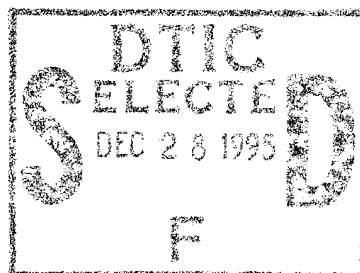


NASA Contractor Report 3559

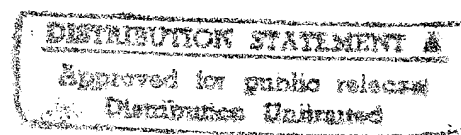
Investigation of Degradation Mechanisms in Composite Matrices

DEPARTMENT OF DEFENSE
PLASTIC TECHNICAL EVALUATION CENTER
AMERICAN POLYMER INC. AND ASSOCIATES

C. Giori and T. Yamauchi



CONTRACT NAS1-15469
JUNE 1982



19951220 034

NASA

DIGITAL QUALITY IN PAPER TEST 3

卷之三

NASA Contractor Report 3559

Investigation of Degradation Mechanisms in Composite Matrices

C. Giori and T. Yamauchi
*IIT Research Institute
Chicago, Illinois*

Prepared for
Langley Research Center
under Contract NAS1-15469

Accesion For	
NTIS	CRA&I
DTIC	TAB
Unannounced	
Justification _____	
By _____	
Distribution / _____	
Availability Codes	
Dist	Avail and/or Special
A-1	



National Aeronautics
and Space Administration

**Scientific and Technical
Information Office**

1982

TABLE OF CONTENTS

SUMMARY	1
1. INTRODUCTION	2
2. MATRIX RESINS EVALUATED	3
2.1 POLYSULFONES	4
2.2 EPOXY RESINS	5
3. COATING STUDIES	12
3.1 IITRI THERMAL CONTROL COATING S13G/LO	12
3.1.1 Adhesion Studies	12
3.1.2 Effect of Surface Preparation	13
3.1.3 Effect of Coating Thickness on Optical Properties	13
3.1.4 Peel Strength Testing	17
3.2 IITRI THERMAL CONTROL COATING Z-93	17
3.3 PREPARATION OF SAMPLES FOR LARC EVALUATION	17
3.3.1 S13G/LO Coated Composites	17
3.3.2 Zinc Orthotitanate - RTV602/LO Coated Composites	19
4. COMPOSITE DEGRADATION STUDIES	20
4.1 EXPERIMENTAL	20
4.1.1 Composite Materials Utilized in Radiation Exposure Tests.	20
4.1.2 Fabrication of T300/Narmco 5208 Laminates	21
4.1.3 Apparatus for Sample Irradiation.	23
4.1.4 Radiation Sources	23
4.1.4.1 Ultraviolet Source	23
4.1.4.2 High Energy Electron Source	23
4.1.5 Radiation Exposure Conditions	28
4.1.6 GC Analysis	31
4.1.6.1 Analysis of SO ₂	31
4.1.6.2 Analysis of H ₂ , CH ₄ , CO, CO ₂ , and Low Molecular Weight Hydrocarbons	31

TABLE OF CONTENTS (CONTINUED)

4.1.7 GC/MS Analysis	32
4.1.7.1 Cryogenic Sample Collection	32
4.1.7.2 Computer Controlled GC/MS	32
4.1.7.3 Data Enhancement and Spectrum Identification	33
4.1.7.4 Quantitative Analysis	36
4.1.8 Compressive and Flexural Strength	37
4.2 RESULTS AND DISCUSSION	37
4.2.1 GC and GC/MS Analysis of Volatile By-Products	37
4.2.1.1 Preliminary UV Studies of Fiberite 705/60	37
4.2.1.2 UV and Electron Exposure Studies of Polysulfone P1700/C6000, Narmco 5208/T300, and Fiberite 934/T300 .	46
4.2.2 Mechanical and Optical Evaluation	86
4.2.3 Dynamic Mechanical Analysis of Electron Exposed Samples .	92
4.3 CONCLUSION AND RECOMMENDATIONS	99
APPENDIX	101

SUMMARY

The work presented in this report describes the initial phase of investigations designed to help establish the degradation mechanisms and radiation effects in graphite composite materials resulting from electron or ultraviolet irradiation. The ultimate objective of these investigations is to predict the long term durability in a space environment of the graphite composite materials. Investigations were also conducted in the application, physical durability and initial optical properties of conventional thermal control coatings on a variety of composite substrates. Good adhesion of S13G/L0 on the composite substrates was achieved by the utilization of γ -amino-propyltriethoxysilane as the primer. The degradation mechanisms have been investigated for graphite/polysulfone and graphite/epoxy laminates exposed to ultraviolet and high-energy electron radiations in vacuum up to 960 equivalent sun hours and 10^9 rads respectively. Based on GC and combined GC/MS analysis of volatile by-products evolved during irradiation, several free radical mechanisms of composite degradation have been identified. The radiation resistance of different matrices has been compared in terms of G values and quantum yields for gas formation. All the composite materials evaluated have shown high electron radiation stability and relatively low ultraviolet stability as indicated by low G values and high quantum yields for gas formation. Mechanical property measurements of irradiated samples did not reveal significant changes, with the possible exception of UV exposed polysulfone laminates. Hydrogen and methane have been identified as the main by-products of irradiation, along with unexpectedly high levels of CO and CO₂. Initial G values for methane relative to hydrogen formation are higher in the presence of isopropylidene linkages, which occur in bisphenol-A based resins.

1. INTRODUCTION

This report entitled "Investigation of Degradation Mechanisms in Composite Matrices" was prepared by IIT Research Institute for NASA - Langley Research Center under contract No. NAS1-15469. The program was conducted under the direction of W.S. Slemp, the NASA-Langley Project Monitor. Work on this program was conducted at IIT Research Institute, Chicago, Ill., under the direction of C. Giori with the assistance of J. Brzuskieicz (coating studies), T. Yamauchi and S. Shelfo (UV exposure testing), R. Butler (GC analysis), S. Gordon (GC/MS analysis) and K. Hofer (composite fabrication and mechanical testing). Electron irradiation tests have been conducted by IRT Corp., San Diego, Ca., under the direction of J. Wilkenfeld.

Composite materials offer substantial advantages over conventional metallic materials for large space system applications due to their superior strength and stiffness-to-weight ratios and their low coefficient of thermal expansion. The major problem in utilizing composites for satellite structural applications is the degradation of material properties under the effect of the vacuum-radiation environment of space. Long-term stability at geosynchronous orbit is of primary concern. The use of composite materials for large geostationary structures presents a number of uncertainties because of the lack of information on the effects of thermal cycling, high vacuum and space radiation. Spacecraft in synchronous earth orbit are periodically eclipsed from the sun by the earth. This may produce a significant thermal shock effect on the composite. Vacuum may cause outgassing and migration of low molecular weight components from the matrix material. Another critical problem is the degradation of the composite matrix under the effect of radiation. This problem is particularly complex because of the nature of the geosynchronous radiation environment and the requirement for stability to ultraviolet as well as high energy radiations. Protection against heat and ultraviolet radiation may be afforded by the use of thermal control coatings. Such coatings, however, add undesired weight to the composite structure and do not provide protection against penetrating radiations such as high energy electrons.

An understanding of the radiation behavior of composite materials is required in order to predict their long-term durability in a space environment. It is particularly important to develop reliable correlations capable of predicting the extent of degradation for 10 to 30 years missions on the basis of short-term laboratory tests. A kinetic analysis of the degradation process is necessary for predicting the long-term behavior based on short-term exposure data, as well as for correlating accelerated exposure data with real time material performance.

The main objective of this study is to establish the mechanisms of degradation and predict the long-term durability of graphite reinforced composites, including epoxies and polysulfone matrix materials. A secondary objective is to establish the feasibility of using thermal control coatings for ultraviolet protection of composite substrates.

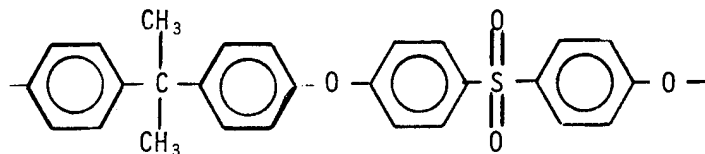
Certain commercial materials and products are identified in this paper in order to specify adequately which materials and products were investigated in the research effort. In no case does such identification imply recommendation or endorsement of the product by NASA, nor does it imply that the materials and products are necessarily the only ones or the best ones available for the purpose. In many cases equivalent materials and products are available and could produce equivalent results.

2. MATRIX RESINS EVALUATED

A study of the mechanisms of radiation damage requires a detailed knowledge of the chemical structure of the matrix resins under evaluation. Unfortunately, the chemical composition of many resins potentially of interest for this study has not been disclosed by the manufacturers. The resins of primary interest for this study are 1) polysulfones, and 2) epoxy resins of high functionality based on the tetraglycidyl derivative of methylenedianiline. The composition of these resins will be reviewed on the basis of information available from the literature or obtained by analysis of samples provided by the manufacturers.

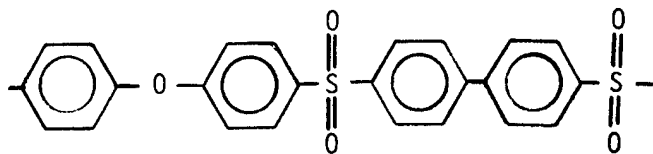
2.1 POLYSULFONES

Polysulfones are a class of high temperature thermoplastic polymers currently available from various commercial sources. Available polysulfones are listed in Table 1. "Udel" P1700 (Union Carbide) is the most widely used of sulfone polymers:



It is obtained by the condensation of bisphenol-A with 4,4'-dichlorodiphenylsulfone. The polymerization involves a nucleophilic displacement reaction. This is made possible by the presence of the sulfone group which is strongly electron attractive and facilitates the displacement of chlorine atoms by the hydroxyl groups of a bisphenol-A.

The second polysulfone was introduced by 3M and later licensed to Carborundum. It is known as "polyarylsulfone":



It is synthesized by a Friedel-Crafts reaction of the disulfonylchloride of diphenylether with biphenyl. It has excellent thermal stability because of the absence of aliphatic groups and the inherent stability of the ether and sulfone bridges.

A third sulfone polymer, introduced by ICI as "polyethersulfone", has the following structure:

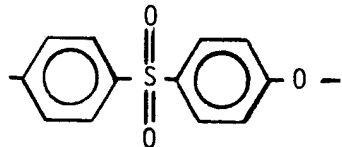


TABLE 1
SULFONE POLYMERS

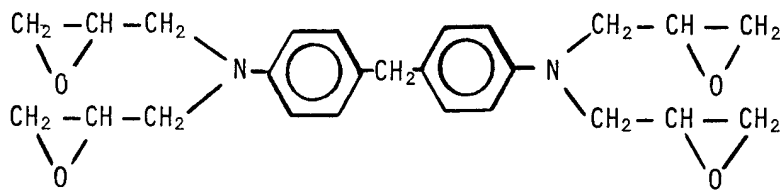
	Union Carbide "Polysulfone" ("Udel", "P1700")
	3M/Carborundum "Polyarylsulfone" ("Astrel") (Discontinued)
	ICI "Polyethersulfone"
UNDISCLOSED	Union Carbide "Polyphenylsulfone" ("Radel")

More recently, a fourth sulfone polymer has been introduced by Union Carbide which is more thermally stable than "Udel." The structure has not been disclosed. The polymer is known as "Radel" or "polyphenylsulfone".

Our study is primarily concerned with the radiation behavior of bis-phenol-A polysulfone ("Udel"). Among the sulfone polymers, "Udel" has shown the greatest potential as composite matrix resin.

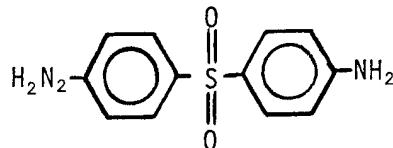
2.2 EPOXY RESINS

The epoxies of interest for this study are high temperature resins based on the tetraglycidyl derivative of methylenedianiline, available from Ciba-Geigy under the trade name MY720:



The high functionality of this resin results in a high degree of crosslinking and high heat distortion temperature of the cured product.

The hardener utilized in conjunction with MY720 is 4,4'-diaminodiphenylsulfone (DDS):



Two epoxy resins based on MY720 and DDS are being evaluated: Fiberite 934 and Narmco 4208. We have conducted a brief analytical study of two batches of Fiberite 934 and Narmco 5208 (neat resins). The following is a summary of our findings:

a. Atomic Absorption Analysis

Boron has been identified in Fiberite 934. Boron trifluoride is used as cocatalyst in Fiberite 934, probably as a complex with ethylamine. Boron was not detected in Narmco 5208.

b. Elemental Analysis

The results obtained for the two resins are quite similar and consistent with structures based primarily on MY720 resin and DDS hardener:

ELEMENTAL ANALYSIS OF RESINS

	C	H	N	S	Cl	Br	P
Fiberite 934	67.48	6.50	7.11	3.00	0.6	0.16	0.05
	67.64	6.62	7.19	3.01			
Narmco 5208	64.83	6.21	7.14	4.18	0.47	0.21	0.05
	64.55	6.20	7.09	4.17			

c. Infrared Analysis

The structural similarity of the two resins is confirmed by their infrared spectra (Figures 1 and 2). The main difference observed is a 5.85 μ band in Fiberite 934 indicative of the presence of carbonyl groups. Carbonyl groups are not believed to be part of the resin structure but are probably due to the presence of acetone or methylethylketone.

d. NMR Analysis

NMR spectra are shown in Figure 3 and 4. Two sets of aromatic protons coupled in a classic AB pattern are observed in each of the NMR spectra. One group which is approximately 1/2 to 1/3 the amount of the other occurs at 6.65 and 7.5 ppm. These two aromatic protons are indicative of protons adjacent to two distinctly different functionalities as might be present in DDS. The second set of aromatic protons located at 6.75 and 7.0 ppm's occur in similar magnetic environments as would be found in MY720 resin. The peak at 5.9 ppm is most likely due to the -NH₂ group of DDS. One -CH₂- group is centered at 2.6 ppm while the other is centered at 3.25 ppm. The -CH- group may be hidden under the aromatic region as it would be expected to be a pentet with low intensity.

No evidence of -CH₃ groups is observed in Fiberite 934. A small amount of -CH₃ groups are present in the Narmco 5208 sample, indicating the presence of minor quantities of a Bisphenol -A based resin.

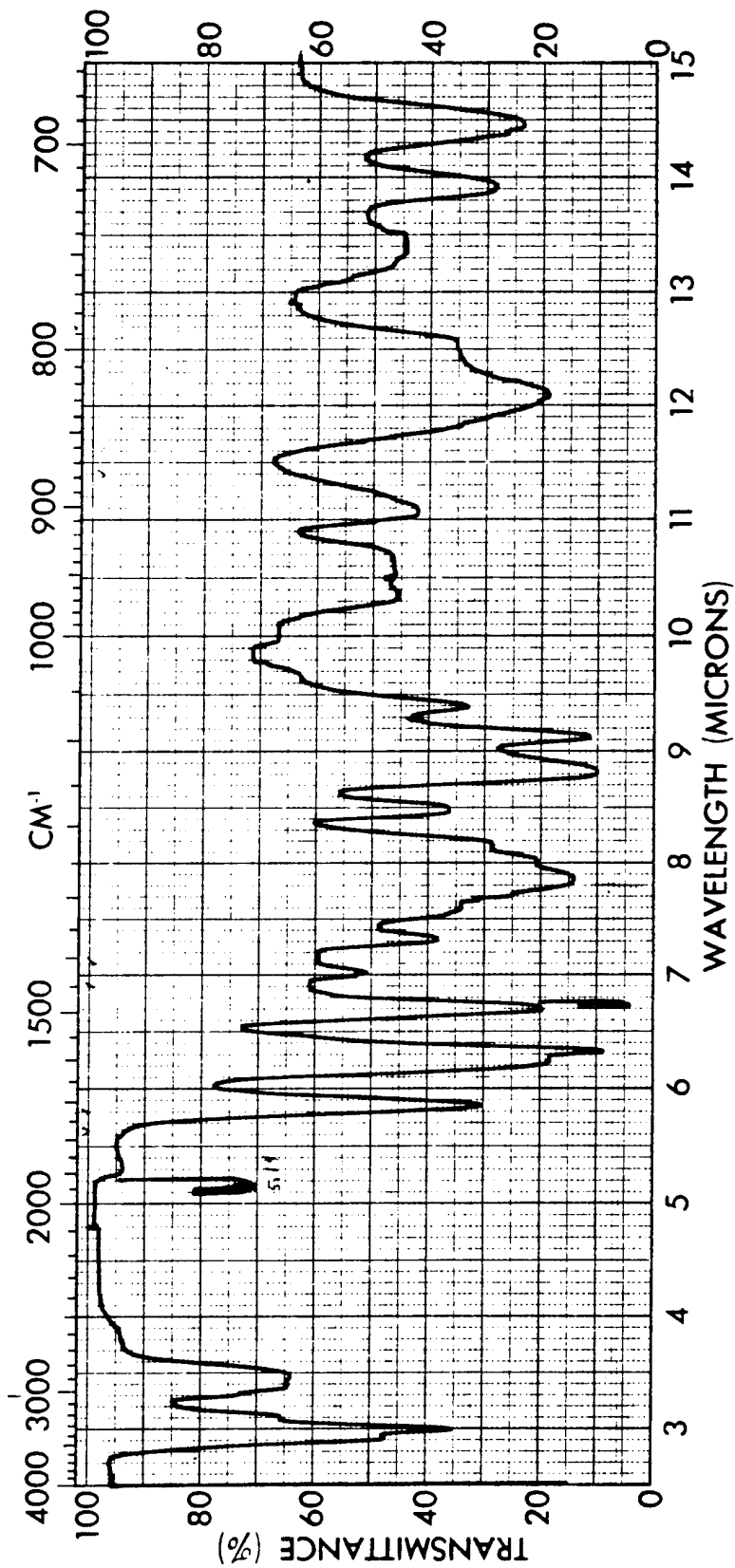


Figure 1. IR Spectrum of Fiberite 934 Resin

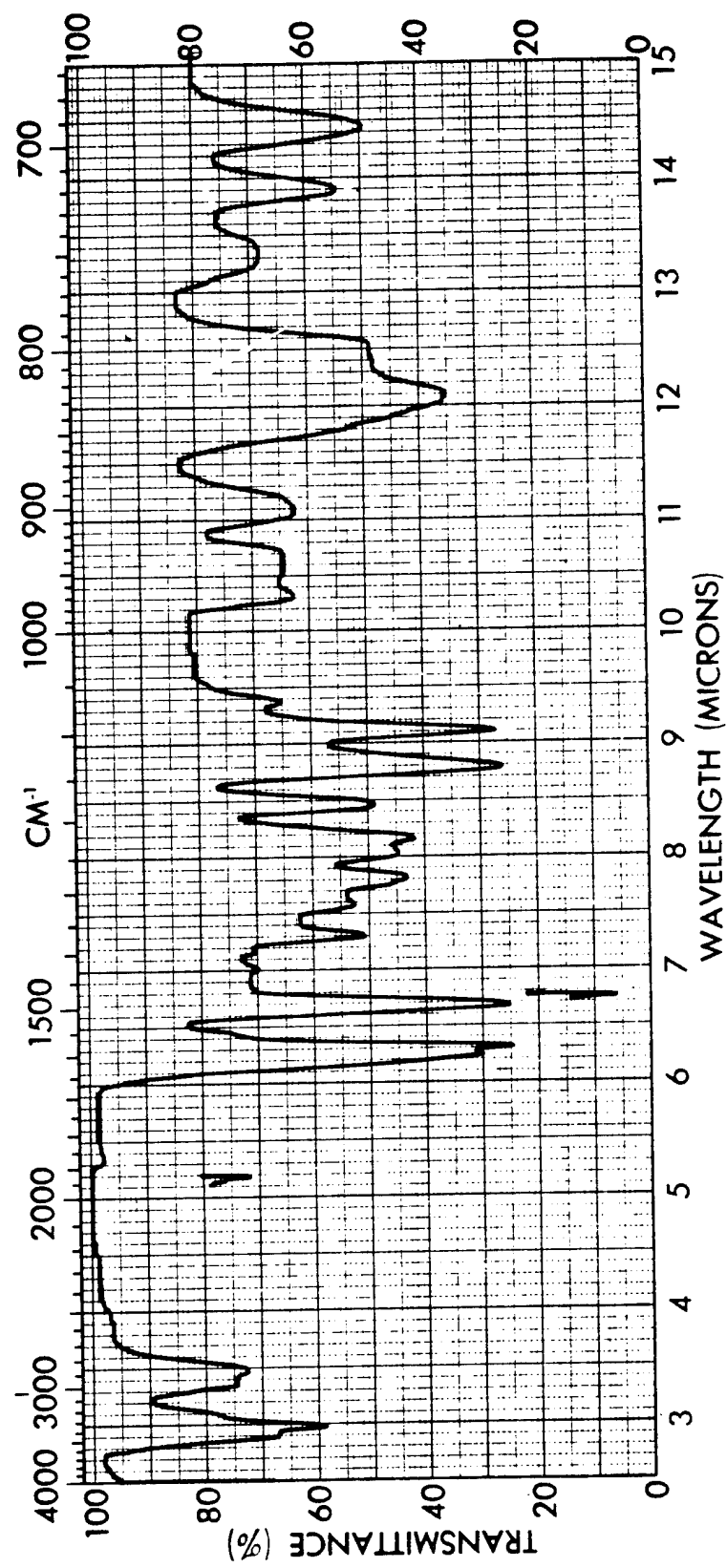


Figure 2. IR Spectrum of Narmco 5208 Resin

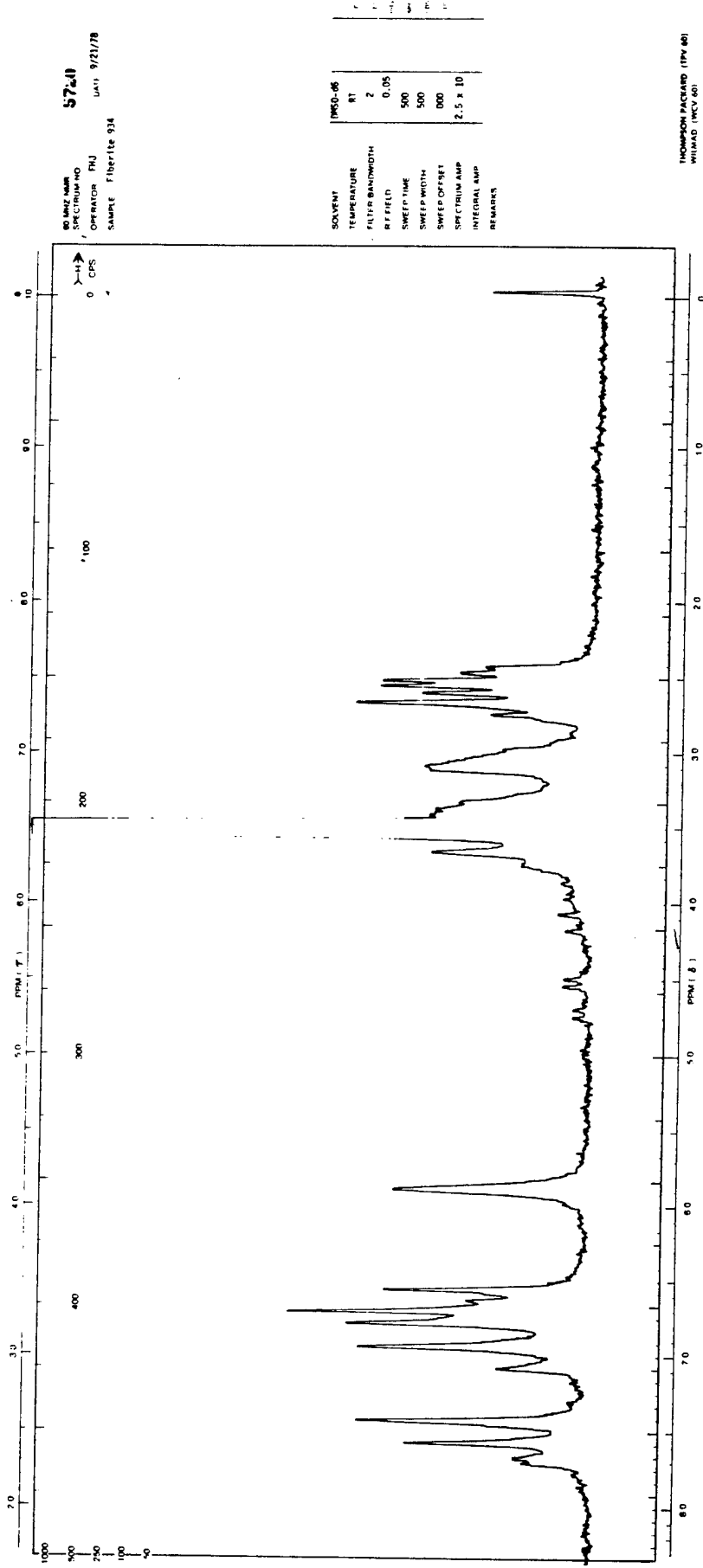


Figure 3. NMR Spectrum of Fiberite 934 Resin

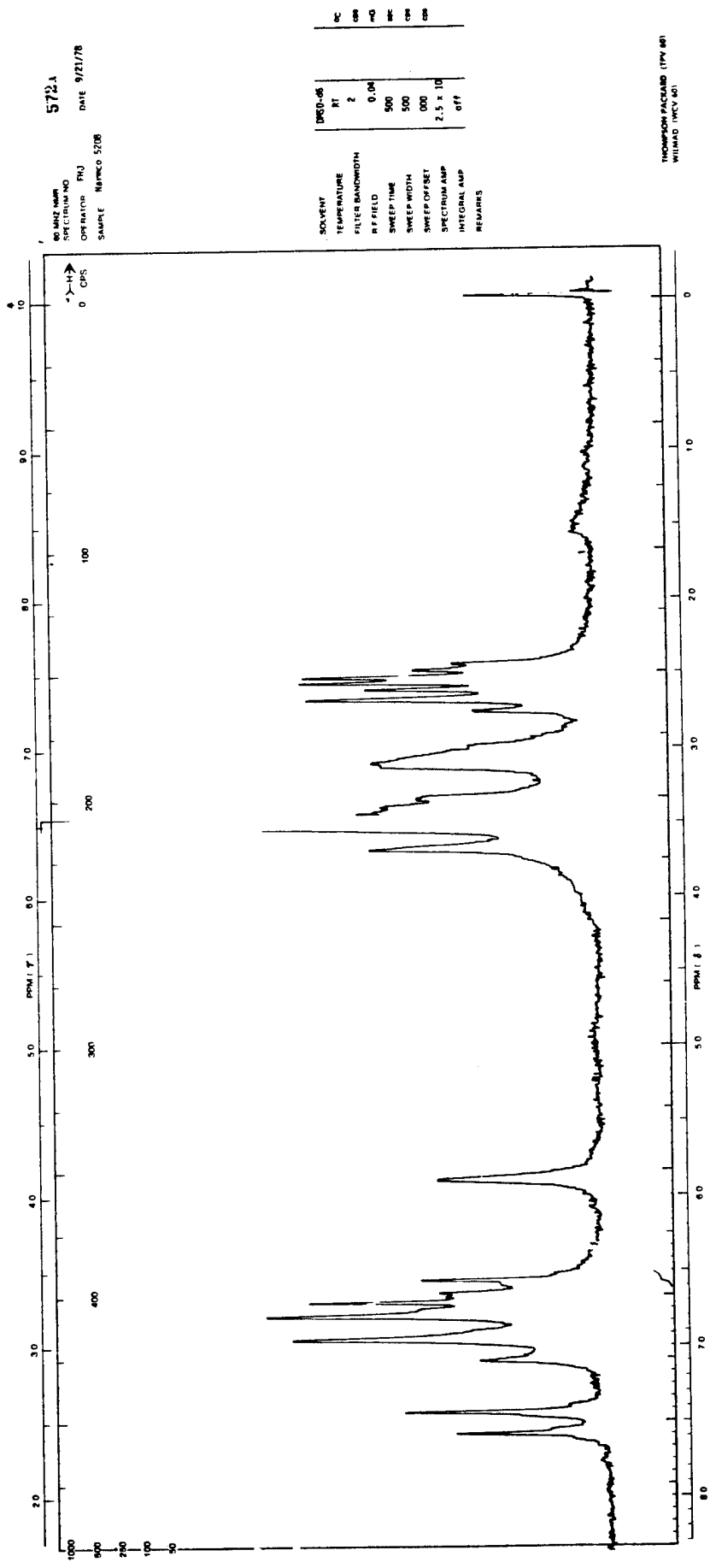


Figure 4. NMR Spectrum of Narmco 5208 Resin

3. COATING STUDIES

3.1 IITRI THERMAL CONTROL COATING S13G/LO

3.1.1. Adhesion Studies

Commercially available silane-type primers have been evaluated as adhesion promoters between the graphite reinforced composite and the silicone-based coating (S13G/LO).

Initial work was carried out utilizing Narmco 5208/T300 composite as the substrate. Four primers listed in Table 2 were applied to the substrate by means of a wipe procedure.

TABLE 2
SILANE TYPE PRIMERS

Trade Name	Composition	Manufacturer
Chemlock AP 133	Undisclosed	Hughson Chemicals, Lord Corp.
SS4044	Undisclosed	General Electric
A4094	Undisclosed	Dow Corning Corp.
A1100 Silane	γ -aminopropyltriethoxysilane	Union Carbide

* No longer available commercially

Primer coated strips were allowed to air dry for 1/2 hour and were then spray coated with S13G/LO (4-6 mil dry film thickness). A control sample (no primer) was also coated for comparative purposes. The coated samples were allowed to cure at room temperature for a period of 48 hours, after which time they were immersed in liquid nitrogen and held until temperature equilibrium was attained (boiling subsided). The samples were then removed from the liquid nitrogen and brought to room temperature. They were then visually examined for signs of coating lifting or delamination. None of the samples failed the immersion test. A cut was therefore made through the coating to the substrate by means of a sharp scalpel and attempts were made to lift the coating by inserting the blade in the cut and turning the blade parallel to the substrate.

Sufficient samples were prepared to evaluate coating adhesion after curing periods of 48 hours and 144 hours. The results obtained are shown in Table 3.

Adhesion of the coating to the primed substrates was cure-time dependent. Samples prepared with A1100 silane primer, however, exhibited superior properties as compared to the others.

3.1.2. Effect of Surface Preparation

The effect of composite surface preparation (abraded and non-abraded) on the adhesion of S13G/L0 coatings has been determined. One set of test specimens was prepared by wiping the surface of the composites with a gauze pad saturated with X-99 solvent (X-99 solvent is the thinner for S13G/L0 paint). Another set of test specimens was abraded with No. 240 grit Alopite cloth and the abraded surface was then wiped with X-99 solvent.

The composite test strips were then wipe primed with a 1:5 ratio (by volume) of A-1100 Silane Primer - X-99 solvent. After air drying for 1/2 hour the primed strips were spray coated with S13G/L0 (Batch No. E-497) and allowed to cure at room temperature.

After curing, the coated strips were thermal-shock-tested by immersion in liquid nitrogen and further checked for coating adhesion by means of the "Knife Adhesion Test." The results obtained are shown in Table 4.

Abrading the surface of the composite materials did not appear to enhance coating adhesion to a marked degree. As a consequence, larger samples submitted to NASA Langley for evaluation were prepared by solvent-wiping of the surfaces only.

3.1.3. Effect of Coating Thickness on Optical Properties

Samples were prepared for determining the effect of coating thickness on solar absorptance (α_s). The solar absorptance was determined by integration of the normal-hemispherical reflectance spectra in the spectral range 325-2600 nm with the solar air-mass-zero spectrum. The values obtained on non-abraded specimens are shown in Table 5. The data indicates that the solar absorptance is coating-thickness-dependent.

TABLE 3
LIQUID NITROGEN ADHESION TEST

Primer	Cure Time	Comments
None	48	Poor adhesion, coating peels away from substrate.
	144	Same as above.
Chemlock AP133	48	Slight degree of adhesion, coating can be peeled from substrate.
	144	Fair adhesion.
SS4044	48	Slight degree of adhesion
	144	Fair to good adhesion. Lifting of coating results in coating residue being left on substrate.
A4094	48	Fair adhesion.
	144	Fair to good adhesion.
A1100 Silane	48	Good adhesion. Coating residue remained on substrate.
	144	<u>Excellent adhesion. Cannot lift coating.</u>

TABLE 4
S13G/L0 COATING STUDIES. A-1100 SILANE PRIMER

Substrate *		Coating Thickness (mm)	Liquid Nitrogen Test	Knife Test	
			(72 hr. cure)	72 hr. cure	264 hr. cure
5208/T300	a)	0.18	Pass	Good	Good
	b)	0.20	Pass	Good	Good
3501-6/AS	a)	0.20	Pass	Good	Good
	b)	0.18	Pass	Good	Good
P1700/ Celion 6000	a)	0.20	Pass	Fair	Fair
	b)	0.25	Pass	Fair	Fair
PMR-15/ Celion 6000	a)	0.15	Pass	Good	Good
	b)	0.18	Pass	Good	Good

* a) Abraded surface.
b) Non-abraded surface.

TABLE 5

OPTICAL PROPERTIES OF S13G/L0 (E-497) ON COMPOSITE SUBSTRATES PRIMED WITH A-1100 SILANE

<u>Substrate</u>	<u>Thickness (mm)</u>	<u>Solar Absorptance (α_s)</u>	<u>Emissance (ϵ)</u>	<u>α_s/ϵ</u>
5208/T300	0.08	0.28	0.90	0.31
	0.13	0.24	0.90	0.27
	0.13	0.23	0.90	0.26
	0.30	Specimen broke		
3501-6/AS	0.08	0.29	0.90	0.32
	0.11	0.24	0.90	0.27
	0.13	0.22	0.90	0.24
	0.25	0.18	0.90	0.20
P1700/Celion 6000	0.08	0.29	0.90	0.32
	0.13	0.24	0.90	0.27
	0.13	0.22	0.90	0.24
	0.28	0.20	0.90	0.22
PMR15/Celion 6000	0.05	0.29	0.90	0.32
	0.13	0.25	0.90	0.28
	0.13	0.22	0.90	0.24
	0.23	0.19	0.90	0.21

3.1.4. Peel Strength Testing

In an effort to evaluate coating adhesion on a quantitative basis, samples were prepared for a 180° peel test. 25 x 150 mm strips of 5208/T300 composite were primed with the various primers and then top-coated with S13G/L0. Before the top coat could dry, strips of cotton cheesecloth were embedded in the coating in such a manner that 20 sq. cm. of the cloth was embedded and a length of the cloth was left free as a pull or peel tab. After curing 120 hours the peel test samples were placed in an Instron Testing Machine, and a 180° peel test was carried out. Peeling was carried out at a rate of 13 mm/min. The results are shown in Table 6.

Preparation of uniform peel test specimens presented a problem in that during the embedment of cloth strips into the coating layer the coating thickness between the substrate and the cloth could not be controlled. Thus the peel strength (which is thickness-dependent) varies. At this stage it appears that the liquid nitrogen/lifting test provided a better indication of coating adhesion.

3.2 IITRI THERMAL CONTROL COATING Z-93

5208/T300, 3501/AS and P1700/Celion 6000 composite samples were coated with Z-93 (2-3 mil thickness). The surface of the composite was abraded slightly to expose clean matrix material. The surface was then rub-primed with the Z-93 and subsequently top coated by spraying. Two top coats were required to effectively hide the substrate. After air drying for 48 hours, the samples passed the liquid nitrogen immersion test, but exhibited some lifting during the knife cut through test.

3.3 PREPARATION OF SAMPLES FOR LARC EVALUATION

3.3.1. S13G/L0 Coating Composites

Coated samples prepared for NASA-Langley evaluation were 50 mm wide strips cut from composite sheets. They were wipe primed with 1:5 ratio of X-1100 Silane in X-99. The primer coating was allowed to air-dry for 1/2 hour and then the strips were spray coated with S13G/L0 (Batch No. E-497). The coated samples are described in Table 7.

Table 6

180° PEEL TEST
SUBSTRATE 5208/T300-S13G/LO COATING

Primer	Comments
None	Poor, peels cleanly from substrate 0.05 kg/cm width
Chemlock AP133	Cohesive strength of coating lower than adhesive strength to substrate. Cloth strip pulls out of coating, 0.49 kg/cm width.
SS4044	Poor, peels cleanly from substrate, 0.18 kg/cm width.
A4094	Cohesive strength of coating lower than adhesive strength to substrate Cloth strip pulls out of coating, 0.54 kg/cm width.
A1100 Silane	Same results as with Chemlock AP133 and A4094, 0.58 kg/cm width.

Table 7
S13G/L0 (E-497) COATED COMPOSITES FOR LARC EVALUATION

<u>Substrate</u>	<u>Average Coating Thickness (mm)</u>
5208/T300	0.25
3501-6/AS	0.23
PMR 15/Celion 6000	0.20
P1700/Celion 6000	0.23

3.3.2. Zinc Orthotitanate - RTV602/L0 Coated Composites

Sample strips of three composite materials (P1700/Celion 6000, 3501-6/AS and 5208/T300) were coated with a zinc orthotitanate - silicone paint formulation (IITRI Batch No. E548). The composite materials were solvent washed (X-99 thinner), air dried for 1/2 hour, and then wipe primed with a 1:5 ratio by volume of A-1100 silane to X-99 thinner. The primed strips were air dried for 1 hour and then spray coated with E-548. At the same time aluminum discs were coated and subsequently used for optical measurements. After curing for 24 hours, coating thickness measurements were made at ten (10) locations on each strip and the average calculated. Substrate description and average coating thickness are shown in Table 8.

Table 8
RTV602/L0 - ZINC ORTHOTITANATE (E-548) COATED
COMPOSITES FOR LARC EVALUATION

<u>Substrate</u>	<u>Average Coating Thickness (mm)</u>
5208/T300	0.20
3501-6/AS	0.15
P1700/Celion 6000	Substrate too irregular to get true reading

The paint was compounded from RTV602/L0 (Batch No. E-538) and Zinc Orthotitanate (Batch No. 1112) to give a pigment-binder ratio (PBR) of 3:1.

The solar absorptance (α_s) of 0.18 mm thick films (on aluminum substrates) in the spectral range 325-2600 nm (solar-air-mass-zero) was 0.16. The emittance was 0.88.

4. COMPOSITE DEGRADATION STUDIES

4.1 EXPERIMENTAL

4.1.1. Composite Materials Utilized in Radiation Exposure Tests

Preliminary exposure tests (UV only) have been conducted on Fiberite 705/60. Samples of Fiberite 705/60 laminates were provided by NASA- Langley. The matrix resin used in 705/60 is P1700 polysulfone, and the fibers employed are graphite T300 and glass (94 and 6 percent respectively).

Ultraviolet and high-energy electron exposure tests have been conducted on 4-ply, undirectional graphite laminates of polysulfone P1700/C6000 and two epoxy systems: Fiberite 934/T300 and Narmco 5208/T300. Fiber volume contents of the laminates tested have been determined using Archimedes principle and assuming zero void content (Table 9). The % resin by weight are given in the same Table. Elemental analysis results (inclusive of the graphite in the composite) are given in Table 10. For comparison, the elemental analysis of clear, extruded P1700 sheet gave:

percent found: C = 72.2; H = 4.93; N = 0.15; S = 6.68; P = 0.007

percent cal.: C = 73.3; H = 5.01; S = 7.24

Table 9

FIBER/RESIN CONTENT OF GRAPHITE LAMINATES

<u>Material</u>	<u>Resin Density</u>	<u>Fiber Density graphite/glass</u>		<u>%-Vol Fiber</u>	<u>%-Wt Resin</u>
705/60	1.3	1.75	2.54	61.2	31.5
P1700/C6000	1.3	1.76	--	47.9	44.5
934/T300	1.3	1.75	--	47.5	45.1
5208/T300	1.3	1.75	--	60.3	32.8

Table 10
ELEMENTAL ANALYSIS OF GRAPHITE LAMINATES*

<u>Material</u>	<u>C</u>	<u>H</u>	<u>N</u>	<u>S</u>	<u>P</u>	<u>Cl</u>	<u>Br</u>	<u>F</u>
705/60	81.6	2.1	3.6	2.8	1.3	0.08	--	--
P1700/C6000	88.6	1.7	3.5	2.1	0.07	0.14	--	0.1
934/T300	76.1	3.0	7.1	1.8	--	0.2	--	0.22
5208/T300	84.8	1.7	7.4	0.86	0.04	0.24	--	0.20

*Inclusive of the graphite present in the composites.

Samples of P1700/C6000 and Fiberite 934/T300 were provided by NASA - Langley. Narmco 5208/T300 laminates were prepared at IITRI according to the procedure given in the following section.

4.1.2. Fabrication of T300/Narmco 5208 Laminates

A 4-ply, unidirectional T300/Narmco 5208 laminate was fabricated using an autoclave to provide the pressure and temperature cycle required.

The autoclave, with internal dimensions of 1.6 meters in length and 0.5 meters diameter allows the fabrication of either one large plate or several smaller plates simultaneously. The movement of the aluminum heating plate into and out of the autoclave is facilitated by a trolley. The autoclave itself is permanently mounted on a steel frame. The heat cycle (maximum capacity 288°C) is automatically controlled. There is provision for two separate vacuum systems that may be used at the same time for fabricating two plates simultaneously. Air pressure to 7 kg/sq cm is obtained directly from an air line in the fabrication laboratory.

The preliminary layup procedures were developed specifically for the autoclave process. The tape is cut to the required length using a conventional paper cutter and is stacked in the appropriate layer orientations. After all plies are stacked the plate is ready for cure.

A stainless steel caul plate, approximately 76mm longer and wider than the laminate, was used during the curing process. A sheet of TX-1040 separator sheet of the same size as the laminate was placed directly on the stainless steel plate. Next the green laminate and a second separator sheet was added. The aggregate was covered with fiberglass bleeder cloth which was

also trimmed to the size of the green laminate. A corprené dam consisting of 9 mm wide strips of corprené was placed around the aggregate. A Mylar* perforated sheet was then added. A sheet of 181 fiberglass cloth was then placed on top this stack. The complete package was then placed on the heater plate in a vacuum bag. Before the cure cycle was initiated, full vacuum was applied to the package, any leaks were corrected, and check was made to insure that there were no wrinkles on the laminate.

The following cure schedule recommended by General Dynamics was used for the T300/Narmco 5208 composite panels:

1. Full Vacuum is applied to the bagged green layup.
2. The panel is heated from room temperature to 135°C (+2.5,-5°C) in 40 ± 8 minutes (corresponding to a 3°C/minute heat up rate.)
3. The layup is held at full vacuum and 135°C (+2.5°C,-5°C) for 60(± 5) minutes.
4. Pressure is then increased to 6 (± 0.35) kg/cm². The vacuum is vented to outside air when the pressure has reached 1.76 kg/cm².
5. Upon reaching 6 (± 0.35) kg/cm², the temperature is increased to 179°C (+5°C,-2.5°C) in 15 (± 3) minutes.
6. The system is held at 6 (± 0.35) kg/cm² and 179°C (+ 5°C,-2.5°C) for 120 (± 5) minutes.
7. The system is then cooled to 60°C maintaining the 6 (± 0.35) kg/cm² pressure for not less than 30 minutes.
8. The panels are postcured subsequently for 240 (± 5) minutes at 204°C ($\pm 5.0^{\circ}\text{C}$). The heatup rate for postcuring panel is from RT to 204°C in 64 (± 10) minutes.

Throughout the postcure, the panels were loosely supported between two layers of 13 to 19 mm thick aluminum honeycomb core. Following the cure, the laminates were cut into 178 by 32 mm size samples using a diamond blade mounted on a saw.

* Mylar: Registered trademark of E.I. Du Pont de Nemours & Co., Inc.

4.1.3. Apparatus for Sample Irradiation

The systems used for ultraviolet exposure consist of 38 mm diam. and 305 mm long quartz tubes sealed on stainless steel and equipped with 70 mm CFF flanges and ultra-high vacuum valves. For electron irradiation, Pyrex* tubes of the same size and valves with gold seals were employed. These vacuum assemblies allow gas collection for GC and GC/MS analysis of volatile by-products evolved from the sample during radiation exposure. The exposure tubes containing the composite samples were dried at 120°C overnight under reduced pressure. The tubes were subsequently evacuated to 10^{-7} torr or less using an ion pump. The vacuum system utilized in this study is shown in Figure 5. Figure 6 shows a tube assembly equipped with a copper-constantan thermocouple to monitor sample temperature variations during electron exposure.

4.1.4. Radiation Sources

4.1.4.1. Ultraviolet Source

The ultraviolet radiation source used in this study is a A-H6 high pressure, quartz-jacketed, water-cooled mercury-arc lamp. The output of this lamp approximates the solar-spectral distribution (Figure 7). Its radiant energy is emitted mainly in a broad continuum spreading all the way down to below 230 nm. Its high ratio of ultraviolet-to-total energy allows accelerated ultraviolet testing at several equivalent solar factors.

4.1.4.2. High Energy Electron Source

The electron linear accelerator of IRT Corp. has been utilized for high energy electron exposure. This system can provide electron beams over a wide range of energies. The samples were irradiated at a mean dose rate of 10.8 krad/sec. Although dose rates as high as 50 krad/sec could be achieved, a lower dose rate was employed to prevent an excessive temperature increase of the samples. At the dose rate employed, the irradiated samples reached a maximum temperature of 49°C.

The samples were mounted in a specially designed holder shown in Figure 8. Concrete block shielding was provided for the valves as shown. The samples

* Pyrex: Trademark of Corning Glass Works.

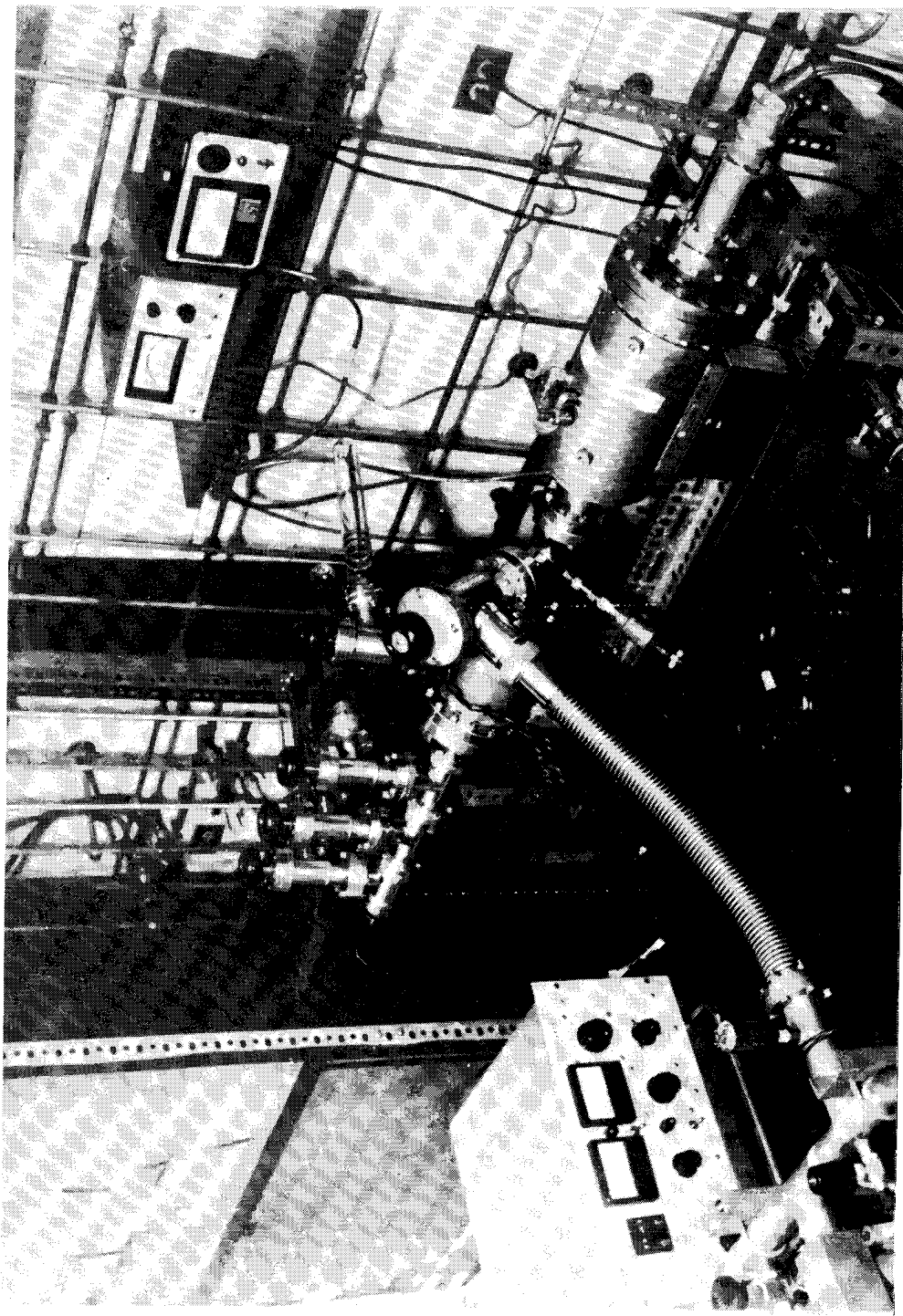


Figure 5. VACUUM SYSTEM

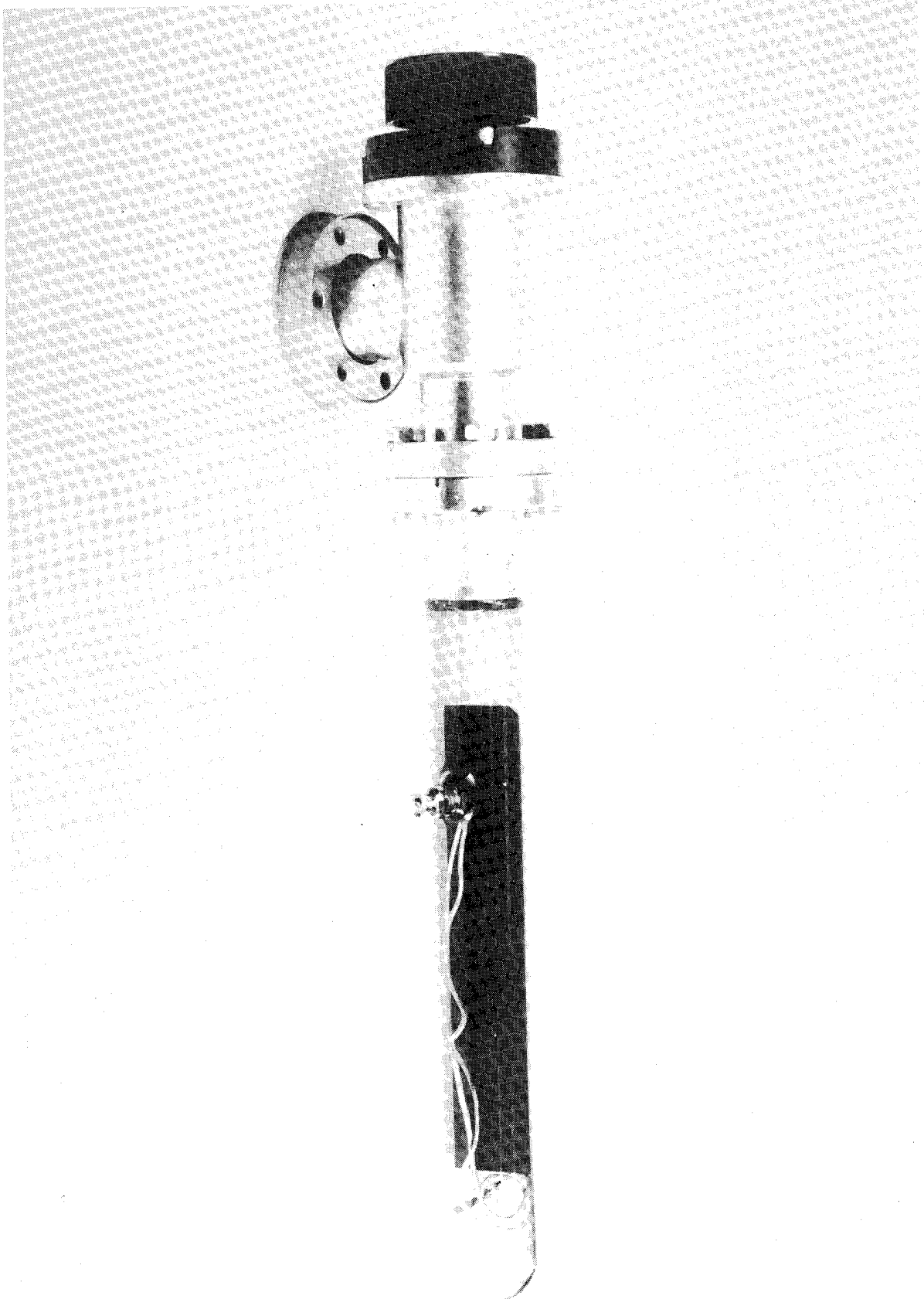


Figure 6. Vacuum Assembly for High-Energy Electron Exposure and Sample Temperature Monitoring

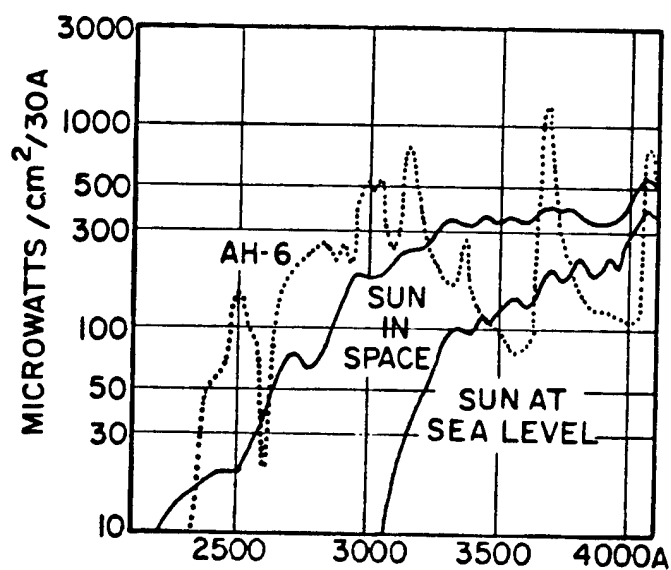


Figure 7. Ultraviolet Spectral Energy Distribution
of AH-6 Lamp, the Sun in Space, and Sun
at Sea Level

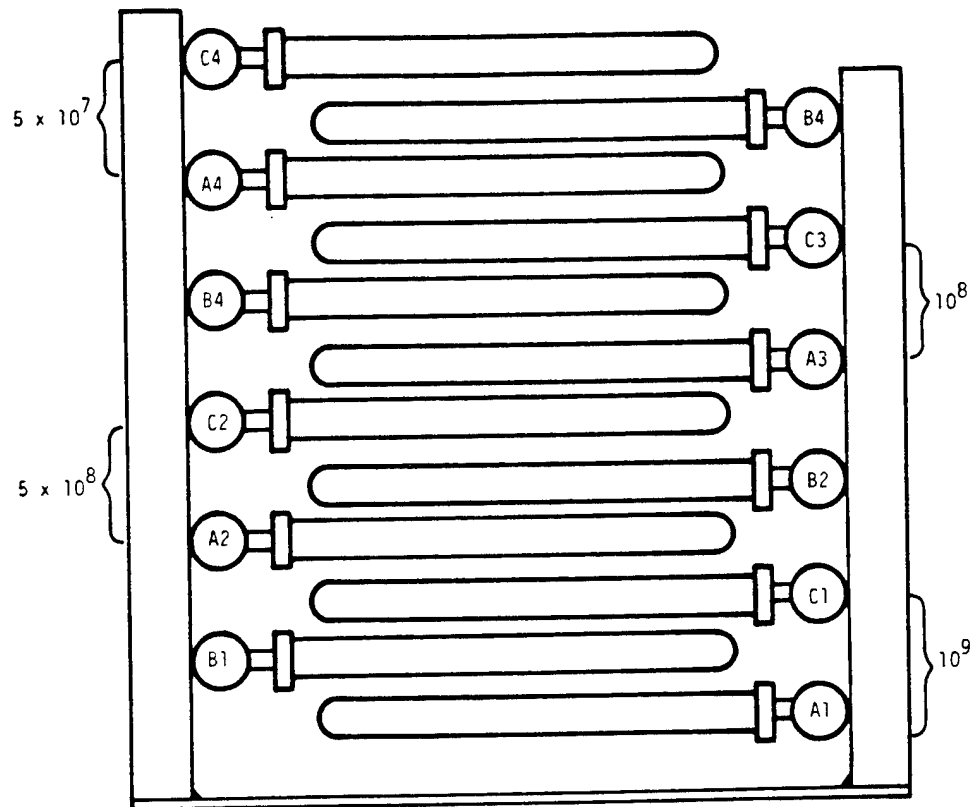


Figure 8. Irradiation configuration for composite samples.
Sample position is indicated as is the total dose (rads) received.

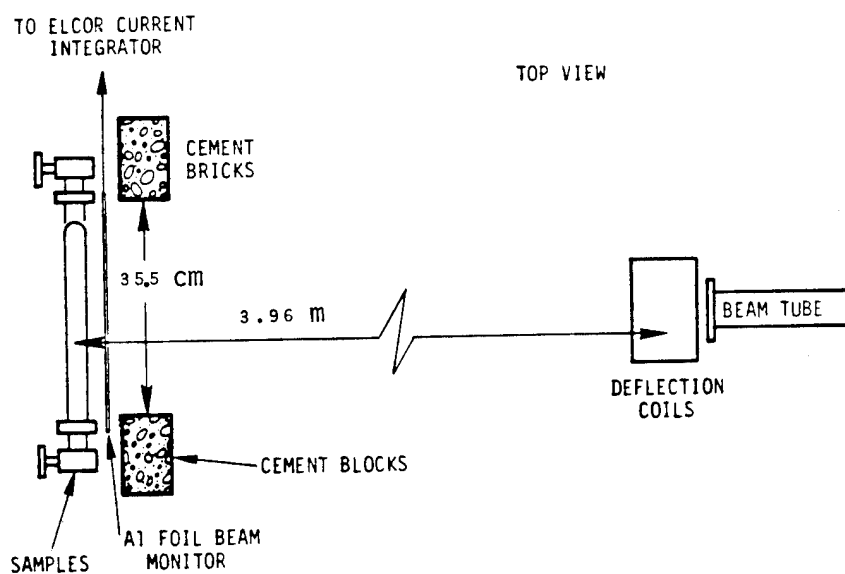


Figure 9. Experimental setup for composite irradiation.

occupied an area of approximately 30 x 56 cm. A fan provided some cooling although, in retrospect, it probably was not necessary. The sample tubes were oriented horizontally with the valves at the outer edges as shown. The samples were placed approximately 3.96 m from the end of the IRT single section Linac as shown in Figure 9. The accelerator was tuned to provide a 12 MeV beam with an average pulse current of 575 μ A, a pulse width of 6 μ s, and a repetition rate of 180 Hz. The beam was rastered across the sample area with an IRT magnetic coil deflection unit.

Dosimetry was provided with plastic film dosimeters. The beam map shown in Figure 10 indicates that beam uniformity was good. As this type of dosimeter is limited to a total dose of about 10 Mrads, much lower than required, a secondary beam monitor was provided. This was an Al foil secondary emission monitor placed in front of the samples. The current generated by secondary electron emission as the primary beam traverses the foil is read by a current integrator whose output is calibrated against the dosimeter. Thus, total dose accumulated could be related to charge collected by the monitor.

4.1.5. Radiation Exposure Conditions

The ultraviolet doses employed are shown in Table 11. Ultraviolet exposure tests were conducted using a space ultraviolet acceleration factor of four, which is equivalent to an ultraviolet flux of ~ 0.7 cal/cm² min in the wavelength region 200-400 nm.

The electron exposure doses are shown in Table 12. The samples were irradiated at a mean dose rate of 10.8 krads per second. Samples A, B, C-4 were irradiated for 79.6 min and received a total dose of 5×10^7 rads. Samples A, B, C-3 were irradiated for 153.8 min and received a dose of 1×10^8 rads. Samples A, B, C-2 were irradiated for 769.2 min and received a total dose of 5×10^8 rads. Finally, samples A, B, C-1 were irradiated for 1538.5 min and received a total dose of 1×10^9 rads. According to the thermocouple, sample C-1 reached a maximum temperature of about 49 °C. Since the sample configurations were basically identical and the dose rate relatively uniform over the entire irradiation area, there is no reason to doubt that the other samples stayed at about the same temperature.

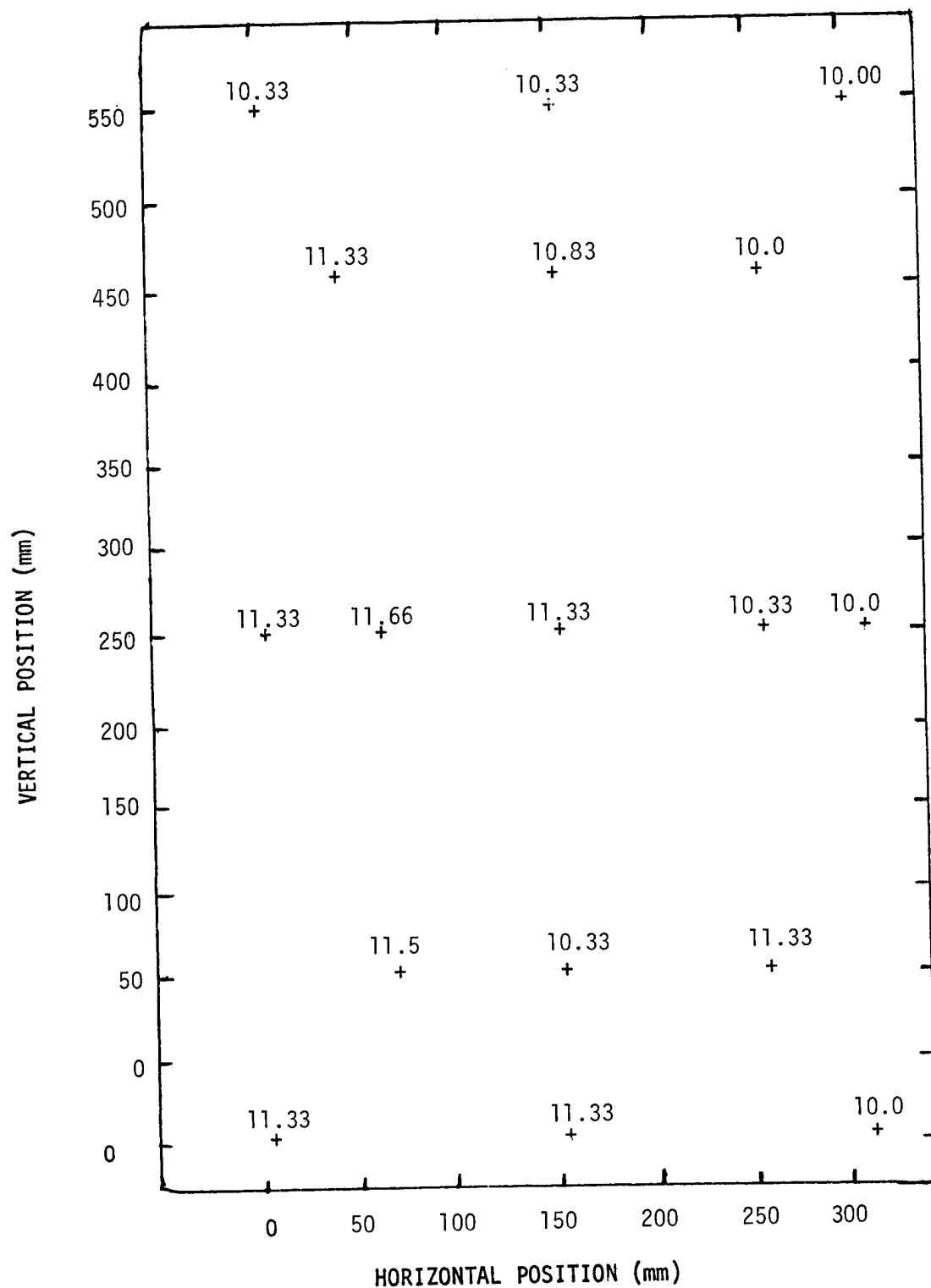


Figure 10. Dose rate map over the irradiation plane.
Dose rates in krads/s.

Table 11
ULTRAVIOLET EXPOSURE TEST CONDITIONS

<u>Sample No.</u>	<u>Material</u>	<u>Ultraviolet Dose, ESH*</u>
5	Fiberite 705/60	20
7	"	420
8	"	592
17	Fiberite 934/T300	210
18	"	480
19	"	720
20	"	960
21	Polysulfone P1700/C6000	240
22	"	480
23	"	720
24	"	960
33	Narmco 5208/T300	240
34	"	480
35	"	720
36	"	960

* ESH = Equivalent Sun Hours

Table 12
ELECTRON EXPOSURE TEST CONDITIONS

<u>Sample I.D.</u>	<u>Material</u>	<u>Dose (rads)</u>
A-4	Fiberite 934/T300	5×10^7
A-3	"	1×10^8
A-2	"	5×10^8
A-1	"	1×10^9
B-4	Polysulfone P1700/C6000	5×10^7
B-3	"	1×10^8
B-2	"	5×10^8
B-1	"	1×10^9
C-4	Narmco 5208/T300	5×10^7
C-3	"	1×10^8
C-2	"	5×10^8
C-1	"	1×10^9

4.1.6. GC Analysis

After irradiation, the sample tube assembly is attached to the vacuum line, filled with zero grade Helium and the gases allowed to mix for one hour prior to analysis. An irradiated blank was run through the analysis procedure with the following results:

H₂ = 25 ppm (v)

CH₄ = not detected (<100 ppb [v])

CO = not detected (<100 ppb [v])

CO₂ = 250 ppb (v)

Both the H₂ and CO₂ were identified as impurities present in the helium used to fill the sample tube, and deducted from the results.

4.1.6.1. Analysis of SO₂

SO₂ analysis was conducted using a gas chromatograph fitted with a sulfur specific flame photometric detector. Separation was accomplished using a 254 x 3 mm stainless steel column packed with Porapak QS. The analysis was run isothermally at 180°C. Helium was used as a carrier gas. Detector instability and wall absorption of SO₂ complicated the analysis and made SO₂ quantification uncertain.

4.1.6.2. Analysis of H₂, CH₄, CO, CO₂, and Low Molecular Weight Hydrocarbons

H₂, CH₄, CO, and hydrocarbons up to C₃ were analyzed using a Trace Gas Analyzer equipped with a Helium ionization detector. For H₂ and CO analysis the analyzer was fitted with 508 x 3 mm stainless steel column packed with 100/120 mesh Molecular Sieve 5A. Helium carrier gas flow was set at 30 ml/min⁻¹ and the analysis was run isothermally at 100°C. CH₄, CO₂, and hydrocarbon analysis was accomplished by fitting the instrument with 254 x 3 mm column packed with a 100/120 mesh Porapak QS. Helium flow was set at 30 ml/min⁻¹ and the analysis run isothermally at 40°C for CO₂ and CH₄ and isothermally at 150°C for higher hydrocarbons. The sample was injected via a 8.9 ml sample loop attached to both the Trace Gas Analyzer and a standard vacuum line. This setup allows the sample loop to be evacuated, filled with sample at a known pressure, and injected without danger of contamination due to atmospheric gases. The

instrument was calibrated using two standard gas mixtures (10 ppm each of H₂, CO, and CH₄, and CO₂ in He; and 50 ppm of C₂H₆, and C₃H₈ in He).

4.1.7. GC/MS Analysis

4.1.7.1. Cryogenic Sample Collection

For GC/MS analysis, the remaining gas sample from the irradiated polymer tube was collected in a cryogenic trap. To accomplish this one exit of the trap was connected to the sample tube and the other exit connected to a standard laboratory vacuum system. Vacuum tight connections were provided with stainless steel fittings equipped with Teflon* ferrules. The sample was slowly withdrawn from the tube through the liquid N₂ cooled trap by utilizing the vacuum system. Rate of sample withdrawal and collection was controlled with a needle valve situated between the trap and the vacuum system. Sample pressure was measured with a Wallace-Tiernan type absolute pressure gauge. The sample was continuously withdrawn until the pressure read zero. Total collection time for the 150-200 ml (STP) of sample was approximately 30 minutes. Upon termination of the collection procedure the trap was filled with UHP He to ambient pressure, removed from the collection apparatus (while maintaining liquid N₂ temperature), sealed off and transported to the GC/MS.

4.1.7.2. Computer Controlled GC/MS

All samples were analyzed for volatile organics by combined gas chromatography-mass spectrometry under computer control (GC-MS-COMP).

After collection of the vaporous components in a liquid-nitrogen-cooled stainless steel trap, the trap was attached to the (modified) injection port of the GC. By rapidly heating the trap (up to 250°C), while reverse-flushing with helium carrier gas for 1 minute, the sample was injected directly onto the GC column for analysis. A 50 m x 0.05 mm I.D. OV-101 SCOT column was used, with a carrier gas flow rate of 3.0 ml/min and an injector split ratio of 10:1. The column was held initially at a temperature of 35°C for 10 minutes, then programmed at 4°C/min to 210°C.

*Teflon: Registered trademark of E.I. Du Pont de Nemours & Co., Inc.

The total column effluent was coupled directly to a double-focusing mass spectrometer operated at low resolution. The ion source of the mass spectrometer consists of a combination standard electron impact source and an electron impact ionization detector (EID). By operating the EID at a low electron energy, the carrier-gas-free total ion current signal from the GC could be monitored in real-time using a strip chart recorder.

On injection, the magnet of the mass spectrometer was set to scan cyclically throughout the GC run from m/e 20 to m/e 250 every 2.4 sec. The data were gathered and stored using data system with disk-based mass storage. At the end of a run, ion abundance data from each scan were numbered and plotted as a function of spectrum scan number using visual display unit. A typical total current profile (TICP) obtained in this way is shown in Figure 11.

The raw GC-MS files were transferred by magnetic tape to an off-line computer system for data "clean-up", followed by spectrum identification and quantitation.

4.1.7.3. Data Enhancement Spectrum Identification

It is well established that the mass spectra obtained from the GC-MS analysis of complex mixtures are often markedly different from the spectra of the corresponding pure compounds, largely due to contributions from background noise and overlapping peaks. These extraneous contributions can severely compromise compound identification efforts and measurements of relative concentrations. Dromey et al.¹ have developed an effective minicomputer-based method (Program CLEANUP) to automatically extract background-free and resolve mass spectra of mixture components from GC-MS data by the systematic application of a tabular peak-modeling technique to mass chromatograms in the data file. The use of this algorithm enhances the GC resolution and also gives "pure" spectra by using masses which have maximized at any given spectrum number.

¹ R.G. Dromey, M.J. Stefik, T.C. Rindfleisch, and A.M. Duffield: Extraction of Mass Spectra Free of Background and Neighboring Component Contributions from Gas Chromatography/Mass Spectrometry Data, Anal. Chem., 48, 1368 (1976).

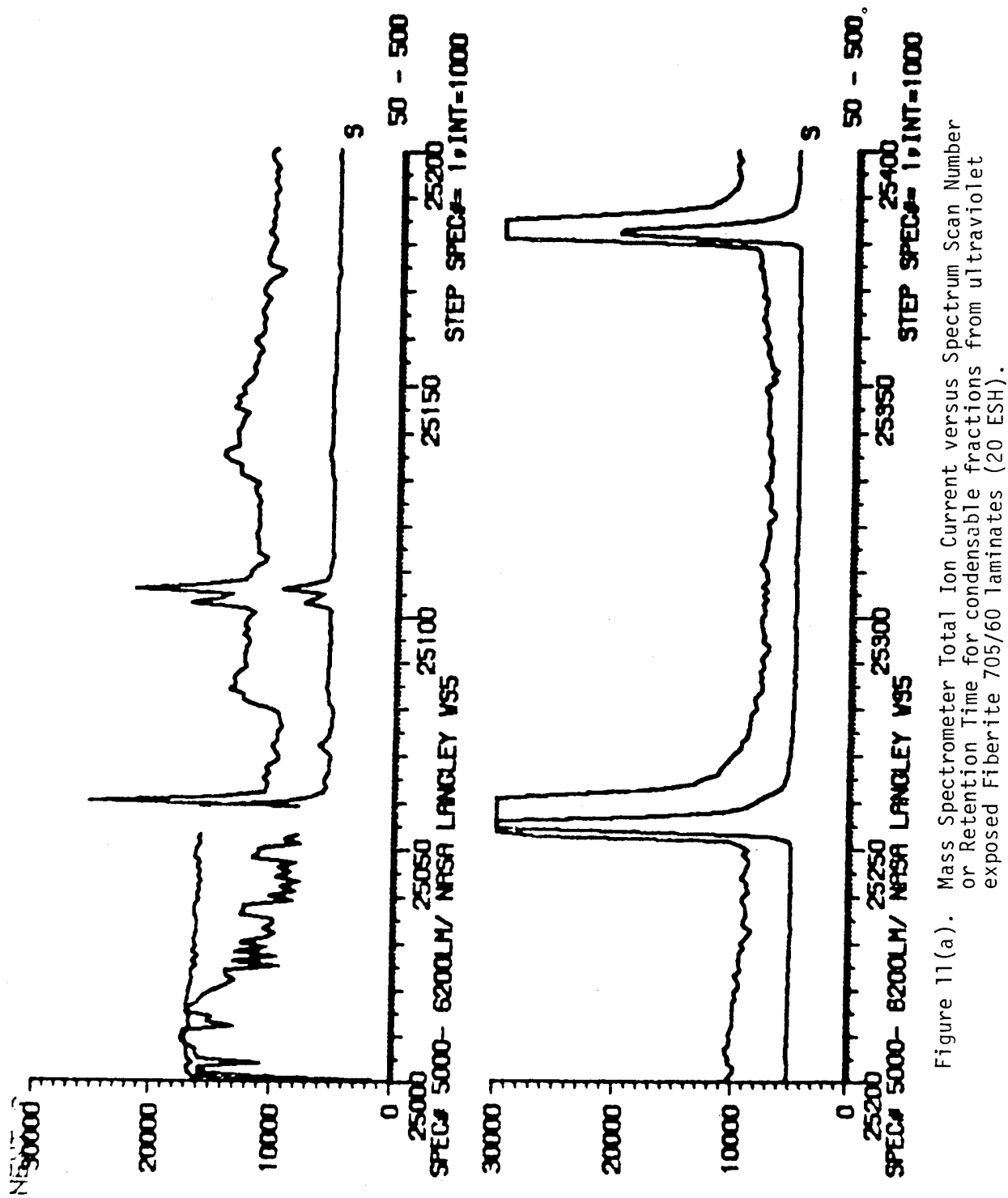


Figure 11(a). Mass Spectrometer Total Ion Current versus Spectrum Scan Number or Retention Time for condensable fractions from ultraviolet exposed Fiberite 705/60 laminates (20 ESH).

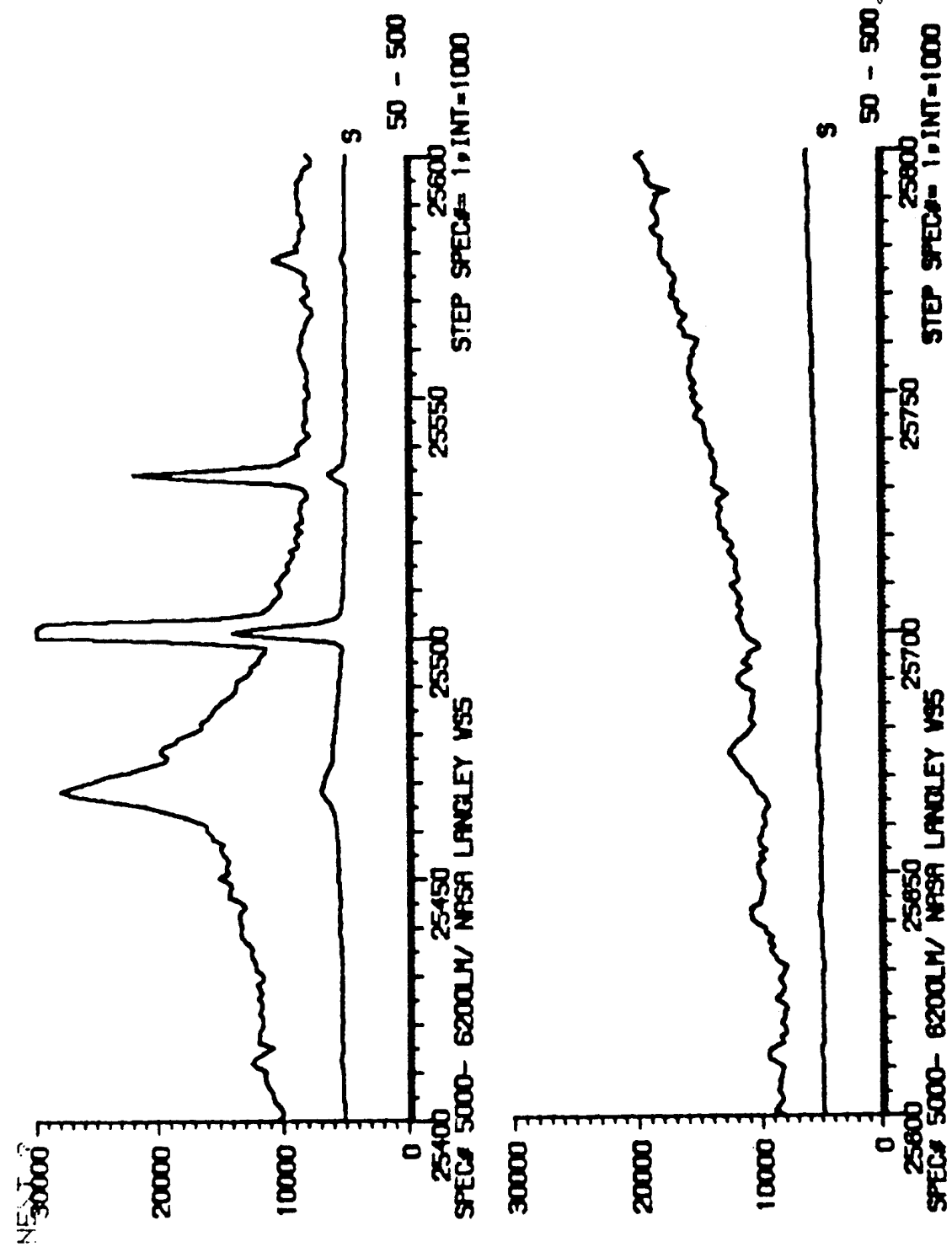


Figure 11(b). Mass Spectrometer Ion Current versus Spectrum Scan Number or Retention Time for condensable fractions from ultraviolet exposed Fiberite 705/60 lamination (20 ESH).

Identification of the resolved spectra is then established using a computer-based mass spectral search system (Biemann Method) or by manual comparison with Eight Peak Index².

4.1.7.4. Quantitative Analysis

Ideally, compounds may be quantitated by first preparing a calibration curve, relating peak area to amount of solute over the concentration range of interest, and then determining the amount of the compound present in the sample from the standard curve. However, because of the complexity of the samples in the present investigation, extensive use of standards throughout the elution range is obviously impractical.

Smith et al.³ have developed a method (program TIMSEK) to compute relative concentrations of components based on one or more standards, using the same "cleaned-up" GC-MS data which previously yielded information on the identity of the individual components. The algorithm can also be used to automatically calculate relative retention indexes using suitable homologous-series standards. Relative retention index data is used to establish identity in those cases where closely-related compounds exhibit very similar mass spectra.

After obtaining the corrected area for each peak from CLEANUP, the relative concentration of the *i*th component is calculated by TIMSEK from

$$\text{Rel. Conc } (i) = \frac{\text{Areal TIC of the } i\text{th component}}{\text{Areal TIC of internal standard}} \quad (1)$$

Determination of relative concentrations provides a means of quantitatively comparing GC-MS profiles but does not measure the actual amount of each component. To obtain an estimate of the amount of a particular component present in the sample, we have simply established, in a separate experiment, the MS response factor for known amounts of a standard (*n*-decane). This factor has then been used to determine the amount of each substance of interest in terms of *n*-decane, by direct conversion of the peak areas.

² "Eight Peak Index of Mass Spectra", Mass Spectrometry Data Center, AWRE, Aldermaston, Reading, U.K., 1970.

³ D.H. Smith, M. Achebach, W.J. Yeager, P.J. Anderson, Fitch, and T.C. Rindfleisch: Quantitative Comparison of Combined Gas Chromatographic/Mass Spectrometric Profiles of Complex Mixtures, *Anal. Chem.*, 49, 1623 (1977).

4.1.8. Compressive and Flexural Strength Measurements

After gas analysis, the laminate samples were removed from the exposure tubes and cut using a diamond blade saw as shown in Figure 12. Compressive strength of laminate samples has been obtained utilizing the IITRI compression test fixture. This fixture provides a method of aligning the specimen for uniaxial loading. As Figure 13 demonstrates, the fixture consists of a pair of trapezoidal wedge grips grasping either end of the specimen. The wedge grips are used to apply the compressive loads to the tabs. This feature ensures plane-to-plane contact for the test specimens throughout the loading. The advantage of this fixture lies in the fact that a straight-sided test specimen can be used. Individual specimen tab thickness variations are permitted, provided only that the tab surfaces are parallel and thus surface-to-surface contact is attained at all wedge positions. In use, prestressing of the specimen tabs transverse to the specimen is accomplished by bolting across the tabs; this measure prevents the slippage of the tabs early in the load cycle. Lateral alignment of the fixture top and bottom halves is assured by a guidance system consisting of two parallel roller bushings in the upper half of the fixture and two corresponding bushing shafts in the lower half of the fixture. This feature insures against misalignment in loading. The compression specimen geometry is shown schematically in Figure 14. It should be noted that all failure loads were below the theoretical buckling loads for the 12.7 mm gauge length shown.

The flexural specimen geometry is shown in Figure 15.

4.2 RESULTS AND DISCUSSION

4.2.1. GC and GC/MS Analysis of Volatile By-Products

4.2.1.1. Preliminary UV Studies of Fiberite 705/60

Preliminary GC and GC/MS analysis of volatile by-products evolved during ultraviolet exposure have been performed on Fiberite 705/60. The GC results obtained are shown in Table 13 for samples exposed 20, 420, and 592 ESH. GC/MS data for 20 ESH samples are shown in Table 14. The helium ionization detector employed for GC analysis was found inadequate for SO₂ measurements. (In subsequent work, SO₂ was measured by separate GC analysis with a flame

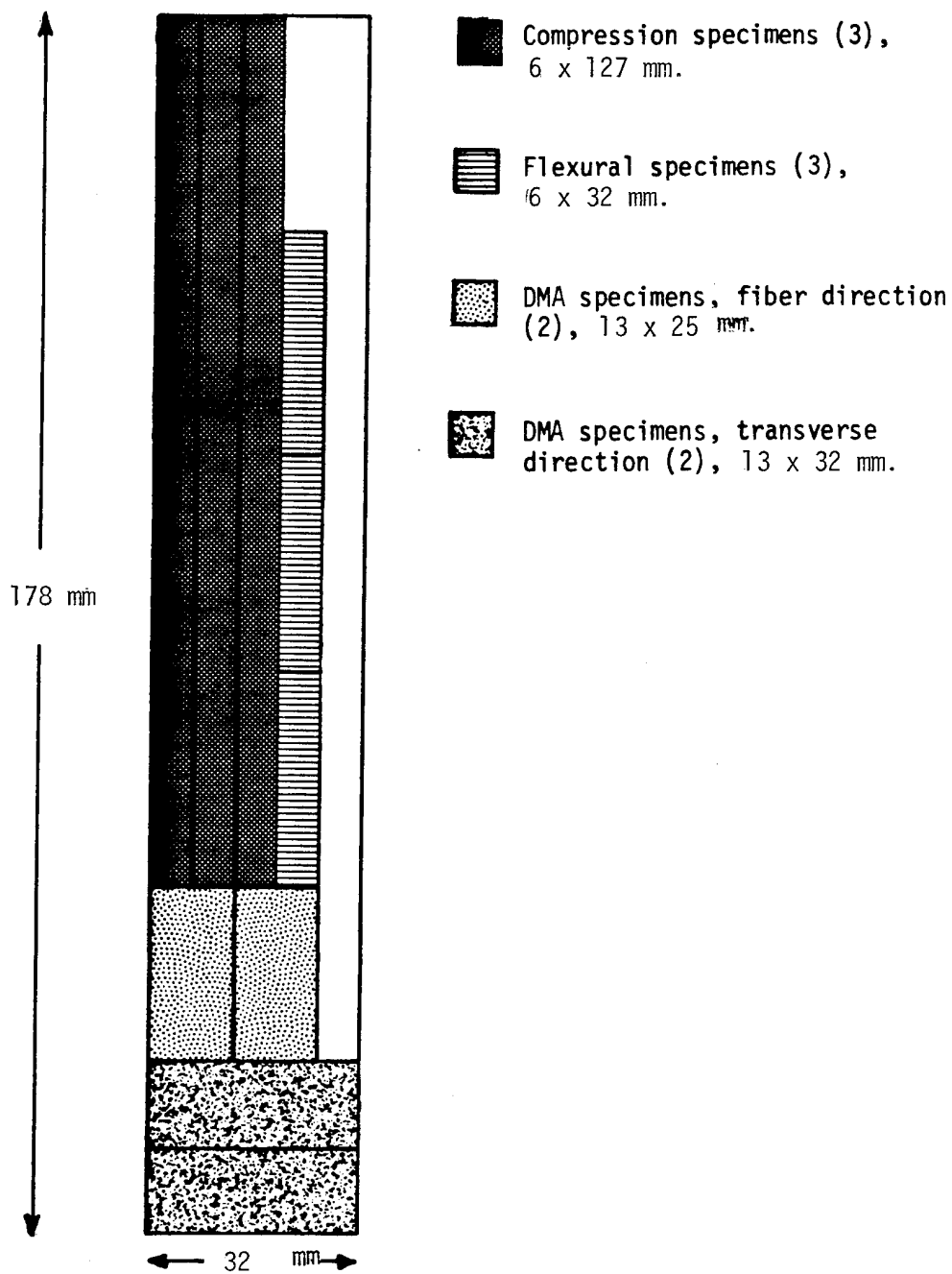


Figure 12. Utilization of exposed samples for mechanical testing.

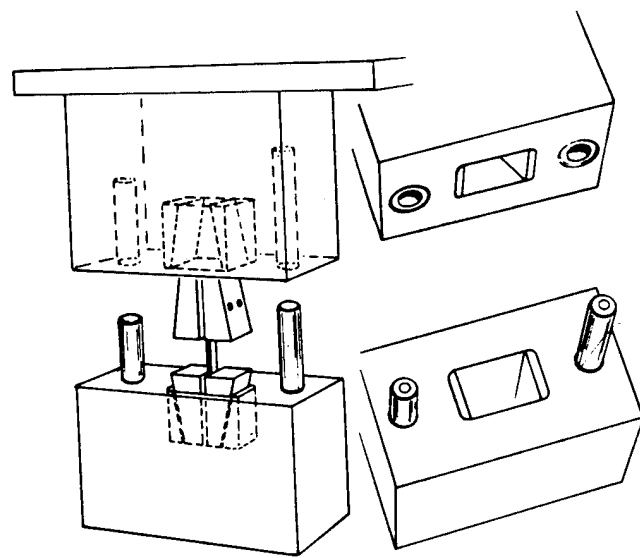


Figure 13. Schematic of the IITRI Compression Test Fixture.

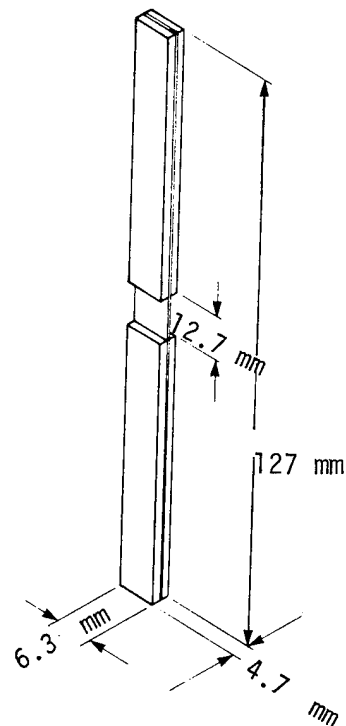


Figure 14. Compression Specimen Geometry

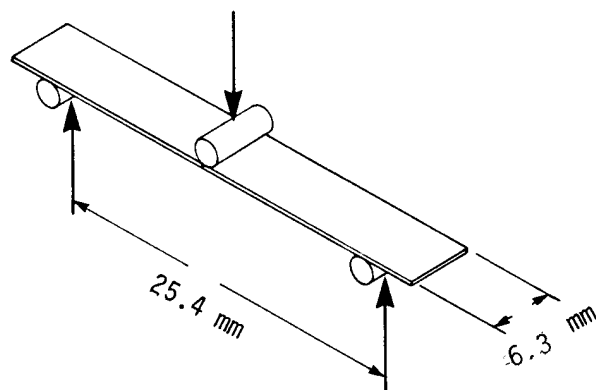


Figure 15. Flexural Specimen Geometry

Table 13

ULTRAVIOLET IRRADIATION OF FIBERITE 705/60 LAMINATES.
GC ANALYSIS OF EVOLVED PRODUCTS BY USING A PORAPAK QS COLUMN.

Product	Yield*, mole x 10 ⁻⁶		
	20 ESH**	420 ESH	592 ESH
H ₂	0.51	0.36	1.70
CH ₄	0.024	0.076	0.16
CO	0.67	2.07	3.28
CO ₂	0.33	1.14	1.13
C ₂ H ₆	traces	traces	0.023
C ₃ H ₈	traces	traces	0.012

* Surface Area of exposed samples, 56.5 cm²

** Equivalent Sun Hours

Table 14

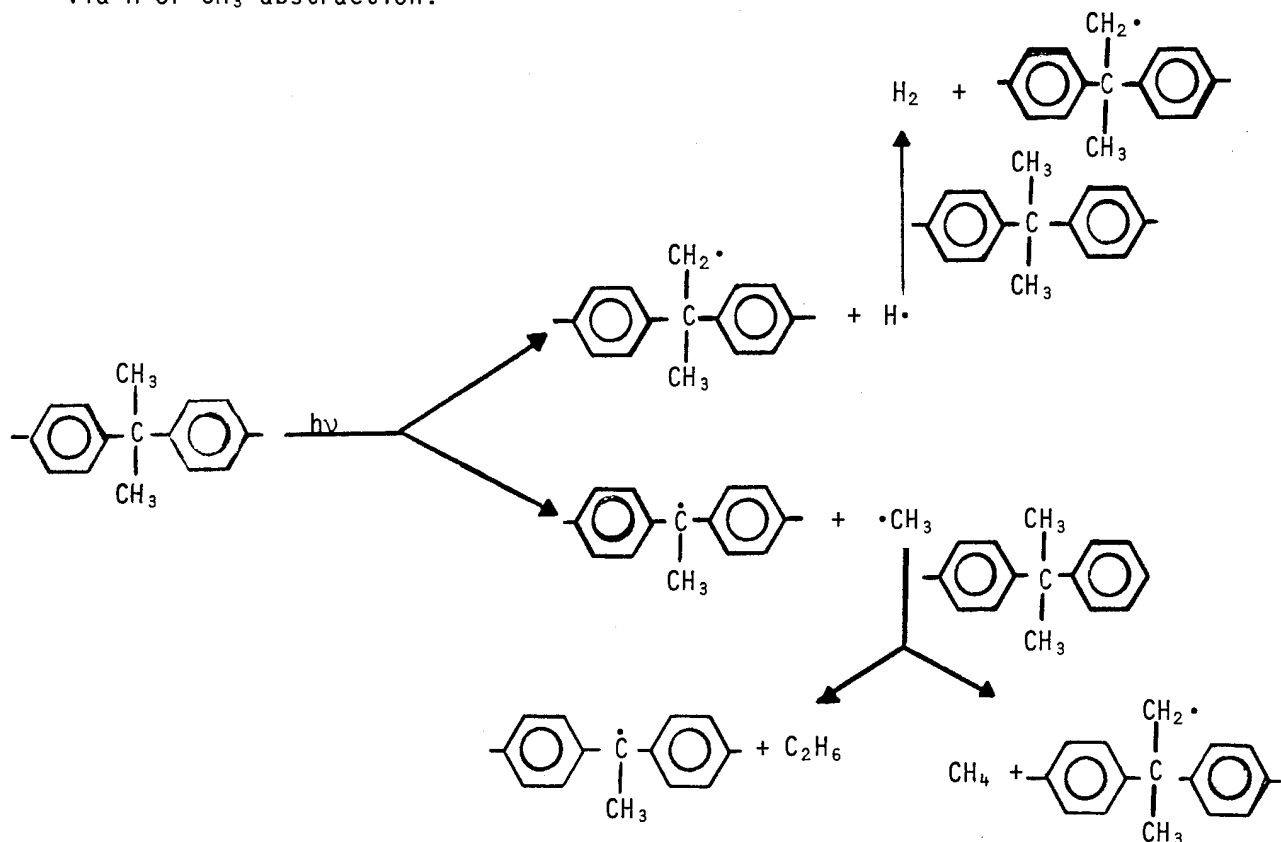
ULTRAVIOLET IRRADIATION OF FIBERITE 705/60
LAMINATE. GC/MS ANALYSIS OF EVOLVED
PRODUCTS BY USING OV-101 COLUMN.
EXPOSURE DOSE, 20 ESH

Product	Yield*
	mole x 10 ⁻¹⁰
Benzene	325
Acetone	153
Toluene	93
Ethylbenzene	31
Stryrene	5.1
Isopropylbenzene	0.8

*Surface area of exposed sample
56.5 cm²

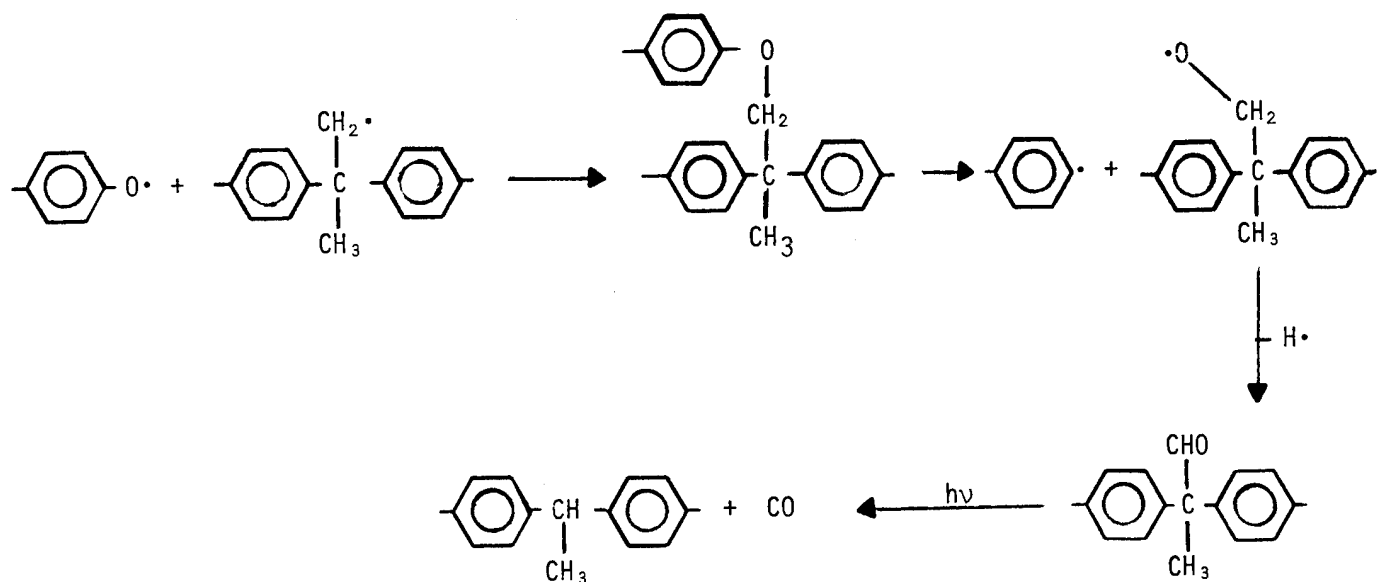
photometric detector). The results obtained indicate that degradation occurs via a free radical process and that several concurrent degradation mechanisms are involved, primarily at the isopropylidene linkage.

Formation of H₂, CH₄, and C₂H₆ can be explained in terms of cleavage of C-C and C-H bonds at the isopropylidene unit followed by free radical quenching via H or CH₃ abstraction:

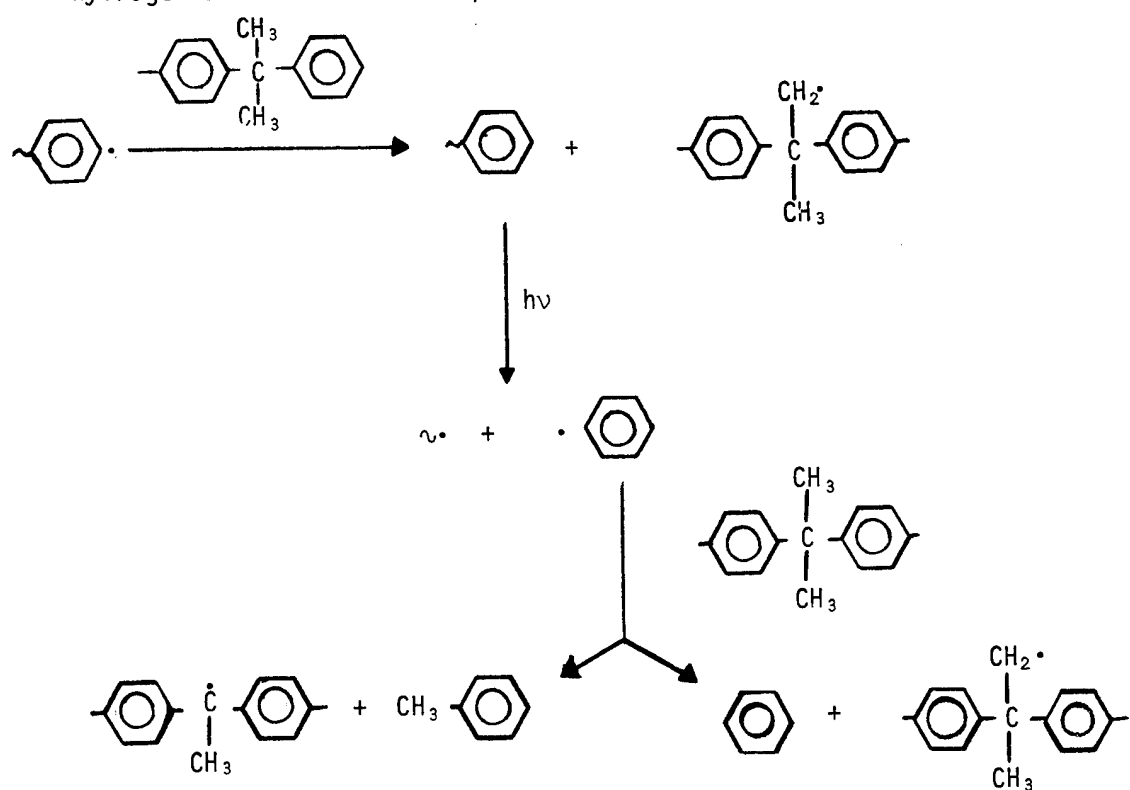


Formation of CO₂ would be expected under photo-oxidative conditions, but in a vacuum it cannot be explained by any reasonable mechanism. It is possible that carbonyl groups were initially present in the polymer as a result of oxidation reactions during processing.

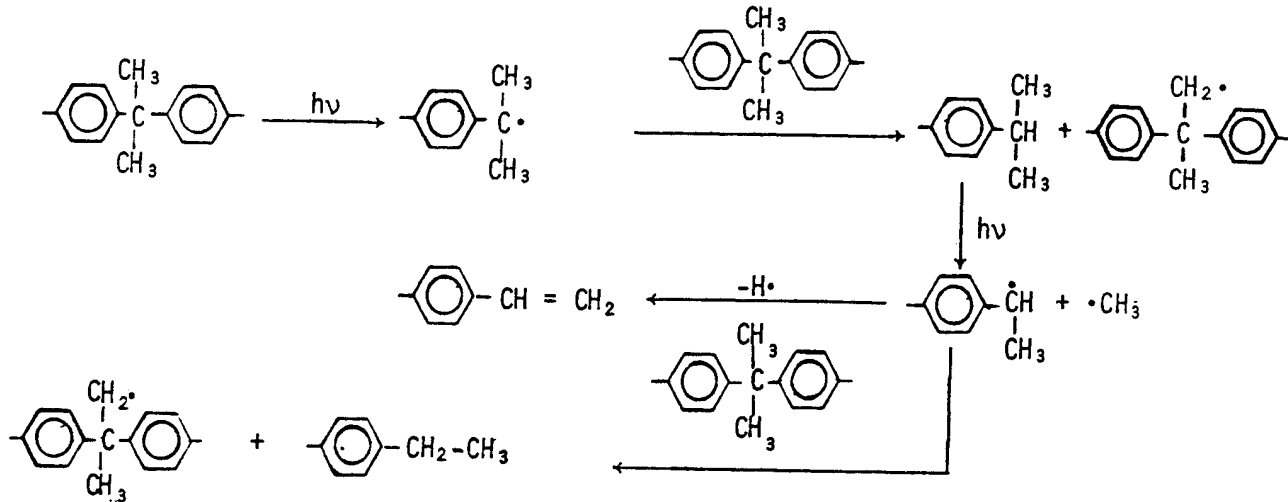
Formation of CO can be ascribed to decarbonylation reactions. A possible path involves recombination of phenoxy radicals with -CH₂· radicals followed by cleavage, disproportionation and decarbonylation:



Formation of benzene requires two cleavage reactions and two hydrogen abstractions.
Toluene is formed by a similar process but methyl abstraction instead of hydrogen abstraction takes place at the phenyl radical:

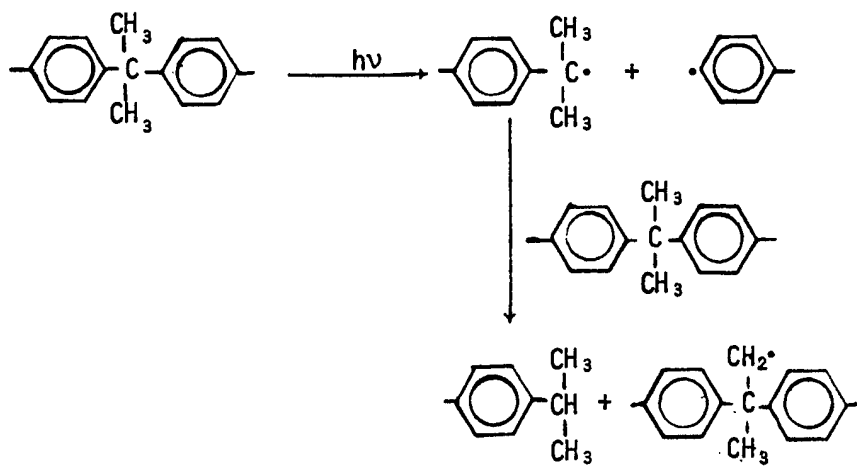


Ethylbenzene and styrene arise from a double process of cleavage and hydrogen abstraction at the isopropylidene unit. The 1-phenyl, 1-ethyl radical is produced which can form styrene end groups (by disproportionation) or ethylbenzene end groups (by hydrogen abstraction):

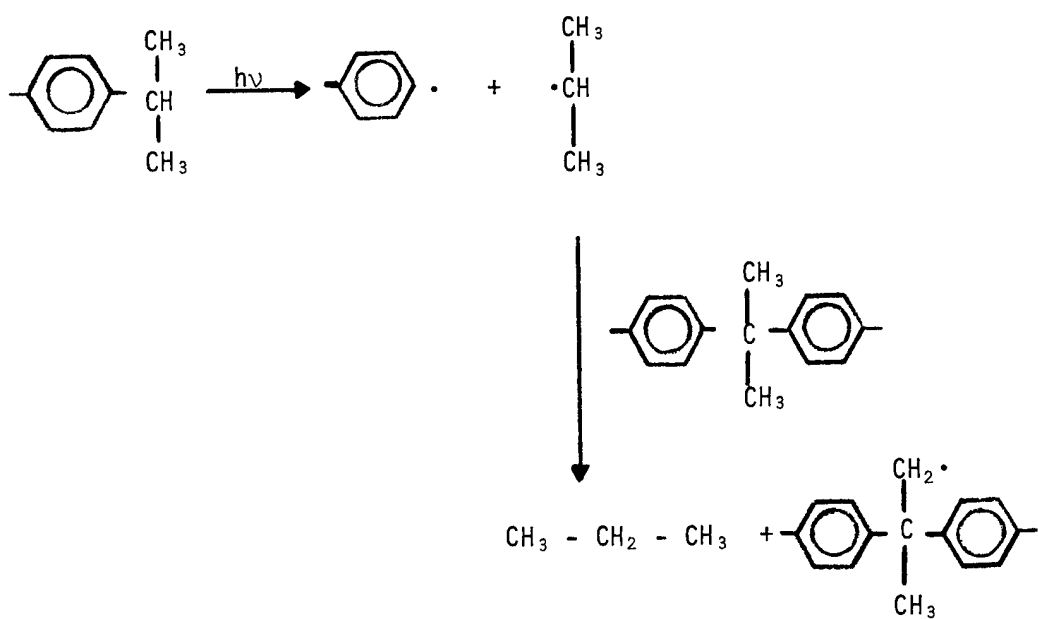


From these end groups, cleavage and hydrogen abstraction at the bond connecting the benzene ring to the polymer chain result in the formation of styrene and ethylbenzene.

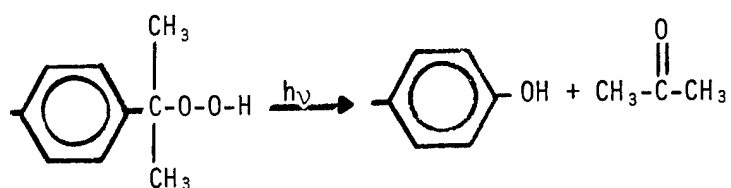
Formation of isopropylbenzene requires the following reaction mechanism:



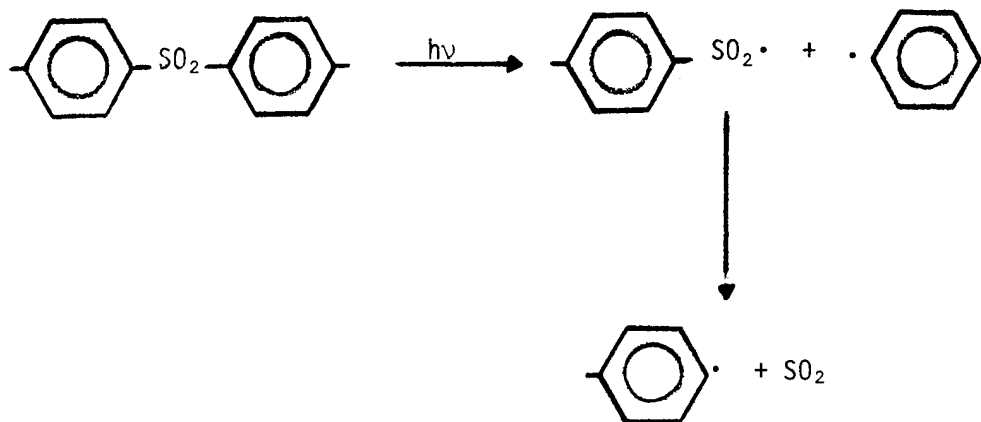
Subsequent cleavage of the phenyl-isopropyl bond explains the formation of propane:



Formation of acetone is ascribed to the decomposition of isopropylbenzene hydroperoxide which is photolytically decomposed to acetone and phenol:



As indicated in the case of CO₂ formation, formation of acetone confirms that oxygen plays a role in the photolytic process, in spite of the fact that the irradiations were conducted under high vacuum. It is difficult to see how the in-chain oxygen atoms of polysulfone could be responsible for these photo-oxidative mechanisms. Most likely, peroxidated groups were originally present in the polymer. Oxidative processes may also arise from the photodecomposition of SO₂ into SO and O₂. These possible mechanisms will be discussed later for other matrix resins evaluated in this study for which analysis of sulfur compounds is available. SO₂ can result from the cleavage of C-S bonds followed by elimination of SO₂:



4.2.1.2. UV and Electron Exposure Studies of Polysulfone P1700/C6000, Narmco 5208/T300, and Fiberite 934/T300

Results of GC analysis of volatile by-products evolved during irradiation are shown in Tables 15-17 and 18-20. The same data are presented graphically in Figures 16-21 and 22-27 for ultraviolet and electron irradiated samples respectively. In the tables, gas formation is expressed as total moles formed during irradiation. In the graphs, gas formation is shown as moles produced per square centimeter of irradiated sample (in the case of ultraviolet exposure) or per gram of irradiated resin (in the case of electron exposure). This allows direct comparison of gas yields for different materials, since the resin content of the three laminates was different and the sample size was also slightly different. These results can be generally interpreted in terms of free radical processes involving several bonds in the polymer structures. Although the primary process of electron radiation damage involves ionization, subsequent steps leading to chain scission and cross-linking, with concurrent gas formation, take place by free radical mechanisms. This explains the similarity of the products obtained by ultraviolet and electron irradiation.

Formation of hydrogen, methane, ethane and propane has been discussed in a previous section for Fiberite 705/60. Formation of these gases was explained in terms of free radical reactions at the isopropylidene linkage. The same mechanisms are expected to take place with P1700/C6000. To some extent, these mechanisms may also apply to Narmco 5208, which contains a small percentage of a bisphenol-A resin. For Fiberite 934, that does not contain bisphenol- A, the

Table 15

ULTRAVIOLET IRRADIATION OF P1700/CELION 6000 LAMINATES.
GC ANALYSIS OF EVOLVED PRODUCTS BY USING A PORAPAK QS COLUMN.

Product	Yield*, mole x 10 ⁻⁶			
	240 ESH**	480 ESH	720 ESH	960 ESH
H ₂	0.18	0.75	1.15	1.25
CH ₄	0.11	0.33	0.81	1.25
CO	2.5	4.29	6.79	7.86
CO ₂	2.25	3.18	4.54	5.0
C ₂ H ₆	0.011	0.056	0.12	0.15
C ₃ H ₈	0.032	0.052	0.093	0.12

* Surface area of exposed samples, 43.1 cm²

** Equivalent Sun Hours

Table 16

ULTRAVIOLET IRRADIATION OF 934/T300 LAMINATES.
GC ANALYSIS OF EVOLVED PRODUCTS BY USING A PORAPAK QS COLUMN.

Product	Yield*, mole x 10 ⁻⁶			
	210 ESH**	480 ESH	720 ESH	960 ESH
H ₂	0.017	0.44	0.6	1.0
CH ₄	0.24	0.22	0.2	0.42
CO	2.0	5.0	7.14	6.78
CO ₂	1.20	3.18	5.0	4.32
C ₂ H ₆	0.066	0.16	0.057	0.24
C ₃ H ₈	0.017	0.03	0.009	0.052

* Surface area of exposed samples, 56.5 cm²

** Equivalent Sun Hours

Table 17

ULTRAVIOLET IRRADIATION OF 5208/T300 LAMINATES.
GC ANALYSIS OF EVOLVED PRODUCTS BY USING A PORAPAK QS COLUMN.

<u>Product</u>	<u>Yield*, mole x 10⁻⁶</u>			
	<u>240 ESH**</u>	<u>480 ESH</u>	<u>720 ESH</u>	<u>960 ESH</u>
H ₂	2.16	3.06	5.09	5.30
CH ₄	0.51	0.88	1.57	1.85
CO	5.55	6.47	8.83	10.3
CO ₂	1.29	1.64	2.57	2.91
C ₂ H ₆	0.30	0.31	0.43	0.45
C ₃ H ₈	0.043	0.054	0.082	0.096
SO ₂	not detected	not detected	-	-

* Surface area of exposed samples, 56.5 cm²

** Equivalent Sun Hours

Table 18

ELECTRON IRRADIATION OF P1700/CELION 6000 LAMINATES.
GC ANALYSIS OF EVOLVED PRODUCTS BY USING A PORAPAK QS COLUMN.

<u>Product</u>	<u>Yield*, mole x 10⁻⁶</u>			
	<u>5 x 10⁷ rads</u>	<u>10⁸ rads</u>	<u>5 x 10⁸ rads</u>	<u>10⁹ rads</u>
H ₂	1.51	2.41	17.5	64.7
CH ₄	0.25	0.37	1.25	2.6
CO	1.76	2.48	8.79	14.4
CO ₂	0.95	1.45	5.79	14.8
C ₂ H ₆	0.0045	0.010	0.043	0.054
C ₃ H ₈	0.0024	0.0074	0.017	0.019
SO ₂	not detected	not detected	0.025	0.087

* Weight of exposed samples, 5.13g (44.5%-wt resin)

Table 19

ELECTRON IRRADIATION OF 934/T300 LAMINATES.
GC ANALYSIS OF EVOLVED PRODUCTS BY USING A PORAPAK QS COLUMN.

Product	Yield*, mole $\times 10^{-6}$			
	5×10^7 rads	10^8 rads	5×10^8 rads	10^9 rads
H ₂	6.65	17.1	78.2	48.9
CH ₄	0.015	0.025	0.15	0.58
CO	0.43	0.66	4.87	10.2
CO ₂	0.80	1.07	2.40	4.33
C ₂ H ₆	0.0013	0.0042	0.017	0.061
C ₃ H ₈	absent	0.0015	0.0090	0.043
SO ₂	0.053	not detected	0.043	not detected

* Weight of exposed samples, 5.83g (45.1%-wt resin)

Table 20

ELECTRON IRRADIATION OF 5208/T300 LAMINATES.
GC ANALYSIS OF EVOLVED PRODUCTS BY USING A PORAPAK QS COLUMN.

Product	Yield*, moles $\times 10^{-6}$			
	5×10^7 rads	10^8 rads**	5×10^8 rads	10^9 rads
H ₂	3.2	-	18.5	190
CH ₄	0.03	-	0.077	1.42
CO	1.76	-	3.22	28.5
CO ₂	6.18	-	17.1	13.5
C ₂ H ₆	absent	-	absent	0.13
C ₃ H ₈	absent	-	absent	0.067
SO ₂	0.017		not detected	not detected

* Weight of exposed samples, 4.47g (52.8%-wt resin)

** Leaking valve, gas sample was not analyzed.

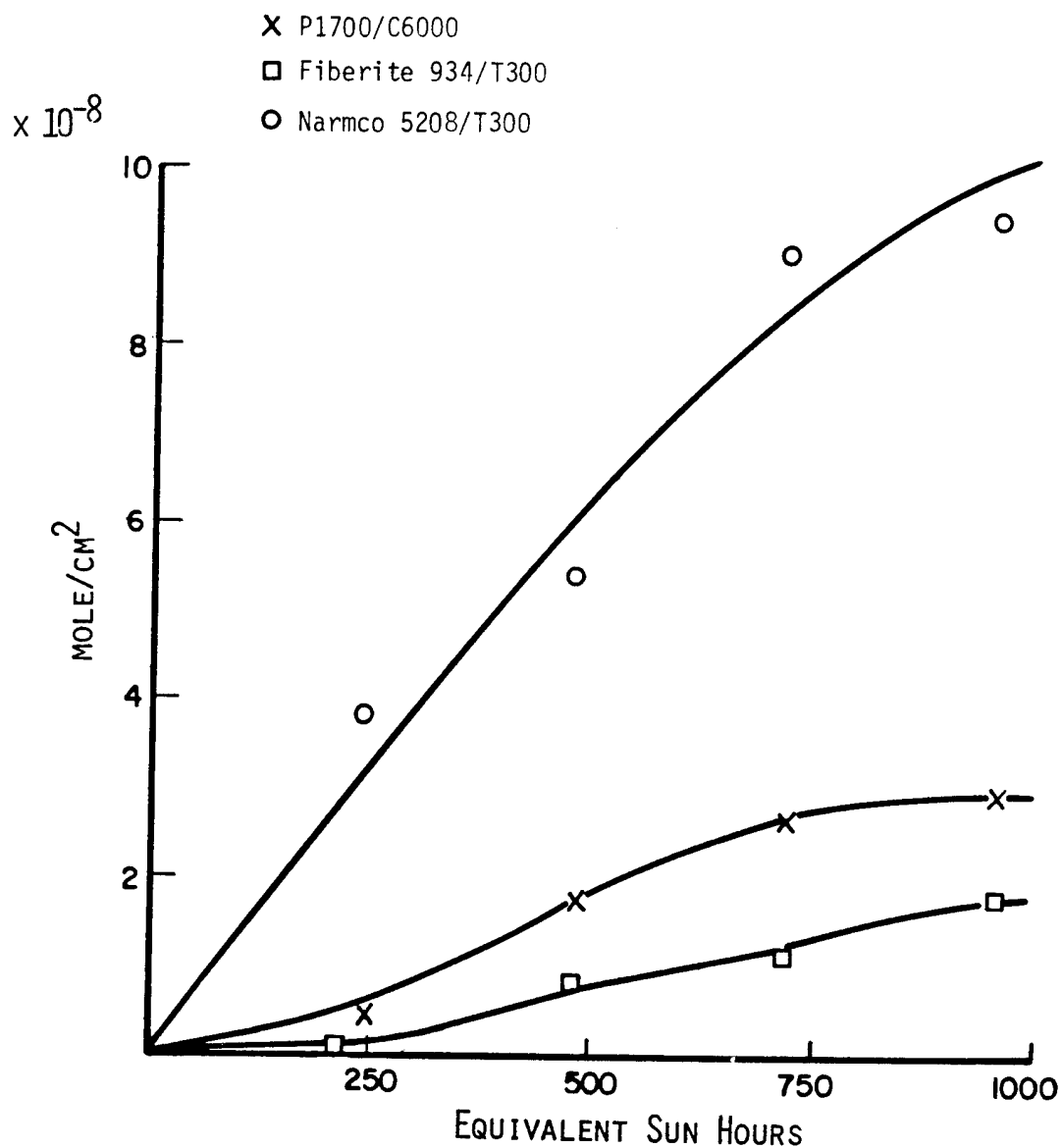


Figure 16. Hydrogen formation during ultraviolet radiation exposure.

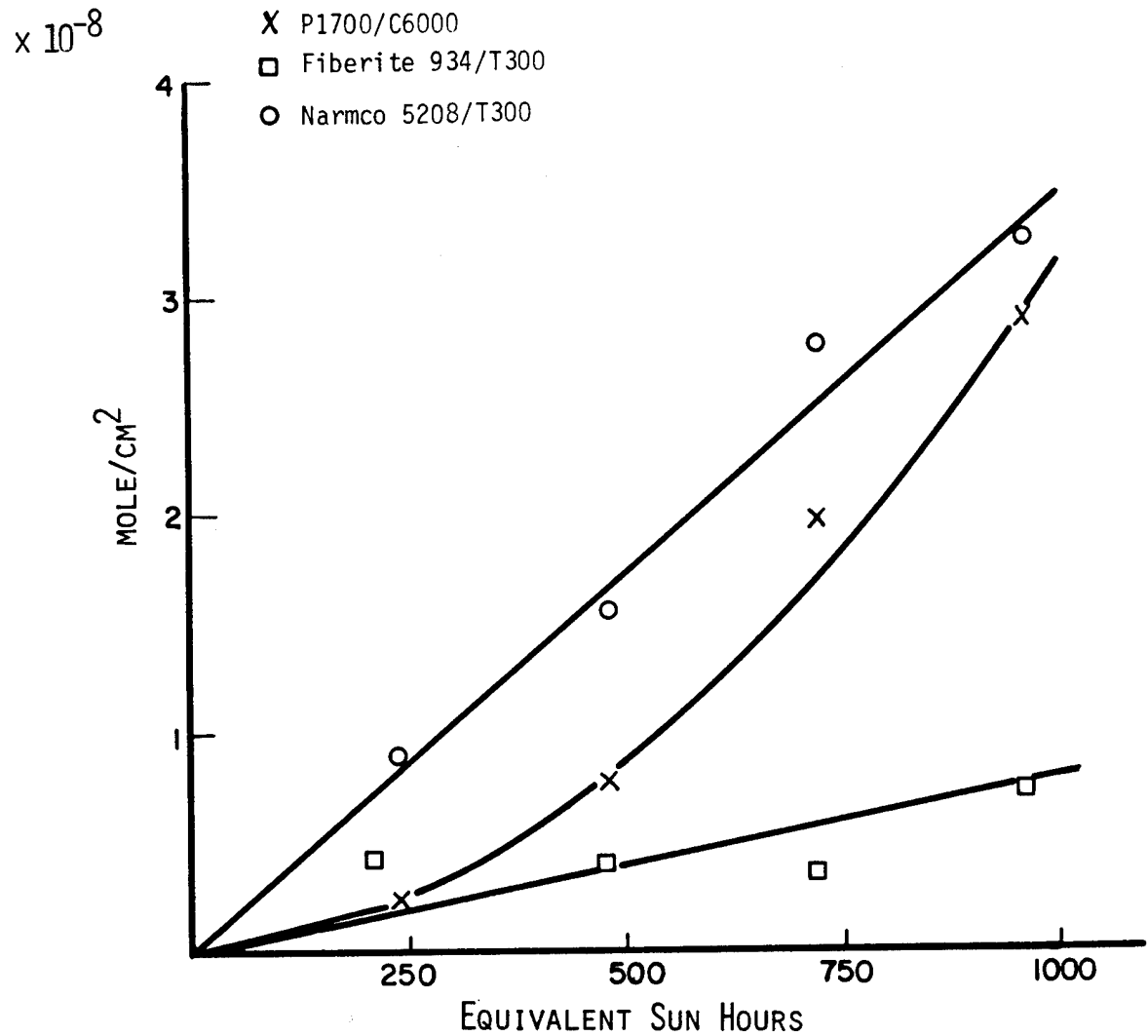


Figure 17. Methane formation during ultraviolet radiation exposure.

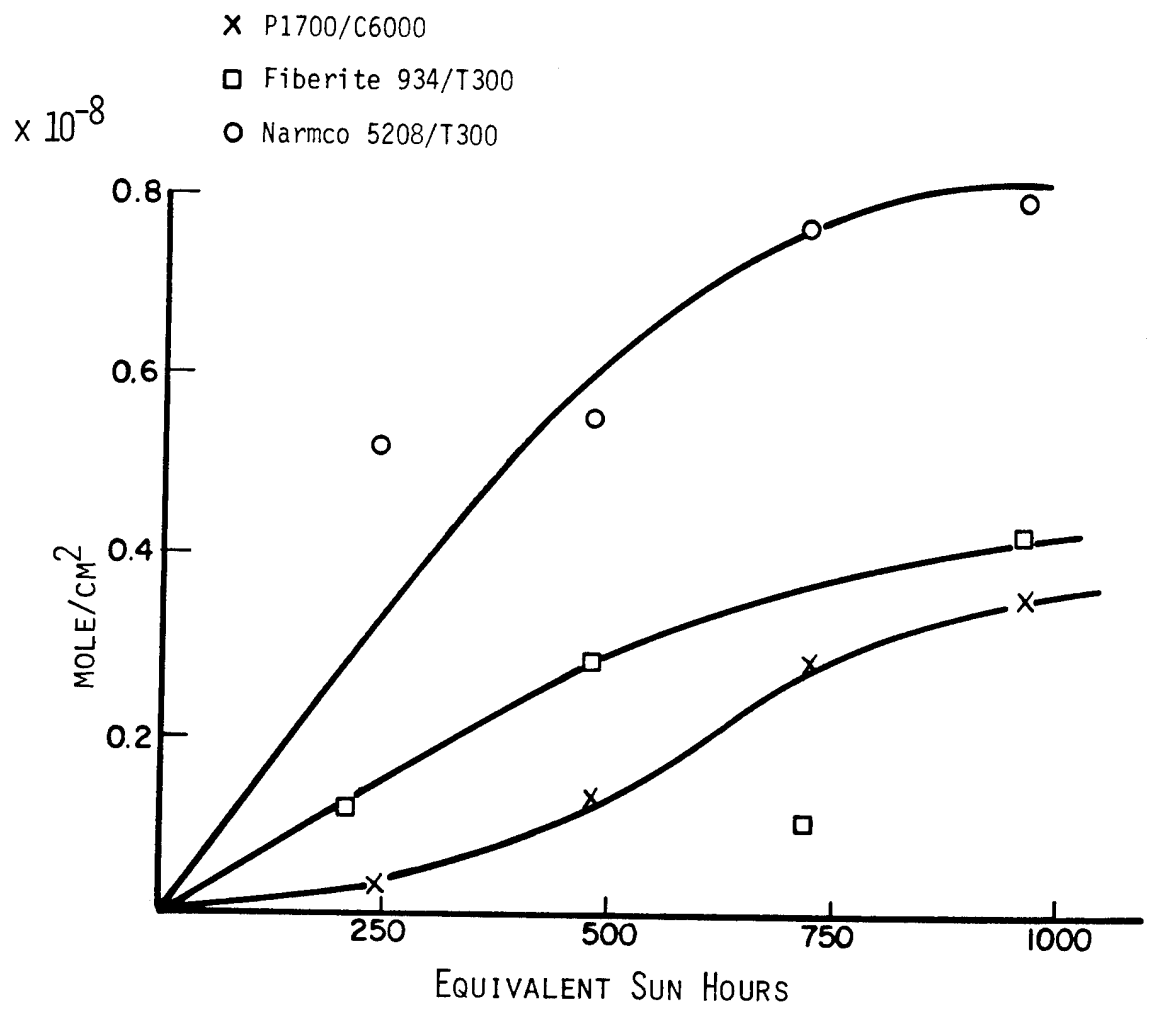


Figure 18. Ethane formation during ultraviolet radiation exposure.

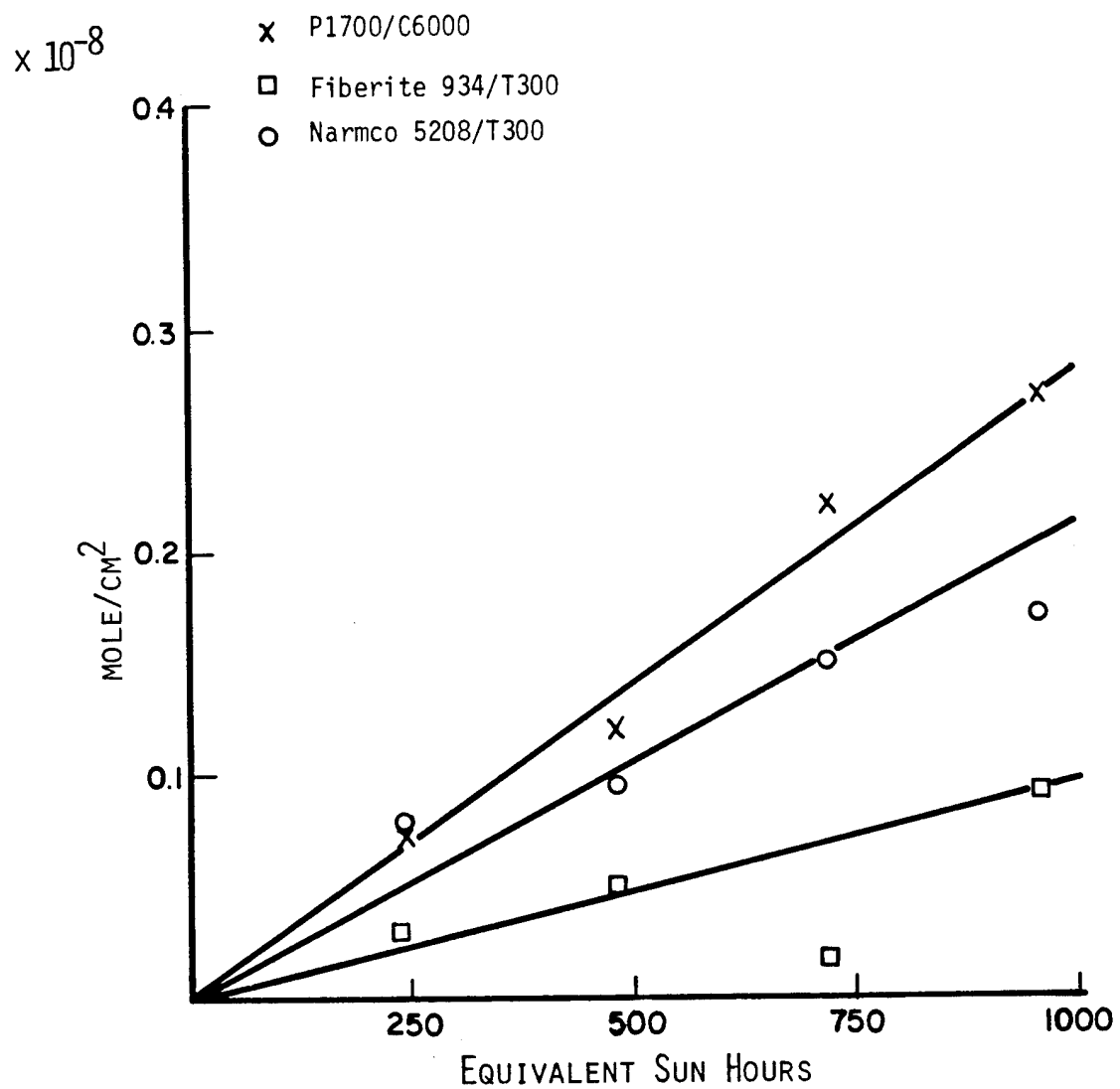


Figure 19. Propane formation during ultraviolet radiation exposure.

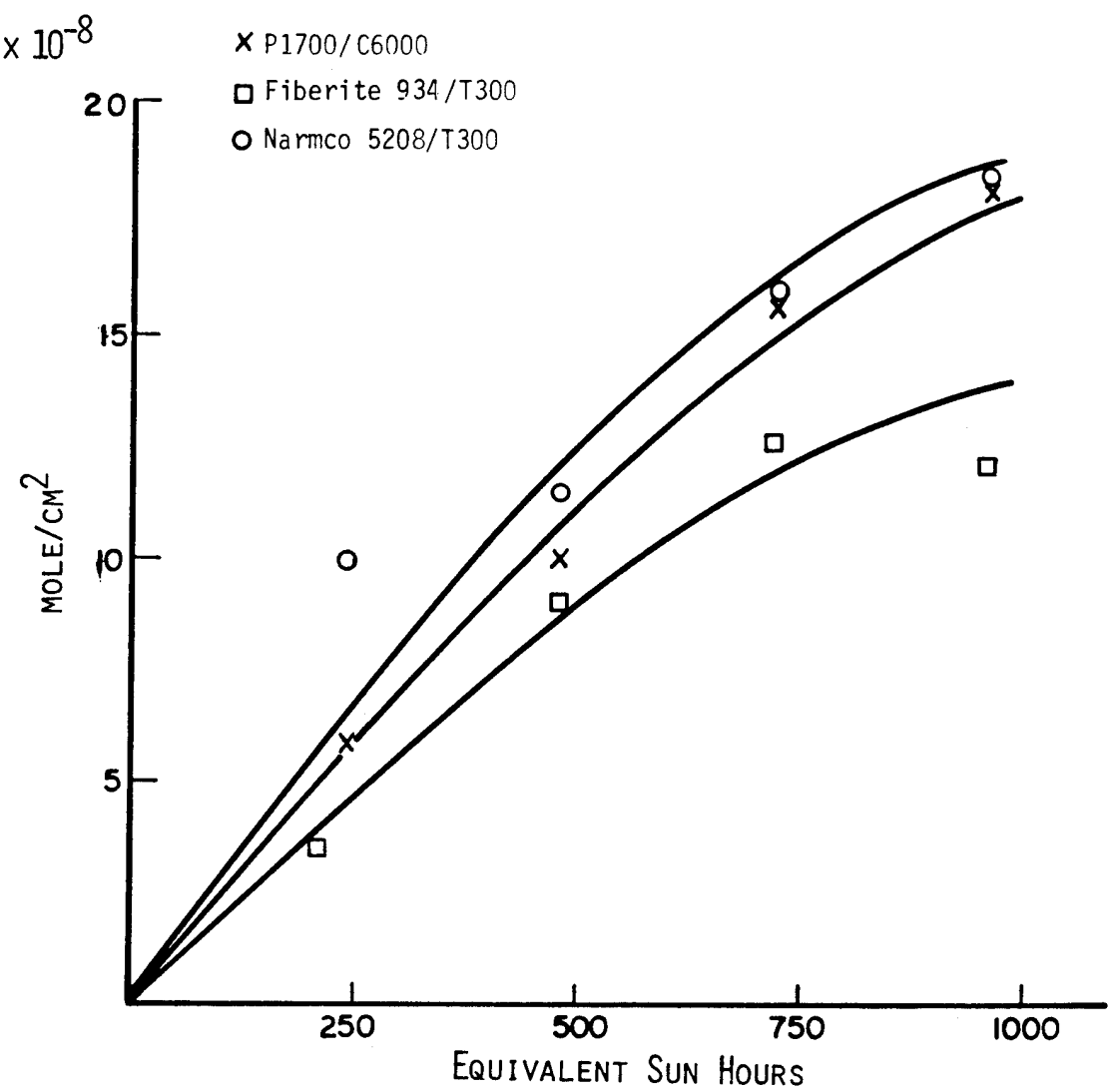


Figure 20. Carbon monoxide formation during ultraviolet radiation exposure.

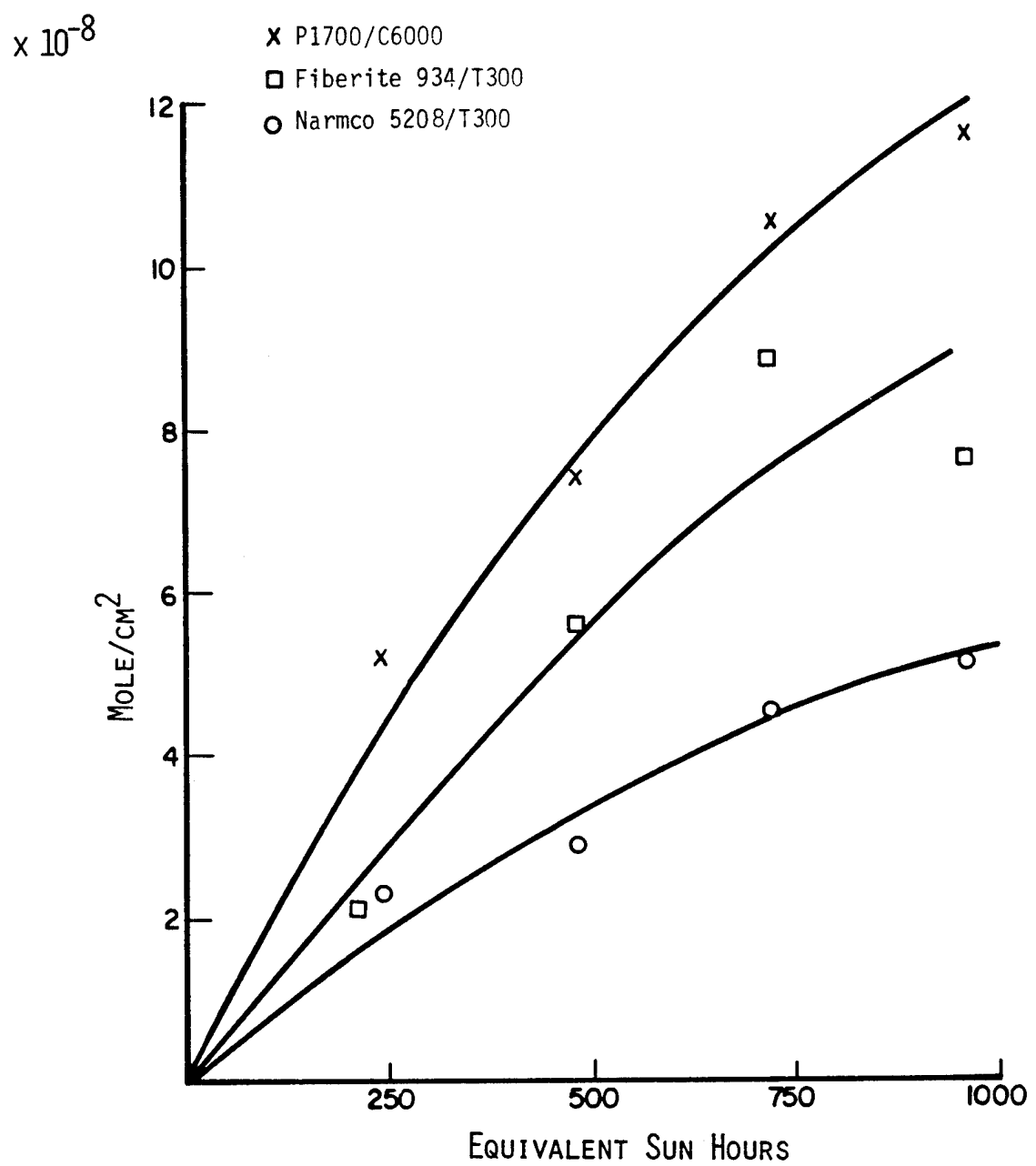


Figure 21. Carbon dioxide formation during ultraviolet radiation exposure.

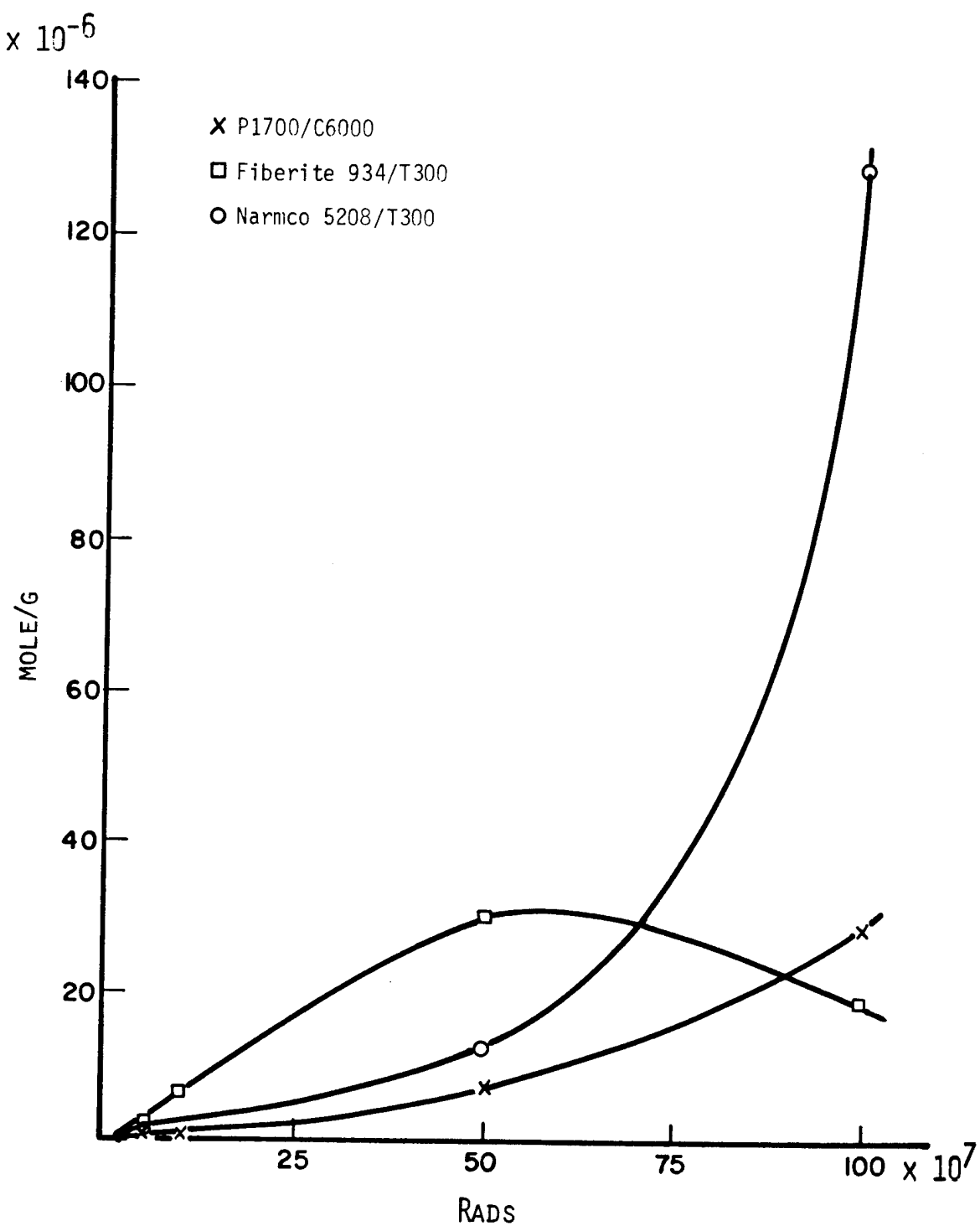


Figure 22. Hydrogen formation during electron radiation exposure.

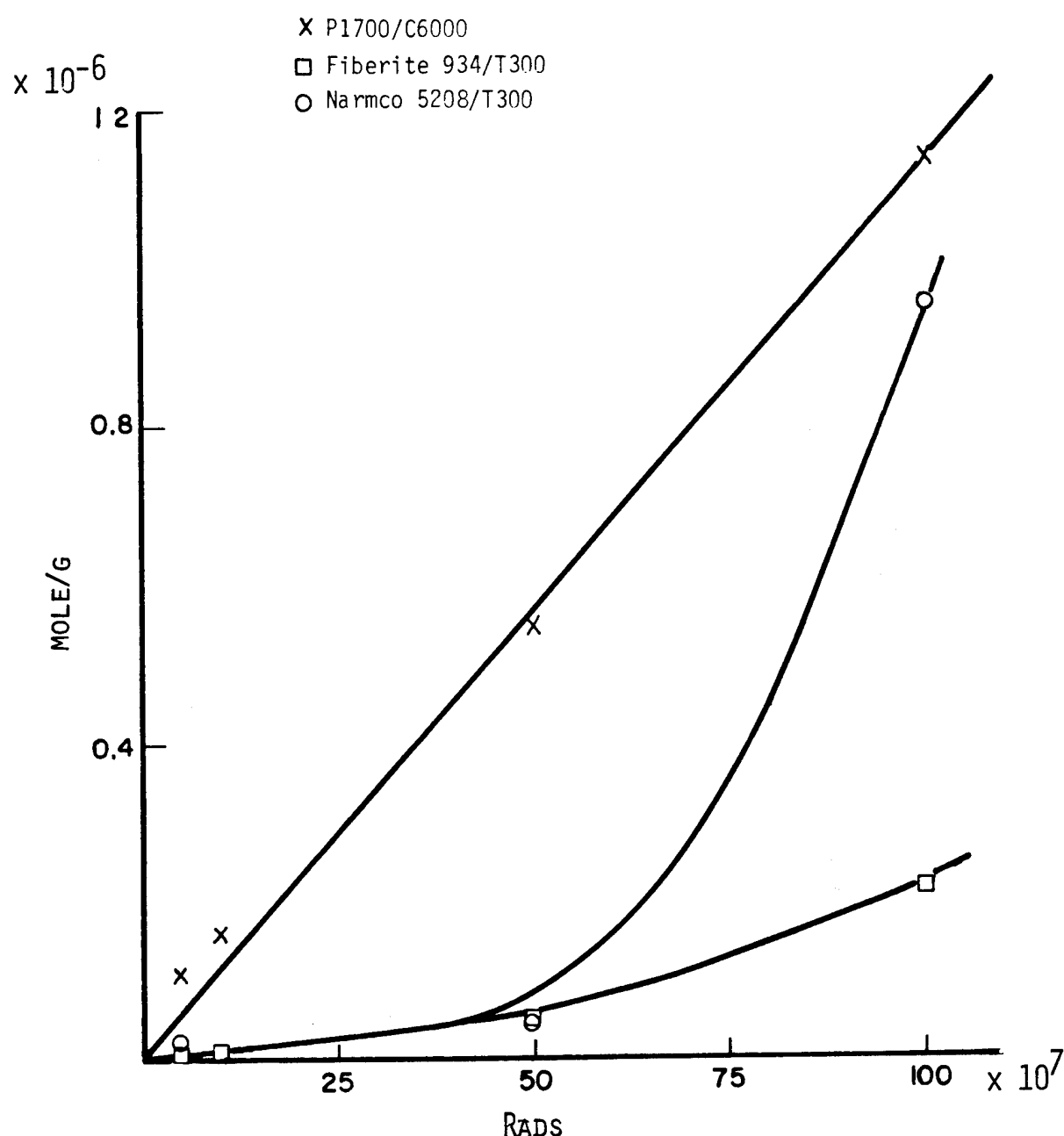


Figure 23. Methane formation during electron radiation exposure.

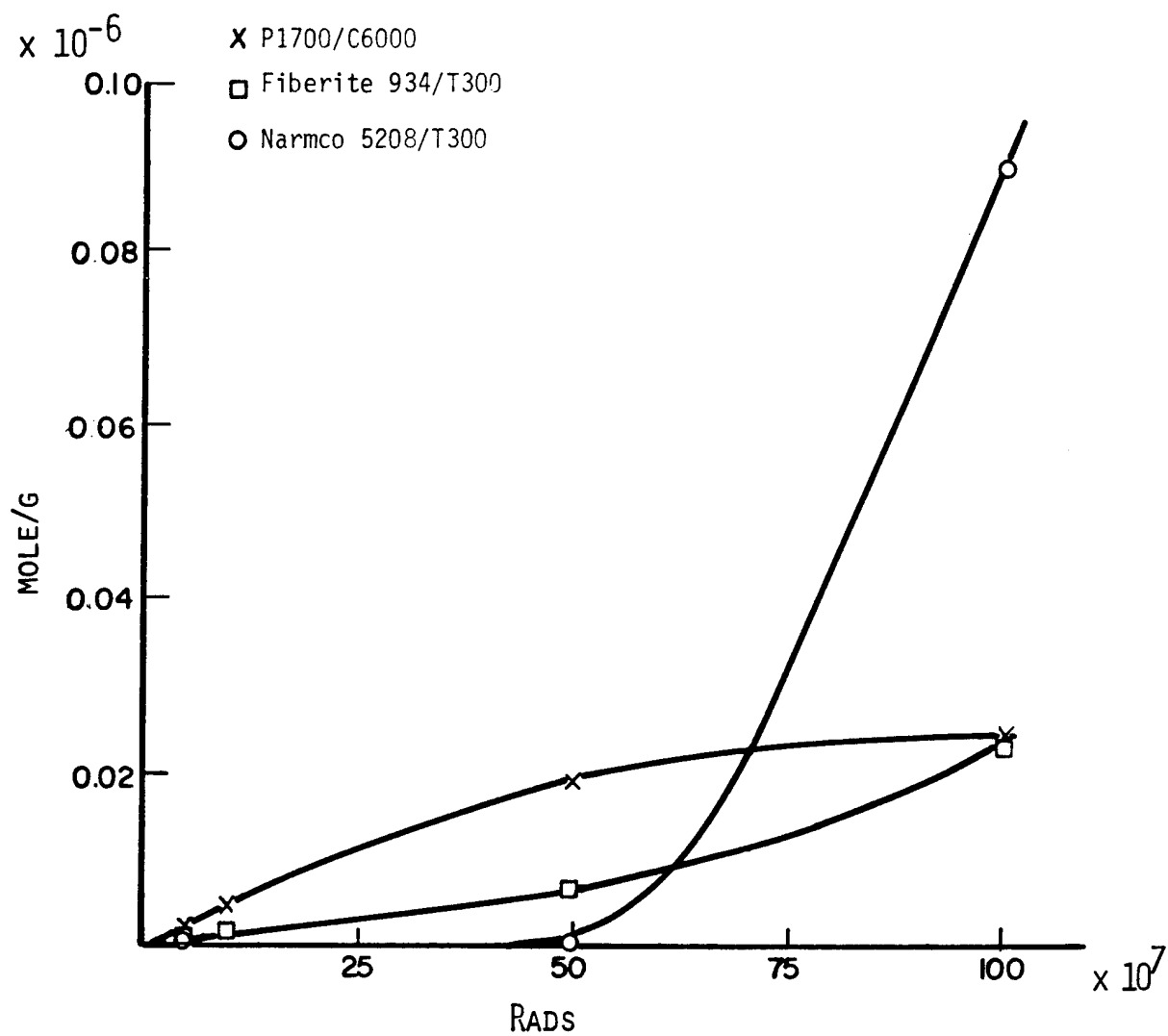


Figure 24. Ethane formation during electron radiation exposure.

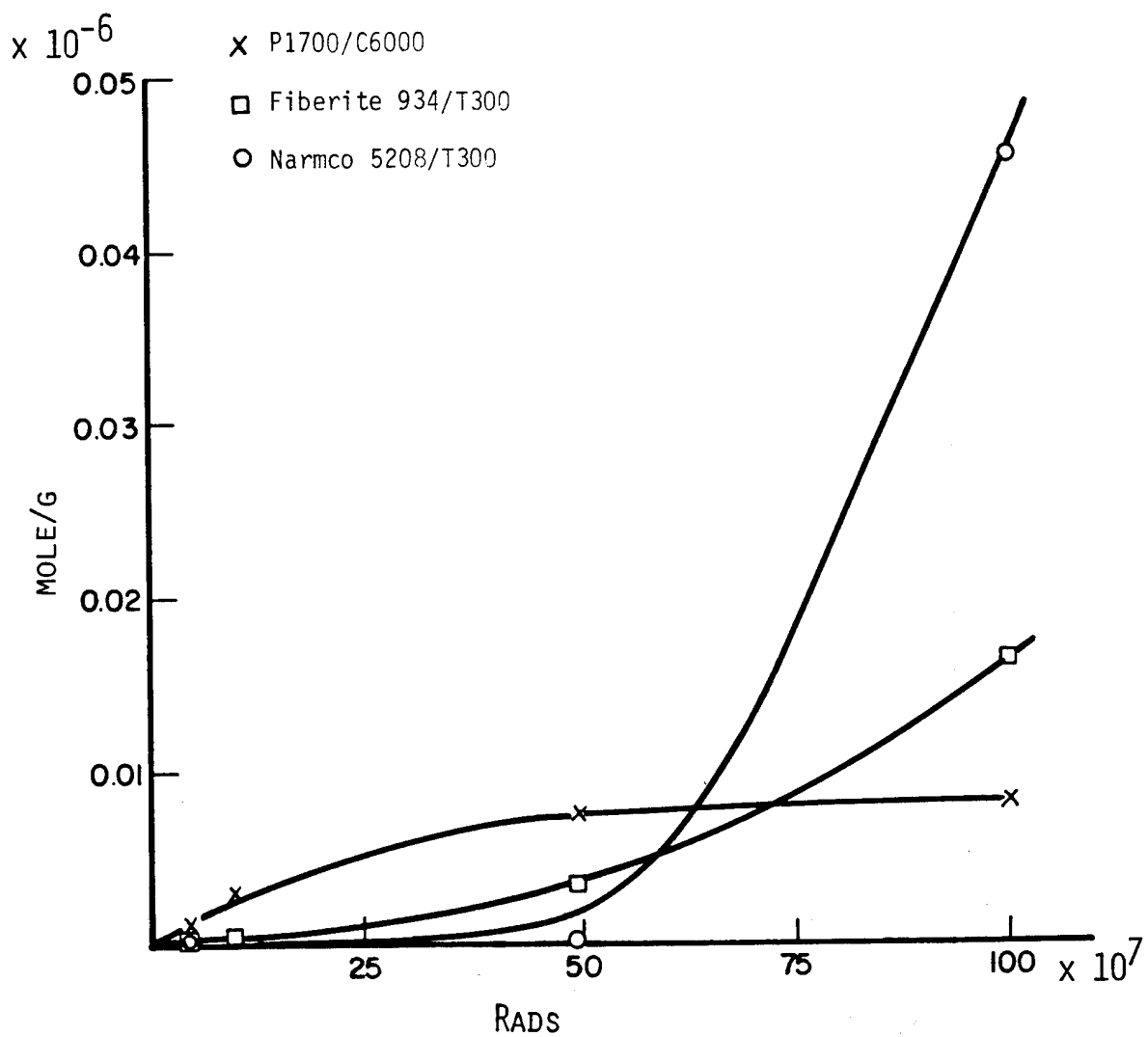


Figure 25. Propane formation during electron radiation exposure.

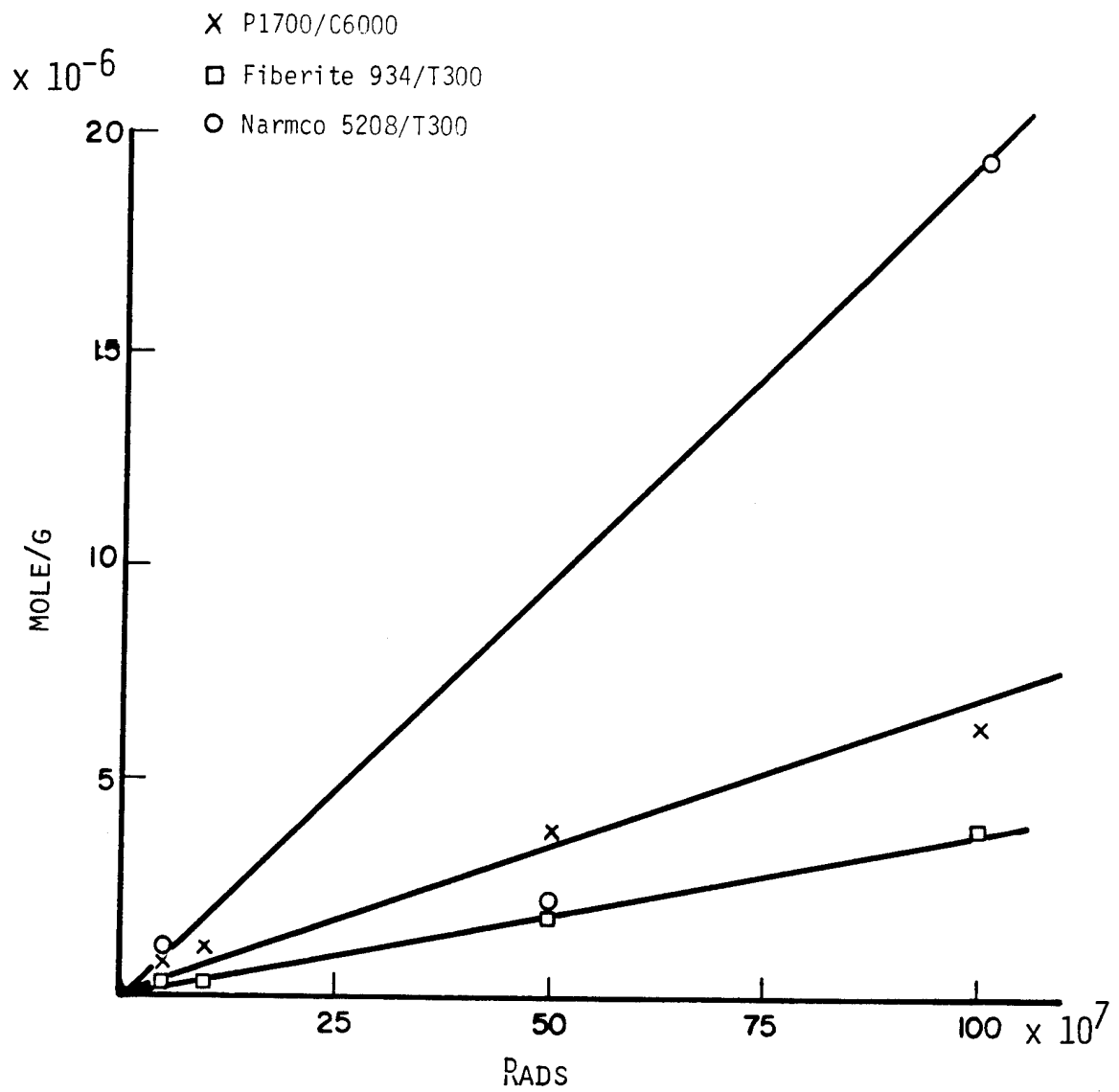


Figure 26. Carbon monoxide formation during electron radiation exposure.

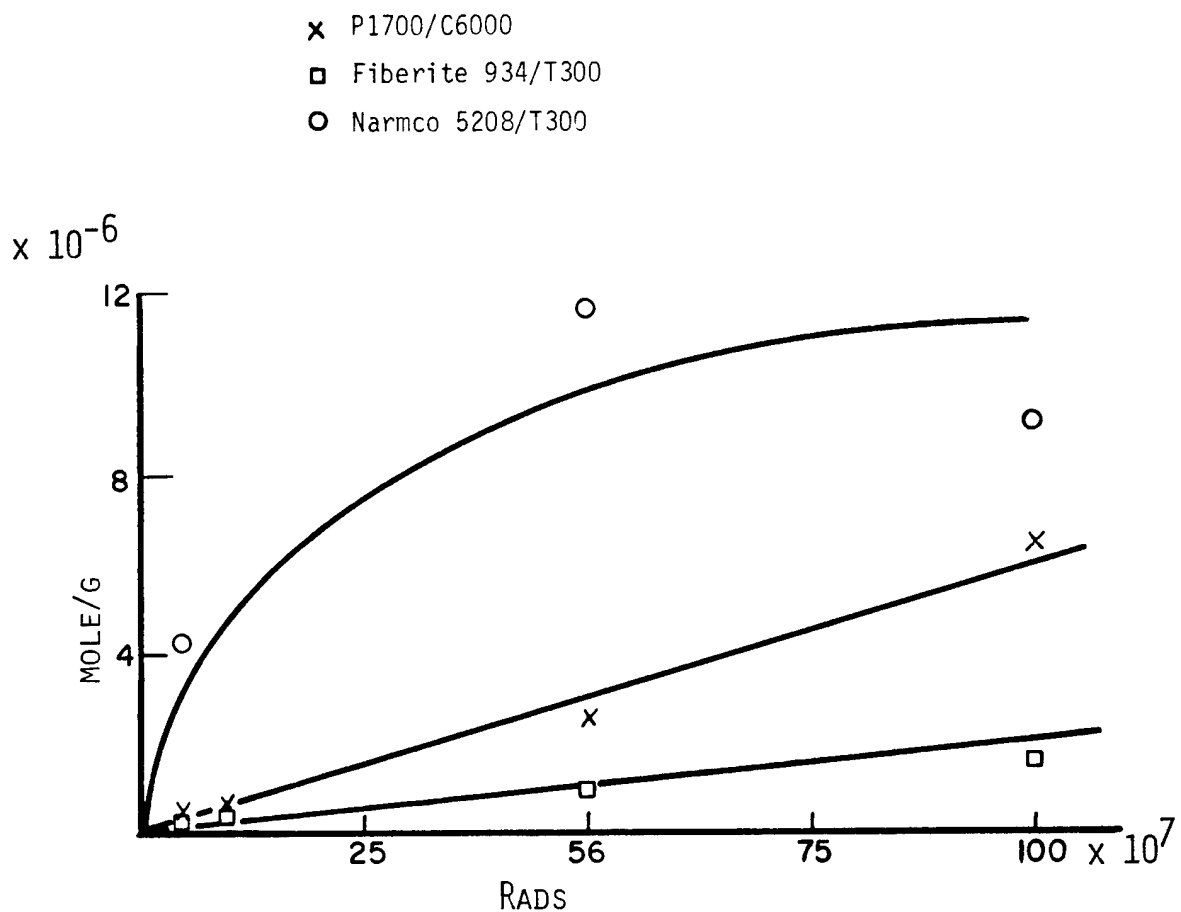


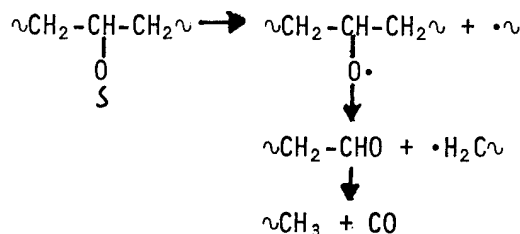
Figure 27. Carbon dioxide formation during electron radiation exposure.

glycidyl groups of MY720 are believed to be mainly responsible for the formation of hydrogen and low molecular weight hydrocarbons.

Initial G values and quantum yields for gas formation are reported in Table 21. Initial values are more significant than average values, since the gas evolved from the samples is retained in the exposure tubes and may undergo further reactions. It is interesting to compare the G values for H₂ and CH₄ for the three laminates tested. These G values can be related to the presence of isopropylidene units (bisphenol-A) in the matrix resins, and show that methane is more readily formed when bisphenol-A is present due to the energetically favored elimination of CH₃· radicals from the isopropylidene units followed by hydrogen abstraction. (Hydrogen abstraction is favored over CH₃· radical recombination, as indicated by the fact that yield of methane is always higher than that of ethane). The concentration of isopropylidene units (due to bisphenol-A) decreases in order P1700>5208>934. In the same order, G_{H₂} increases (from 9.3 to 24.9 to 48.6) and G_{CH₄} decreases (from 2.1 to 0.13 to 0.11). However, this trend is not apparent for the quantum yields of ultraviolet exposed sample.

With the exception of the oxides of carbon, H₂ is by far the predominant product of electron irradiation (on a molar basis), particularly in the case of Fiberite 934 and Narmco 5208, for which G_{CH₄} is low. In the case of ultraviolet irradiation, H₂ and CH₄ are both important products.

High yields of CO and CO₂ have been found for all samples exposed to ultraviolet and electron irradiation. Likewise, high yields of CO and CO₂ have been reported by Gesner and Kelleher⁴ for ultraviolet irradiation of polysulfone in a vacuum. A possible mechanism of CO formation from P1700 has been discussed previously for Fiberite 705/60. For epoxy type systems, such as Fiberite 934 and Narmco 5208, CO may arise from the decomposition of alkoxy linkages:



⁴B.D. Gesner and P.G. Kelleher: Thermal and Photo-Oxidation of Polysulfone. J. Appl. Polym. Sci. 12, 1199 (1968).

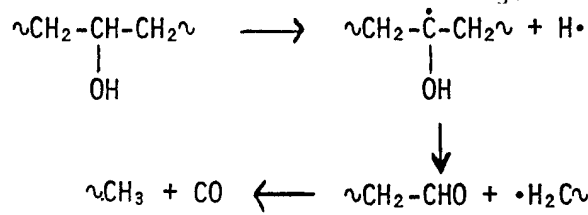
Table 21
INITIAL QUANTUM YIELDS AND G-VALUES FOR MAIN GAS FORMATION

Product	Initial quantum yields*, $\times 10^{-3}$		$P1700/C6000$	$934/T300$	$5208/T300$	$P1700/C6000$	$934/T300$	$5208/T300$	Initial G values**, $\times 10^{-3}$
	$P1700/C6000$	$934/T300$							
H ₂	0.20	0.037		1.11		9.3		48.6	24.9
CH ₄	0.078	0.18		0.33		2.1		0.11	0.13
C ₂ H ₆	0.01	0.05		0.11		0.042		0.012	<10 ⁻³
C ₃ H ₈	0.027	0.013		0.025		0.028		0.0045	<10 ⁻³
CO	1.90	1.47		3.26		10.5		3.1	23.0
CO ₂	1.57	0.92		0.66		6.1		3.9	80.8
C ₆ H ₆	0.002	0.0015		0.026		0.0034		<10 ⁻³	<10 ⁻³
SO ₂	not measured	not measured		0.0027		0.014	not determined	not determined	not determined
Total	3.79	2.67		5.52		28.1		55.7	128

* Molecules formed per photon absorbed in the ultraviolet region. Calculations based on a quantum flux of 1.327×10^{-10} Einsteins/sec cm² in the 200-400 nm range.

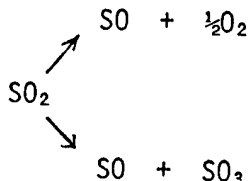
** Molecules formed per 100 eV absorbed. Only the polymer portion of the laminates has been taken into account for the calculations.

A somewhat similar reaction has been proposed⁵ to explain high evolution of CO from a bisphenol-A/epichlorohydrin resin exposed to ultraviolet radiation in vacuum. Another possible mechanism is the following:



Formation of CO₂ in relatively high yields is surprising and cannot be readily explained. Presence of carboxylated groups formed by oxidation during processing is a possible explanation. In the case of Narmco 5208 exposed to electron irradiation, the rate of CO₂ formation was unusually high. These experiments should be repeated to determine whether thermal oxidation during processing was responsible for the high CO₂ yields.

Possible oxidative mechanisms leading to CO₂ formation may arise from oxygen formed by the decomposition of SO₂. SO₂ is known to decompose photochemically and radiochemically according to the following mechanism⁶:



Sulfur monoxide rapidly disproportionates to sulfur and SO₂; likewise, SO₃ decomposed photochemically to SO₂ and O₂:



Reaction of oxygen with aldehydic groups (formed by the mechanisms discussed previously) followed by decarboxylation may lead to CO₂ formation.

⁵B.D. Gesner and P.G. Kelleher: Oxidation of Bisphenol A Polymer, J. Appl. Polym. Sci. 13, 2183 (1969).

⁶"Inorganic Sulfur Chemistry", G. Nickless ed., Elsevier Publ. Co., 1968, p 374.

SO_2 quantification was not positively achieved in this study, mainly due to detector instability and wall absorption and retention of the polar SO_2 . However, the available data indicates that SO_2 is not a major product of UV and electron exposure. Relatively low values for SO_2 formation have been reported by Davis et al.⁷ for electron irradiation and by Gesner and Kelleher⁴ for ultraviolet irradiation of polysulfone. Interestingly, SO_2 has been reported to be the major gas product in γ -irradiation^{8,9} and thermal degradation^{10,11} of polysulfone in vacuum.

High quantum yields for gas formation have been determined for the three systems evaluated (Table 21). These values indicate photolytic instability. For comparison, the quantum yields for total gas are of the same order of magnitude as in polystyrene, and about an order of magnitude higher than polymethyl-methacrylate.

G values have been previously reported for polysulfone (clear film). Brown⁸ reported an average G (total gas) of 0.04 for γ -irradiation. Davis⁷ reported an average G (total gas) of 0.01 for electron irradiation. Our value for initial G (total gas) for P1700 is approximately 0.03 (Table 21). G (total gas) are higher for Fiberite 934 and Narmco 5208 (G (total gas) = 0.05 and 0.12 respectively) mainly because of a higher G_{H_2} (and a higher G_{CO_2} for Narmco 5208). However, all values are quite low (for comparison G (total gas) in polystyrene is 5.7), indicating high electron radiation resistance. The lower G (total gas) for P1700 compared to the two epoxy systems indicates greater electron stability of P1700 resin, at least in terms of gas formation. Although, as a rule, higher radiation stability in terms of gas formation is reflected in higher radiation stability in terms of mechanical properties, this may not be true in this case, because P1700 is a linear polymer and its mechanical properties are likely to be more sensitive to molecular changes than Narmco 5208 and Fiberite 934 which are highly cross-linked thermosets.

⁷A. Davis, M.H. Gleaves, J.H. Golden and M.S. Huglin: The Electron Irradiation Stability of Polysulphone., Makromol. Chem. 129, 63 (1969).

⁸J.R. Brown and J.H. O'Donnell: Effect of Gamma Radiation on Two Aromatic Polysulfones, J. Appl. Polym. Sci. 19, 405 (1975).

⁹J.R. Brown and J.H. O'Donnell: Effects of Gamma Radiation on Two Aromatic Poly-sulfones. II. A Comparison of Irradiation at Various Temperatures in Air-Vacuum Environment, J. Appl. Polym. Sci. 23, 2763 (1979).

¹⁰A. Davis, Thermal Stability of Polysulphone, Makromol. Chem. 128, 242 (1969).

¹¹W.F. Hale, A.G. Farnham, R.N. Johnson and R.A. Clendining: Poly(Aryl Ethers) by Nucleophilic Aromatic Substitution. II. Thermal Stability, J. Polym. Sci. A-1, 5, 2399 (1967).

Results of GC/MS analyses on higher molecular weight compounds condensable at liquid nitrogen temperature are shown in Tables 22-24 and 25-27 for ultraviolet and electron exposed samples respectively. Although a large number of products have been identified, particularly for ultraviolet exposed samples, the majority of these products is present only in trace quantities. These products do not contribute significantly to the total gas yield, and, with the possible exception of benzene and acetone, do not play a significant role in the overall degradation process. However, they contribute toward some understanding of the mechanisms of radiation damage. Although a much greater variety of compounds were identified from ultraviolet exposed samples, there are remarkable similarities between the products obtained with ultraviolet and electron irradiation, indicating that similar free radical processes take place. The same observation was made earlier for the products identified by GC with a Porapak column.

A surprisingly large number of linear alkanes up to C₁₆ have been identified, along with alkenes, cycloalkanes and cycloalkenes. These compounds indicate that, although radiation attack of the benzene ring relative to the aliphatic portion of the polymers is not favored, decomposition of the benzene ring does take place under ultraviolet and electron irradiation. Hydrogen abstraction from the benzene ring is not energetically favored and is unlikely to occur. Phenyl radicals are certainly formed by main chain cleavage, but they are not expected to lead to decomposition of the ring. The most likely explanation is an attack of the benzene ring by hydrogen atoms to form cyclohexadienyl radicals:



Formation of cyclohexadienyl radicals has been conclusively demonstrated by Lyons¹² in a ESR study of γ -irradiated polysulfone, in which cyclohexadienyl radicals were detected together with phenoxy and phenylsulfone radicals. From cyclohexadienyl radicals, cycloalkenes and cycloalkanes can be readily formed by subsequent hydrogen attack. Quenching of cyclohexadienyl radicals may lead

¹²A.R. Lyons, M.C.R. Symons and J.K. Yandell: An Electron Spin Resonance Study of the Radiation Damage of Polysulphone, *Makromol. Chem.* 157, 103 (1972).

Table 22. Ultraviolet irradiation of P1700/C6000 Laminates. GC/MS analysis of evolved products by using OV-101 column. Surface area of exposed laminate samples, 43.1 cm²

TOTAL DOSE (ESH)		240		480		720		960	
TYPE OF COMPOUND	Formula	mole x10 ⁻¹⁰	g x10 ⁻⁸						
Alkanes, open chain									
2-methylpropane	C ₄ H ₁₀					4.48	2.59	7.38	4.28
n-butane	C ₄ H ₁₀	19.3	11.2	74.0	42.9	130	75.7	not resolved	
2-methylbutane	C ₅ H ₁₂			5.23	3.77	2.43	1.75	not resolved	
n-pentane	C ₅ H ₁₂	13.2	9.51	226	163	113	81.3	25.0	18.0
n-hexane	C ₆ H ₁₄	2.01	1.74	8.08	6.95	22.0	19.0	38.8	33.4
2-methylhexane	C ₇ H ₁₆			1.68	1.69	2.08	2.08	5.22	5.11
branched alkane	C ₈ H ₁₈			0.85	0.97			2.19	2.49
n-heptane	C ₇ H ₁₆	2.12	2.12	12.9	12.9	19.8	19.9	38.7	38.7
n-octane	C ₈ H ₁₈	1.22	1.39	4.75	5.42	12.4	14.1	20.1	23.0
branched alkane	C ₉ H ₂₀	0.20	0.26	1.40	1.79	1.02	1.16	2.87	3.68
n-nonane	C ₉ H ₂₀	1.36	1.74	5.20	6.66	12.5	16.1	16.4	21.1
n-decane	C ₁₀ H ₂₂	0.22	0.30	0.83	1.20	2.63	3.75	4.6	6.54
branched alkane	C ₁₀ H ₂₂					0.39	0.55	0.32	0.46
n-undecane	C ₁₁ H ₂₄	0.40	0.65	1.19	3.21	5.73	8.94	7.3	11.4
branched alkane	C ₁₁ H ₂₄			0.11	0.18	0.44	0.69	0.73	1.14
n-dodecane	C ₁₂ H ₂₆					0.30	0.50	0.35	0.61
branched alkane	C ₁₂ H ₂₆					0.23	0.39	0.12	0.21
n-tridecane	C ₁₃ H ₂₈	0.14	0.25			1.73	3.17	0.70	1.29
branched alkane	C ₁₃ H ₂₈					0.06	0.11		
n-tetradecane	C ₁₄ H ₃₀					0.19	0.39		
branched alkane	C ₁₄ H ₃₀					0.11	0.23		
n-pentadecane	C ₁₅ H ₃₂					0.32	0.63		
Alkenes, open chain									
1-butene or 2-methylpropene	C ₄ H ₈	10.7	6.01	59.6	33.4	52.3	29.3	68.5	38.4
2-butene	C ₄ H ₈			5.55	3.11	20.0	11.2	9.38	5.25
1-pentene (or ethylcyclopropane)	C ₅ H ₁₀	217	152	232	163	79.3	55.4	202	141
methylbutene	C ₅ H ₁₀			1.94	1.36			0.70	0.49
2-pentene (or 2-Me-2-butene)	C ₅ H ₁₀			1.93	1.35	34.3	24.0		
2-hexene	C ₆ H ₁₂			0.23	0.20	1.03	0.86	1.40	1.17
1-hexene	C ₆ H ₁₂	1.76	1.48	1.11	0.94	4.01	3.38	7.09	5.96

Table 22. (con't.)

TOTAL DOSE (ESH)		240		480		720		960	
TYPE OF COMPOUND	Formula	mole x10 ⁻¹⁰	g x10 ⁻⁸						
2-heptene	C ₇ H ₁₄					0.71	0.70	2.06	2.02
1-heptene	C ₇ H ₁₄	8.90	8.72	7.45	7.31	15.0	14.7	14.4	14.1
4-methyl-2-hexene	C ₇ H ₁₄					0.22	0.21		
2-or 3-methyl-2-hexene	C ₇ H ₁₄	1.15	1.13	0.55	0.53	0.95	0.93	1.30	1.27
1-octene	C ₈ H ₁₆	0.36	0.41	0.28	0.32	1.93	2.16	1.84	2.07
1-nonene	C ₉ H ₁₈	3.35	4.22	2.32	2.92	2.89	3.65	2.64	3.33
t-butylcyclohexene	C ₁₀ H ₁₈					0.27	0.38		
<u>Alkanes, cyclic</u>									
cyclobutane	C ₄ H ₈	3.66	2.06	10.3	5.78	20.9	11.7	39.5	22.1
ethylcyclopropane (or 1-pentane)	C ₅ H ₁₀	217	152	232	163	79.3	55.4	202	141
dimethylcyclopropane	C ₅ H ₁₀	12.8	8.96	23.4	19.9	48.3	33.8	82.2	57.5
methylcyclobutane	C ₅ H ₁₀	4.26	2.98	8.94	6.25	8.03	5.62	62.8	44.0
cyclopentane	C ₅ H ₁₀	116	81.0	142	99.7	85.0	59.6	173	121
methylcyclopentane	C ₆ H ₁₂	0.98	0.83	3.98	3.34	12.8	10.7	20.0	16.7
cyclohexane	C ₆ H ₁₂	11.3	9.55	34.6	29.0	85.2	71.6	92.7	78.0
ethylcyclobutane	C ₅ H ₁₂					0.32	0.27		
ethylcyclopentane	C ₇ H ₁₄					0.36	0.35	0.60	0.59
dimethylcyclopentane	C ₇ H ₁₄					0.66	0.65	0.87	0.86
methylcyclohexane	C ₇ H ₁₄					3.43	3.36	5.48	5.37
ethylcyclohexane	C ₈ H ₁₆			0.27	0.31	2.98	3.34	1.24	1.40
trimethylcyclohexane	C ₉ H ₁₈	0.42	0.53			0.43	0.54	0.27	0.34
methylethylcyclohexane	C ₉ H ₁₈					0.59	0.74	0.58	0.73
isopropylcyclohexane	C ₉ H ₁₈					0.38	0.49		
sec-butylcyclohexane	C ₁₁ H ₂₂					0.16	0.26	0.29	0.41
n-pentylcyclohexane	C ₁₁ H ₂₂					0.16	0.26	0.26	0.41
<u>Alkenes, cyclic</u>									
cyclopentene	C ₅ H ₈	2.92	1.98	3.86	2.62	7.65	5.20	9.84	6.69
methylcyclopentene	C ₆ H ₁₀	0.59	0.49	0.49	0.40	3.17	2.60	3.74	3.06
cyclohexene	C ₆ H ₁₀	63.9	52.4	63.2	51.8	128	104	123	101
4-methylcyclohexene	C ₇ H ₁₂	2.46	2.37						

Table 22. (con't.)

TOTAL DOSE (ESH)		240	480	720	960		
TYPE OF COMPOUND	Formula	mole x10 ⁻¹⁰	g x10 ⁻⁸	mole x10 ⁻¹⁰	g x10 ⁻⁸	mole x10 ⁻¹⁰	g x10 ⁻⁸
methylenecyclohexane	C ₇ H ₁₂	0.09	0.09	0.12	0.12	0.72	0.72
1-or 3-methylcyclohexene	C ₇ H ₁₂			1.15	1.11	3.38	3.25
t-butylcyclohexene	C ₁₀ H ₁₈			0.16	0.22		0.50
cyclohexylpent-2-ene	C ₁₁ H ₂₀			0.23	0.35	0.57	0.87
<u>Aromatic hydrocarbons</u>							
benzene	C ₆ H ₆	27.3	21.3	74.0	57.7	128	99.8
toluene	C ₇ H ₈	1.36	1.25	6.06	5.57	18.6	17.1
ethylbenzene	C ₈ H ₁₀	39.6	42.0	42.0	44.5	78.6	83.3
xylene	C ₈ H ₁₀	124	131	143	151	155	164
isopropylbenzene	C ₉ H ₁₂	0.26	0.32	0.53	0.64	2.17	2.60
n-propylbenzene	C ₉ H ₁₂					0.52	0.64
ethyltoluene	C ₉ H ₁₂					2.16	2.60
trimethylbenzene	C ₉ H ₁₂					0.97	1.17
n-butylbenzene	C ₁₀ H ₁₄					0.07	0.09
naphthalene	C ₁₀ H ₈					0.08	0.11
n-pentylbenzene	C ₁₁ H ₁₆					6.79	10.0
cyclohexylbenzene	C ₁₂ H ₁₆					0.05	0.08
<u>Aldehydes and ketones</u>							
acetone	C ₃ H ₆ O	120	70.0	4.54	2.64	32.2	18.7
cyclobutanone	C ₄ H ₆ O			2.09	1.46		
methacrylaldehyde	C ₄ H ₆ O					78.7	55.1
methylcyclopentanone	C ₆ H ₁₀ O	0.67	0.66			1.17	1.15
cyclohexanone	C ₆ H ₁₀ O	51.1	59.8	2.72	2.67	67.6	66.3
<u>Esters</u>							
cyclohexylacetate	C ₈ H ₁₄ O ₂					0.95	1.36
cyclohexylhexanoate	C ₁₂ H ₂₂ O ₂					0.87	1.72
<u>Alcohols, ethers and related compounds</u>							
methanol	CH ₄ O	3.49	1.12	4.78	1.53		

Table 22. (con't.).

TOTAL DOSE (ESH)		240	480	720	960				
TYPE OF COMPOUND	Formula	mole x10 ⁻¹⁰	g x10 ⁻⁸						
ethanol	C ₂ H ₆ O			2.50	1.15			1.01	0.46
tetrahydro-2-methylpyran	C ₆ H ₁₂ O	0.09	0.09	0.21	0.21	1.34	1.34	1.92	1.92
1-pentanol	C ₅ H ₁₂ O			0.41	0.36	1.00	0.87	2.53	2.22
cyclopentenediol	C ₅ H ₈ O ₂					12.4	12.4		
phenylether	C ₁₂ H ₁₀ O					0.05	0.09		
oxybiscyclohexane	C ₁₂ H ₂₂ O	0.10	0.18			0.63	1.06		
<u>Sulfur containing compounds</u>									
carbon disulfide	CS ₂	2.81	2.14	3.77	2.89	3.79	2.88	4.19	3.18
carbonylsulfide	COS			8.20	4.93	3.08	1.84	9.33	5.60
thiophene	C ₄ H ₆ S			1.90	1.61	3.60	3.02	12.6	10.6
2-or 3-methylthiophene	C ₅ H ₆ S			0.28	0.28	0.95	0.93	2.29	2.24
methyleneethylsulfide	C ₃ H ₈ S					0.12	0.09		
cyclobutanethiol	C ₄ H ₈ S					0.12	0.11		
methylthioacetate	C ₃ H ₆ OS					0.10	0.09		
<u>Nitrogen containing compounds</u>									
NONE									
<u>Halogen containing compounds</u>									
chloromethane	CH ₃ Cl	1.17	0.58			2.27	1.14	2.49	1.24
trichloroethylene	C ₂ HC ₁ ₃	0.27	0.36			1.79	2.35	0.45	0.59
chlorobenzene	C ₆ H ₅ Cl	0.92	1.03	1.33	1.50	3.33	3.75	3.58	4.00
tetrachloroethylene	C ₂ Cl ₄					0.84	1.40	0.05	0.08

Table 23. Ultraviolet irradiation of 934/T300 laminates. GC/MS analysis of evolved products by using OV-101 column. Surface area of exposed laminate sample, 56.5 cm².

TOTAL DOSE (ESH)		210		480		720		960	
TYPE OF COMPOUND	Formula	mole x10 ⁻¹⁰	g x10 ⁻⁸						
<u>Alkanes, open chain</u>									
n-butane	C ₄ H ₁₀			3.84	2.23	1.69	0.98	4.70	2.73
n-pentane	C ₅ H ₁₂	0.14	0.10	3.28	2.36	2.36	1.71	5.70	4.10
2-methylpentane	C ₆ H ₁₄							0.92	0.79
3-methylpentane	C ₆ H ₁₄	0.07	0.06	0.16	0.14			0.90	0.77
2,2-dimethylbutane	C ₆ H ₁₄	0.17	0.15	2.71	2.34				
n-hexane	C ₆ H ₁₄	0.86	0.74			1.42	1.22	6.40	5.50
n-heptane	C ₇ H ₁₆	0.99	0.99	3.46	3.46	1.94	1.94	17.4	17.4
3-methylhexane	C ₇ H ₁₆			0.09	0.09			0.41	0.41
2-methylhexane	C ₇ H ₁₆			0.12	0.12			0.52	0.52
branched alkane	C ₇ H ₁₆			0.06	0.06				
branched alkane	C ₈ H ₁₈	0.10	0.12	0.77	0.91			2.25	2.57
n-octane	C ₈ H ₁₈	0.79	0.90	3.79	4.33	0.80	0.91	5.43	6.20
branched alkane	C ₉ H ₂₀			0.31	0.40			0.69	0.88
n-nonane	C ₉ H ₂₀	0.40	0.51	2.63	3.38	0.37	0.48	3.03	3.87
branched alkane	C ₁₀ H ₂₂			0.11	0.16			0.20	0.28
n-decane	C ₁₀ H ₂₂	0.15	0.22	0.68	0.96	0.12	0.18	1.26	1.78
branched alkane	C ₁₁ H ₂₄					0.07	0.10	0.26	0.40
n-undecane	C ₁₁ H ₂₄	0.32	0.50	2.01	3.14	0.99	1.55	5.28	8.25
branched alkane	C ₁₂ H ₂₆			0.03	0.05			0.13	0.23
n-dodecane	C ₁₂ H ₂₆	0.03	0.05	0.06	0.11	0.08	0.14	0.69	1.18
n-tridecane	C ₁₃ H ₂₈	0.22	0.41	0.14	0.26			4.80	8.84
branched alkane	C ₁₃ H ₂₈							0.12	0.23
n-tetradecane	C ₁₄ H ₃₀	0.04	0.08	0.03	0.06			0.63	1.25
branched alkane	C ₁₄ H ₃₀							0.21	0.41
n-pentadecane	C ₁₅ H ₃₂	0.10	0.21	0.05	0.11			1.43	3.05
<u>Alkenes, open chain</u>									
propene (tentative)	C ₃ H ₆	8.24	3.46			35.4	14.8	2.59	1.45
butene or 2-methylpropene	C ₄ H ₈	3.12	1.75	1.65	0.93	8.61	4.82		
1-pentene	C ₅ H ₁₀	0.71	0.50	0.65	0.46			0.40	0.28

Table 23. (con't.)

TOTAL DOSE (ESH)		210		480		720		960	
TYPE OF COMPOUND	Formula	mole x10 ⁻¹⁰	g x10 ⁻⁸						
1-hexene	C ₆ H ₁₂	0.71	0.60	0.55	0.47	0.20	0.17	0.55	0.45
1-heptene	C ₇ H ₁₄	0.40	0.40	0.41	0.40	0.08	0.08	0.79	0.77
2-heptene	C ₇ H ₁₄							0.21	0.20
octene	C ₈ H ₁₆	0.12	0.13	0.21	0.23			0.34	0.37
nonene	C ₉ H ₁₈	0.04	0.05	0.09	0.12	0.45	0.57	0.05	0.07
decene	C ₁₀ H ₂₀					0.16	0.23		
undecene	C ₁₁ H ₂₂							0.04	0.07
dodecene	C ₁₂ H ₂₄					0.11	0.18	0.08	0.14
<u>Alkanes, cyclic</u>									
cyclobutane	C ₄ H ₈			0.14	0.08				
methylcyclobutane	C ₅ H ₁₀							0.31	0.21
methylcyclopentane	C ₆ H ₁₂	0.07	0.06	0.19	0.16			0.51	0.43
cyclohexane	C ₆ H ₁₂	0.36	0.30	1.81	1.52	0.15	0.13	2.24	1.88
methylcyclohexane	C ₇ H ₁₄	0.06	0.06					0.35	0.34
dimethylcyclopentane	C ₈ H ₁₄			0.12	0.12				
ethylcyclopentane	C ₇ H ₁₄							0.10	0.10
<u>Alkenes, cyclic</u>									
cyclohexene	C ₆ H ₁₀	0.22	0.18	0.24	0.20			0.15	0.12
<u>Aromatic hydrocarbons</u>									
benzene	C ₆ H ₆	20.2	15.7	84.7	66.1	40.2	31.4	55.3	43.1
toluene	C ₇ H ₈	0.18	0.17	3.38	3.10	0.53	0.50	6.90	6.35
ethylbenzene	C ₈ H ₁₀			0.15	0.16	0.28	0.30	0.29	0.31
xylene	C ₈ H ₁₀			0.08	0.09			0.11	0.12
<u>Aldehydes and ketones</u>									
acetone	C ₃ H ₆ O	1.48	0.86	10.8	6.25	18.3	10.6	12.3	7.14
2-pentanone	C ₅ H ₁₂ O	0.31	0.27					0.07	
unidentified aldehyde									

Table 23. (con't.)

TOTAL DOSE (ESH)		210	480	720	960		
TYPE OF COMPOUND	Formula	mole x10 ⁻¹⁰	g x10 ⁻⁸	mole x10 ⁻¹⁰	g x10 ⁻⁸	mole x10 ⁻¹⁰	g x10 ⁻⁸
methyl ethyl ketone	C ₄ H ₈ O				0.66	0.47	
acetophenone	C ₈ H ₈ O				0.28	0.34	
<u>Esters</u>							
methyl acetate	C ₃ H ₆ O ₂			1.14	0.85	19.6	14.5
ethyl formate	C ₃ H ₆ O ₂			3.68	2.72		1.30
isopropyl formate	C ₄ H ₈ O ₂					0.81	0.72
n-propyl formate	C ₄ H ₈ O ₂					1.02	0.89
methyl propionate	C ₄ H ₈ O ₂					2.05	1.80
methyl n-butanoate	C ₅ H ₁₀ O ₂					0.09	0.09
methyl benzoate	C ₆ H ₈ O ₂					0.07	0.09
methyl 2-ethyl hexanoate	C ₉ H ₁₈ O ₂						0.07
<u>Alcohols, ethers and related compounds</u>							
methanol	CH ₃ O			0.54	0.17		3.45
ethanol	C ₂ H ₆ O					17.0	7.8
isopropanol	C ₃ H ₈ O					2.32	1.39
methylethylether	C ₃ H ₆ O			9.27	5.56		
furan	C ₄ H ₆ O	0.18	0.12	1.33	0.91		0.61
alcohol, unidentif	C ₄ H ₈ O						0.42
2-methylfuran	C ₅ H ₆ O			0.33	0.27		0.53
2-methyl-1,3-dioxolane	C ₄ H ₈ O ₂						0.24
1-pentanol	C ₅ H ₁₂ O	0.07	0.06			1.39	1.23
<u>Sulfur containing compounds</u>							
carbonylsulfide	COS	15.9	9.53	64.3	38.5	2.94	1.77
dimethylsulfide	C ₂ H ₆ S	1.06	0.65	14.0	8.7	30.0	18.6
dimethyldisulfide	C ₂ H ₆ S ₂	0.06	0.06	1.08	1.01	0.07	0.07
carbodisulfide	CS ₂			1.39	1.06	0.31	0.23
methylethylsulfide	C ₃ H ₈ S			1.00	0.77		1.67
thiophene	C ₄ H ₄ S			0.09	0.08		0.13
methylthioacetate	C ₃ H ₆ OS			0.30	0.27	13.3	12.0
propanethiol	C ₃ H ₆ S					5.43	4.13

Table 23. (con't.)

TOTAL DOSE (ESH)		210	480	720	960				
TYPE OF COMPOUND	Formula	mole x10 ⁻¹⁰	g x10 ⁻⁸	mole x10 ⁻¹⁰	g x10 ⁻⁸	mole x10 ⁻¹⁰	g x10 ⁻⁸	mole x10 ⁻¹⁰	g x10 ⁻⁶
2-methyl-2-butanethiol (or 2-pentane-thiol)	C ₅ H ₁₂ S					0.42	0.45		
methyl n-propylsulfide	C ₄ H ₁₀ S							0.09	0.08
methylthiophene	C ₅ H ₆ S							0.12	0.09
methyl n-propyldisulfide	C ₄ H ₁₀ S ₂							0.07	0.08
<u>Nitrogen containing compounds</u>									
propionitrile	C ₃ H ₅ N					0.34	0.19	0.21	0.11
isopropynitrile	C ₄ H ₇ N					0.06	0.04		
methylcinnoline	C ₉ H ₆ N ₂					0.10	0.15		
<u>Halogen containing compounds</u>									
chloromethane	CH ₃ Cl	0.39	0.20	1.33	0.66	41.5	20.7		
chloroethane	C ₂ H ₅ Cl			0.24	0.15	1.17	0.75		
trichlorotrifluoroethane	C ₂ Cl ₂ F ₃			0.02	0.05	0.11	0.21	0.05	0.10
tetrachloroethylene	C ₂ Cl ₄			0.02	0.05				
vinylchloride	C ₂ H ₃ Cl					4.66	2.89		
dichloromethane	CH ₂ Cl ₂					1.25	1.06		
2-chloropropane	C ₃ H ₇ Cl					3.1	2.46		
1,1,1,3,3-pentafluoro-2,2,3-trichloropropane	C ₃ Cl ₃ F ₅					0.12	0.30		
1,2 dichloroethane	C ₂ H ₄ Cl ₂					0.19	0.19		
dichlorobutane	C ₄ H ₈ Cl ₂					0.09	0.11		
chlorobenzene	C ₆ H ₅ Cl					0.05	0.06		

Table 24. Ultraviolet irradiation of 5208/T300 laminates. GC/MS analysis of evolved products by using OV-101 column. Surface area of exposed laminate sample, 56.5 cm².

TOTAL DOSE (ESH)		240	480	720*	960
TYPE OF COMPOUND	Formula	mole x10 ⁻¹⁰	g x10 ⁻⁸	mole x10 ⁻¹⁰	g x10 ⁻⁸
<u>Alkanes, open chain</u>					
2-methylpropane	C ₄ H ₁₀	12.5	7.27		
n-pentane	C ₅ H ₁₂				106 73
2-methylbutane	C ₅ H ₁₂				6.59 4.74
alkane, unidentified	C ₅ H ₁₂		0.81 0.58		
n-hexane	C ₆ H ₁₄	2.61	2.25	22.1 19.1	25.3 21.8
branched alkane	C ₆ H ₁₄			2.88 2.47	5.75 4.94
branched alkane	C ₇ H ₁₄	1.05	1.05	1.89 1.89	4.04 4.04
n-heptane	C ₇ H ₁₆	4.58	4.58	13.4 13.4	23.3 23.3
2-methylheptane	C ₈ H ₁₈				0.79 0.90
3-methylheptane	C ₈ H ₁₈				4.90 5.60
branched alkane	C ₈ H ₁₈	1.13	1.28	3.68 4.19	
n-octane	C ₈ H ₁₈	2.93	3.34	6.53 7.46	8.44 9.61
branched alkane	C ₉ H ₂₀			0.51 0.66	1.01 1.30
n-nonane	C ₉ H ₂₀	1.38	1.77	2.74 3.50	3.49 4.47
n-decane	C ₁₀ H ₂₂	0.28	0.40	1.14 1.62	0.86 1.22
n-undecane	C ₁₁ H ₂₄	1.50	2.35	2.10 3.27	0.93 1.46
n-dodecane	C ₁₂ H ₂₆	0.25	0.43	0.40 0.68	0.16 0.27
n-tridecane	C ₁₃ H ₂₈	0.42	0.77	0.70 1.29	0.36 0.66
n-tetradecane	C ₁₄ H ₃₀	0.60	1.18	0.40 0.79	0.41 0.81
n-pentadecane	C ₁₅ H ₃₂	0.90	1.91	0.12 0.25	
n-hexadecane	C ₁₆ H ₃₄	0.82	1.84	0.42 0.95	0.43 0.97
<u>Alkenes, open chain</u>					
butene or 2-methylpropene	C ₄ H ₆	10.2	5.75		1.50 0.66
1-pentene	C ₅ H ₁₀	1.53	1.07	6.67 4.67	11.9 8.36
1-hexane or 2-methyl-1-pentene	C ₆ H ₁₂	0.84	0.70		
alkene, unidentified	C ₆ H ₁₂				0.25 0.21
alkene, unidentified	C ₆ H ₁₆				0.42 0.48

*Sample analyzed using a Porapak column to confirm the identity of components detected by GC only

Table 24. (con't.)

TOTAL DOSE (ESH)		240		480		720*		960	
TYPE OF COMPOUND	Formula	mole x10 ⁻¹⁰	g x10 ⁻⁸						
<u>Alkanes, cyclic</u>									
methylcyclopentane	C ₆ H ₁₂	0.59	0.50	1.52	1.28			2.8	2.39
cyclohexane	C ₆ H ₁₂	0.57	0.48	3.31	2.78			8.44	7.08
methylcyclohexane	C ₇ H ₁₄			0.67	0.66			1.17	1.15
<u>Alkenes, cyclic</u>									
cyclopentane	C ₅ H ₈			0.36	0.24				
cyclohexene	C ₆ H ₁₀	0.47	0.38	1.05	0.86			0.40	0.33
<u>Aromatic hydrocarbons</u>									
benzene	C ₆ H ₆	423	332	798	623			675	526
toluene	C ₇ H ₈	6.35	5.84	16.5	15.2			18.5	17.1
ethylbenzene	C ₈ H ₁₀	0.65	0.69	3.18	3.37			0.25	0.26
xylene	C ₈ H ₁₀	4.13	4.36	33.8	23.8			2.28	2.42
<u>Aldehydes and ketones</u>									
acetone	C ₃ H ₆ O	209	121	104	60.4				
<u>Esters</u>									
diethylphthalate	C ₁₂ H ₁₄ O ₄	0.89	1.98	1.36	3.02			0.93	2.06
di-n-butylphthalate	C ₁₆ H ₂₂ O ₄	0.60	1.68					6.90	19.2
<u>Alcohols, ethers and related compounds</u>									
2-methylfuran	C ₅ H ₆ O	0.56	0.46						
paraldehyde	C ₆ H ₁₂ O ₃	16.6	21.9	18.3	22.0				
<u>Sulfur containing compounds</u>									
carbonyl sulfide	COS	5.51	3.31						
carbon disulfide	CS ₂			0.82	0.63			1.32	1.0
dimethylsulfide	C ₂ H ₆ S	25.0	15.5	6.67	4.14			10.9	6.79
methylethylsulfide	C ₃ H ₈ S	1.21	0.92	0.77	0.59			0.63	0.48
thiophene	C ₄ H ₄ S	0.51	0.43	1.55	1.30			1.61	1.35
methyl n-propyl sulfide	C ₄ H ₁₀ S	0.65	0.59						
dimethyldisulfide	C ₂ H ₆ S ₂	0.36	0.81						
<u>Nitrogen containing compounds</u>									
NONE									

Table 24. (con't.)

TOTAL DOSE (ESH)		240	480	720*	960
TYPE OF COMPOUND	Formula	mole x10 ⁻¹⁰	g x10 ⁻⁸	mole x10 ⁻¹⁰	g x10 ⁻⁸
<u>Halogen containing compounds</u>					
chloromethane	CH ₃ Cl	0.79	0.40		
chloroethane	C ₂ H ₅ Cl				0.48 0.31
dichloromethane	CH ₂ Cl ₂				1.02 0.87
trichloromethane	CHCl ₃	0.22	0.27		
perfluorotoluene	C ₇ F ₈	0.18	0.42		0.47 0.56

Table 25. Electron irradiation of P1700/C6000 laminate. GC/MS analysis of evolved products by using OV-101 column. Weight of exposed laminate samples, 5.13g (44.5%-wt resin).

TOTAL DOSE (rads)		5x10 ⁷	10 ⁸	5x10 ⁸	10 ⁹
TYPE OF COMPOUND	Formula	mole x10 ⁻¹⁰	g x10 ⁻⁸	mole x10 ⁻¹⁰	g x10 ⁻⁸
<u>Alkanes, open chain</u>					
2-methylpropane	C ₄ H ₁₀	4.26	2.47	1.03	0.60
n-butane	C ₄ H ₁₀	3.65	2.12		1.10
n-pentane	C ₅ H ₁₂	2.49	1.79		4.43
2-methylbutane	C ₅ H ₁₂				3.19
n-hexane	C ₆ H ₁₄	0.99	0.85	0.43	0.37
n-heptane	C ₇ H ₁₆	1.41	1.41	1.16	1.16
branched alkane	C ₇ H ₁₆				1.39
branched alkane	C ₈ H ₁₈				1.04
n-octane	C ₈ H ₁₈	1.14	1.30	0.53	0.61
n-nonane	C ₉ H ₂₀	0.83	1.06		2.49
n-decane	C ₁₀ H ₂₂	0.29	0.41	0.15	0.22
n-undecane	C ₁₁ H ₂₄	1.28	2.00		0.76
n-dodecane	C ₁₂ H ₂₆	0.29	0.49	0.52	0.88
n-tridecane	C ₁₃ H ₂₈	0.83	1.54		1.15
n-tetradecane	C ₁₄ H ₃₀			0.40	0.79
branched alkane	C ₁₃ H ₂₈				1.43
branched alkane	C ₁₄ H ₃₀				2.64
branched alkane	C ₁₅ H ₃₂				0.37
n-pentadecane	C ₁₅ H ₃₂				0.63
n-hexadecane	C ₁₆ H ₃₄				1.33
					2.66
					1.78
					4.02
					1.52
					3.46
<u>Alkenes, open chain</u>					
1-pentene	C ₅ H ₁₀	1.44	1.01		
1-hexene	C ₆ H ₁₂	0.57	0.48		1.31
1-heptene	C ₇ H ₁₄	0.87	0.85	1.51	1.27
2,4,4-trimethyl-1-pentene	C ₈ H ₁₆	0.80	0.90	0.43	0.42
		0.19	0.21		
<u>Alkanes, cyclic</u>					
ethylcyclopropane	C ₅ H ₁₀	0.96	0.67		
cyclohexane	C ₆ H ₁₂	0.44	0.37	0.50	0.42
methylcyclohexane				0.93	0.78
alkylcycloalkane, unidentif					1.45
					1.42
					0.48

Table 25. (con't.)

TOTAL DOSE (rads)		5x10 ⁷	10 ⁸	5x10 ⁸	10 ⁹
TYPE OF COMPOUND	Formula	mole x10 ⁻¹⁰	g x10 ⁻⁸	mole x10 ⁻¹⁰	g x10 ⁻⁸
<u>Alkenes, cyclic</u>					
cyclohexene	C ₆ H ₁₀	13.3	10.9	5.50	4.51
<u>Aromatic hydrocarbons</u>					
Benzene	C ₆ H ₆	4.59	3.58	7.14	5.57
Toluene	C ₇ H ₈	0.37	0.34	0.38	0.35
Ethylbenzene	C ₈ H ₁₀	9.43	10.0	6.93	7.35
Xylene	C ₈ H ₁₀	40.8	43.3	28.1	29.8
<u>Aldehydes and ketones</u>					
cyclohexanone	C ₆ H ₁₀ O	1.76	1.73	2.27	2.23
acetone				9.02	8.84
methylisopropylketone				45.3	26.3
				0.82	0.71
<u>Esters</u>					
diethylphthalate	C ₁₂ H ₁₄ O ₄			5.13	11.4
di-n-butylphthalate	C ₁₅ H ₂₂ O ₄				9.09
					25.3
<u>Alcohols, ethers and related compounds</u>					
Alcohol, unidentif				0.35	10.5
Oxygen compound, unidentif				2.10	2.72
Oxygen compound, unidentif				6.85	
<u>Sulfur containing compounds</u>					
Carbonyl sulfide	CO ₂	25.1	15.1	1.82	1.09
				1.06	0.64
				156	93
<u>Nitrogen containing compounds</u>					
Unidentified				0.73	8.19
					9.81
<u>Halocarbons and halosilanes</u>					
chloromethane	CH ₃ Cl	2.01	1.01	0.20	0.10
dichloromethane	CH ₂ Cl ₂	2.81	2.39		
chlorobenzene	C ₆ H ₅ Cl	0.18	0.30	0.36	0.40
perfluorotoluene	C ₇ F ₈			0.17	0.41
chloroethane	C ₂ H ₅ Cl				8.50
					5.45

Table 26. Electron irradiation of 934/T300 laminate. GC/MS analysis of evolved products by using OV-101 column. Weight of exposed laminate samples, 5.83g (45.1%-wt resin).

TOTAL DOSE (rads)		5x10 ⁷	10 ⁸	5x10 ⁸	10 ⁹
TYPE OF COMPOUND	Formula	mole x10 ⁻¹⁰	g x10 ⁻⁸	mole x10 ⁻¹⁰	g x10 ⁻⁸
Alkanes, open chain					
2-methylpropane	C ₄ H ₁₀			1.60	0.93
n-butane	C ₄ H ₁₀			2.07	1.20
branched alkane	C ₅ H ₁₂			1.49	1.07
n-pentane	C ₅ H ₁₂			1.57	1.13
n-hexane	C ₆ H ₁₄				0.07 0.06
2-methylpentane	C ₆ H ₁₄			0.56	0.47 0.38 0.33
3-methylpentane	C ₆ H ₁₄			0.37	0.31 0.75 0.65
n-hexane	C ₆ H ₁₄			1.42	1.19
branched alkane	C ₇ H ₁₆			0.78	0.78
n-heptane	C ₇ H ₁₆			1.47	1.47 0.84 0.84
n-octane	C ₈ H ₁₈			0.60	0.69 0.80 0.91
branched alkane	C ₉ H ₂₀				0.68 0.78
n-nonane	C ₉ H ₂₀			0.25	0.32 0.63 0.80
branched alkane	C ₉ H ₂₀				0.21 0.27
n-decane	C ₁₀ H ₂₂	4.02	5.71	0.38	0.54 0.12 0.17
branched alkane	C ₁₁ H ₂₄	2.04	0.94		
n-undecane	C ₁₁ H ₂₄				0.26 0.40
n-dodecane	C ₁₂ H ₂₆	10.6	18.1	1.00	1.71 0.25 0.43
branched alkane	C ₁₃ H ₂₈	0.23	0.42		
n-tridecane	C ₁₃ H ₂₈			0.11	0.21 0.24 0.44
n-tetradecane	C ₁₄ H ₃₀	9.44	18.7	0.76	1.50 0.21 0.43 0.22 0.43
n-pentadecane	C ₁₅ H ₃₂			0.20	0.44 0.49 1.04
branched alkane	C ₁₅ H ₃₄	0.49	1.11		
n-hexadecane	C ₁₆ H ₃₄	3.67	8.31	0.29	0.66 0.43 0.97 0.41 0.94
Alkenes, open chain					
propene	C ₃ H ₆			0.88	0.37 0.69 0.29
Alkanes, cyclic					
cyclopropane (tentative)	C ₃ H ₆	0.95	0.40		
cyclohexane	C ₆ H ₁₂			0.36	0.30 0.43 0.36

Table 26. (con't.)

TOTAL DOSE (rads)		5x10 ⁷	10 ⁸	5x10 ⁸	10 ⁹		
TYPE OF COMPOUND	Formula	mole x10 ⁻¹⁰	g x10 ⁻⁸	mole x10 ⁻¹⁰	g x10 ⁻⁸	mole x10 ⁻¹⁰	g x10 ⁻⁸
<u>Alkenes, cyclic</u>							
NONE							
<u>Aromatic hydrocarbons</u>							
Benzene	C ₆ H ₆			0.52	0.41	0.34	0.26
<u>Aldehydes and ketones</u>							
acetone			2.77	1.61			
<u>Esters</u>							
diethylphthalate	C ₁₂ H ₁₄ O ₄			1.39	3.08	0.86	1.92
di-n-butylphthalate	C ₁₆ H ₂₂ O ₄	0.44	1.23	0.15	0.43	3.11	8.66
<u>Alcohols, ethers and related compounds</u>							
paraldehyde (or isomer)	C ₅ H ₁₂ O ₂			5.51	7.28		
<u>Sulfur containing compounds</u>							
NONE							
<u>Nitrogen containing compounds</u>						2.51	
unidentified							
<u>Halogen containing compounds</u>							
dimethyldifluorosilane	C ₂ H ₆ SiF ₂			0.23	0.20		
trimethylfluorosilane	C ₃ H ₉ SiF			0.37	0.34		
perfluorotoluene	C ₇ F ₈					0.24	0.56

Table 27. Electron irradiation of 5208/T300 laminate. GS/MS analysis of evolved products by using OV-101 column. Weight of exposed laminate samples, 4.47g (32.8%-wt resin).

TOTAL DOSE (rads)		5x10 ⁷ (*)	10 ⁸ (**) mole x10 ⁻¹⁰ g x10 ⁻⁸	5x10 ⁸ mole x10 ⁻¹⁰ g x10 ⁻⁸	10 ⁹ mole x10 ⁻¹⁰ g x10 ⁻⁸
TYPE OF COMPOUND	Formula				
<u>Alkanes, open chain</u>					
n-pentane	C ₅ H ₁₂				7.43 5.36
Alkane, unidentif.					2.57
<u>Alkenes, open chain</u>					
butene or 2-methylpropene	C ₄ H ₈				2.01 1.13
<u>Alkanes, cyclic</u>					
NONE					
<u>Alkenes, cyclic</u>					
NONE					
<u>Aromatic hydrocarbons</u>					
benzene					5.47 4.26
toluene					2.82 2.60
<u>Aldehydes and ketones</u>					
NONE					
<u>Esters</u>					
NONE					
<u>Alcohols, ethers and related compounds</u>					
1,4-dioxane					0.93 0.83
<u>Sulfur containing compounds</u>					
NONE					
<u>Nitrogen containing compounds</u>					
unidentified					4.17
fluoro-nitrogen compd, unidentif.				3.60	18.8

*only traces of gas detected in this sample

**leaking valve, gas sample was not analyzed

Table 27. (con't.)

TOTAL DOSE (rads)		5x10 ⁷	10 ⁸	5x10 ⁸	10 ⁹
TYPE OF COMPOUND	Formula	mole x10 ⁻¹⁰	g x10 ⁻⁸	mole x10 ⁻¹⁰	g x10 ⁻⁸
<u>Halogen containing compounds</u>					
chlorotrifluoromethane	CClF ₃			2.97	3.09
trifluoromethane	CHF ₃			4.80	3.36
fluorocarbons, unidentif				28.2	41.2
dimethyldifluorosilane	C ₂ H ₆ F ₂ Si			7.20	6.91
1-H-perfluorohexane	C ₆ HF ₁₃			0.16	0.53
dichloromethane	CH ₂ Cl ₂			4.88	4.15
tetrafluoroethane	C ₂ H ₂ F ₄				12.3 12.5
trimethylfluorosilane	C ₃ H ₉ FSi				2.60 2.40
chloroethane	C ₂ H ₅ Cl				11.4 7.28

to the formation of cyclohexa-1,3-diene, which is known to rearrange under the effect of UV light to form hexa-1,3,5-triene¹³



Either this reaction or a direct cleavage of cyclohexadienyl radicals followed by recombination of hydrocarbon fragments is probably responsible for the formation of linear alkenes and alkanes.

Aromatic compounds identified by GC/MS include benzene, toluene, ethylbenzene, xylene and several more in the case of ultraviolet irradiated polysulfone. Their formation can be explained by free radical mechanisms, some of which have been discussed previously for Fiberite 705/60. Xylene must be present as residual solvent in P1700, because the amount of xylene detected from ultraviolet and electron irradiated P1700 samples is excessively high.

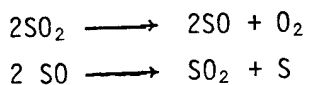
Among the compounds containing carbonyl groups, acetone is the most important. A possible mechanism for acetone formation was suggested previously for Fiberite 705/60. From epoxy type systems, evolution of acetone cannot be readily explained. Acetone formation does not show a clear dependence on exposure time, indicating possible residual solvent or vapor phase reactions.

Several alcohols and ethers have been identified, mainly from ultraviolet exposed samples. Particularly interesting was the identification of paraldehyde, the trimer of acetaldehyde, from ultraviolet irradiated 5208 and electron irradiated 934. Acetaldehyde was never detected, although it was certainly formed, probably because it undergoes decomposition into CO and CH₄.

¹³

R.J. DeKock, N.G. Minaard and E. Habinga: The Photochemical Reactions of 1,3 Cyclohexadiene and α -Phellandrene, Rec. Trav. Chem. 79, 922 (1960).

A variety of sulfur compounds have been identified from ultraviolet irradiated samples, such as carbonyl sulfide (COS), carbon disulfide (CS₂), dimethylsulfide (CH₃-S-CH₃), dimethyldisulfide (CH₃-S-S-CH₃) and methylethylsulfide (CH₃-S-C₂H₅). Formation of small quantities of COS was previously reported for electron irradiation⁷, γ -irradiation⁸, and UV irradiation⁴ of polysulfone in vacuum. These sulfur compounds must arise from secondary reactions of SO₂. SO₂ must act as an oxidant, since the sulfur compounds identified by GC/MS have a lower oxidation number. It was mentioned earlier that SO₂ can undergo photochemical and radiochemical decomposition into SO and O₂ and that SO can undergo disproportionation to SO₂ and elemental sulfur⁶:



Elemental sulfur may react with CO to form COS: CO + S \longrightarrow COS

CS₂ can form from COS by the following reaction¹⁴: 2COS \longrightarrow CS₂ + CO₂

COS may also undergo photolytic decomposition into CO and elemental sulfur¹⁵. Other reaction mechanisms could be proposed for the formation of thiols and thioethers, however, these reactions are of limited interest because the formation of these gases is negligible.

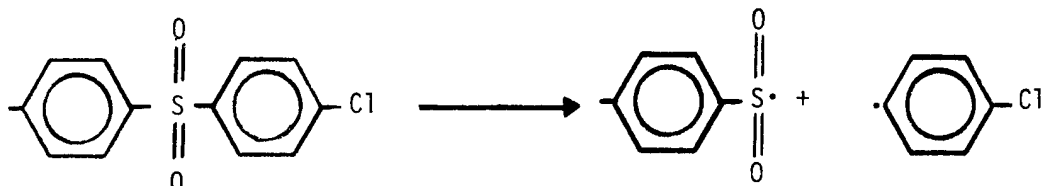
The nearly total absence of nitrogen containing compounds in the gas mixtures is quite remarkable. Nitrogen is present in Fiberite 934 and Narmco 5208 (4,4'-diaminodiphenyl sulfone (DDS) is used as hardener for these resins). Only in the case of UV exposed Fiberite 934 traces of nitriles have been identified. Ammonia or amines were not detected. This indicates good radiation stability for the portion of the molecule linking DDS to the epoxy system.

A variety of fluorocarbons, chlorocarbons and fluorosilanes have been identified. Most of these are freon type gases and constituents of mold releases used in composite fabrication. The only compound of interest in the group is chlorobenzene, detected in the ultraviolet and electron irradiation of P1700. Chlorobenzene arose from chlorophenyl end-groups present in P1700 (which is

¹⁴J.R. Parkinson and H.H. Neville: The Thermal Decomposition of Carbonyl Sulphide, J. Chem. Soc. 1951, 1230.

¹⁵S. Oae, Organic Chemistry of Sulfur, Plenum Press, N.Y., 1977, 39.

prepared from 4,4'-dichlorodiphenylsulfone). Formation of chlorobenzene is an indirect proof of the occurrence of chain cleavage at C-S bonds:



Likewise, benzene formation results from chain cleavage reactions taking place at random points in the polymer chain at both ends of a benzene ring. Similar curves are obtained for benzene and chlorobenzene formation from ultraviolet and electron irradiated P1700 (Figure 28 and 29).

4.2.2. Mechanical and Optical Evaluation

Compressive and flexural strength measurements have been conducted on control samples, ultraviolet exposed samples (960 ESH) and electron exposed samples (10^9 rads) of P1700/C6000, Fiberite 934/T300 and Narmco 5208/T300. Compressive strengths for these materials are presented in Table 28. These data are presented graphically in Figures 30, 31 and 32, where the probability of failure vs. the compressive strength is shown.

As can be seen in Figure 30 for the 934/T300 material, there is no statistical evidence to indicate that the UV or electron exposed samples are different in strength from the control samples. Figure 31 presents the data obtained for P1700/C6000. The control group and the electron exposed group show little difference, but there may well be a deleterious effect of UV exposure on this material. Figure 32 shows negligible variation in 5208/T300 exposed to UV or electrons.

Flexural test results are given in Table 29. Again, these data were plotted relating the probability of failure to the flexural strength (see Figures 33, 34 and 35). The behavior is essentially the same as that shown for compressive strength. The 934/T300 and 5208/T300 materials show no significant variation in strength. There may be flexural strength degradation in UV exposed P1700/C6000 (noted previously in Figure 31 for compressive strength.).

SEM examination of UV exposed P1700/6000 has been conducted in an attempt to identify possible radiation induced surface damage. Surface defects showing

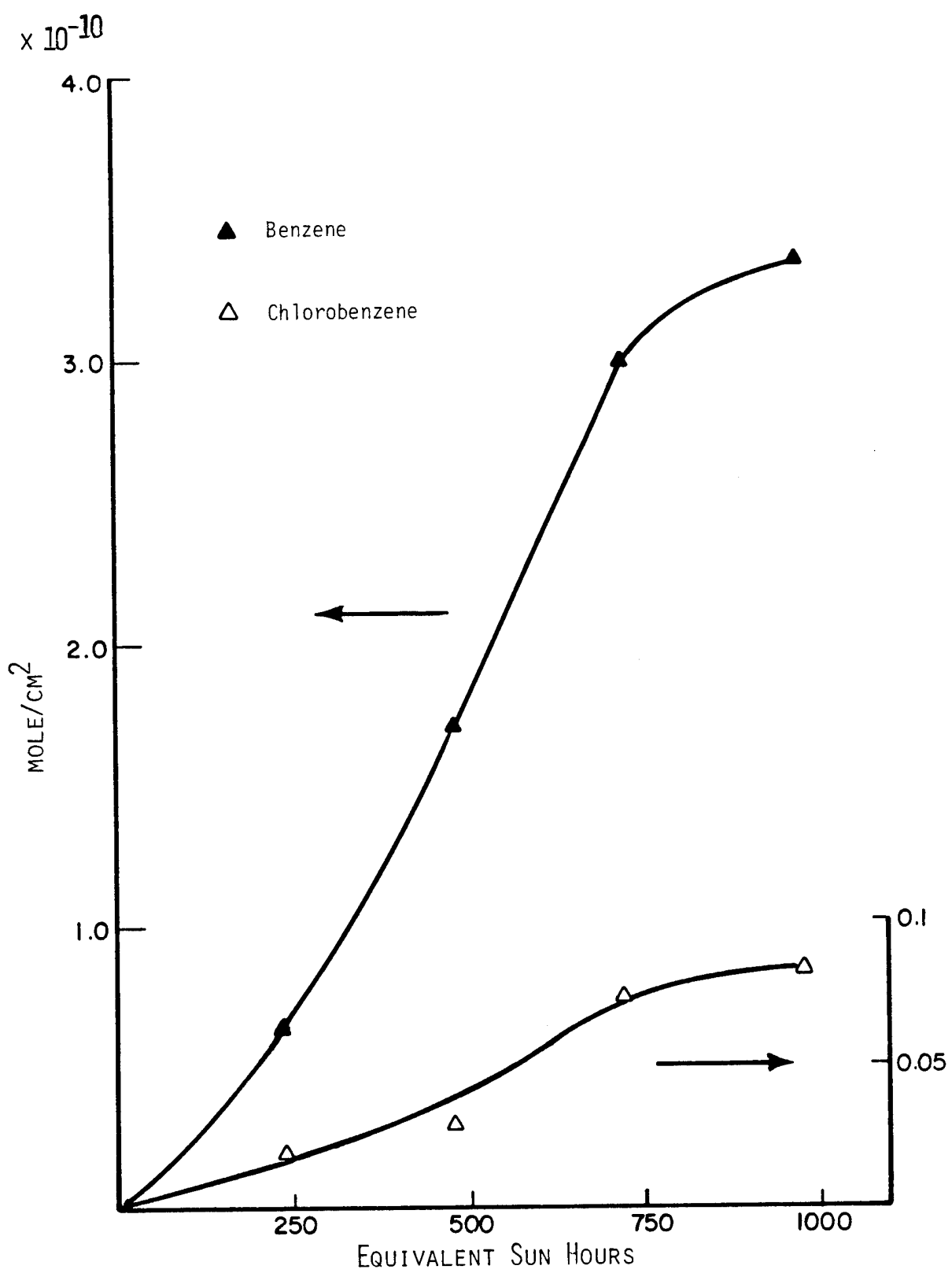


Figure 28. Benzene and chlorobenzene formation during ultraviolet irradiation of P1700/C6000.

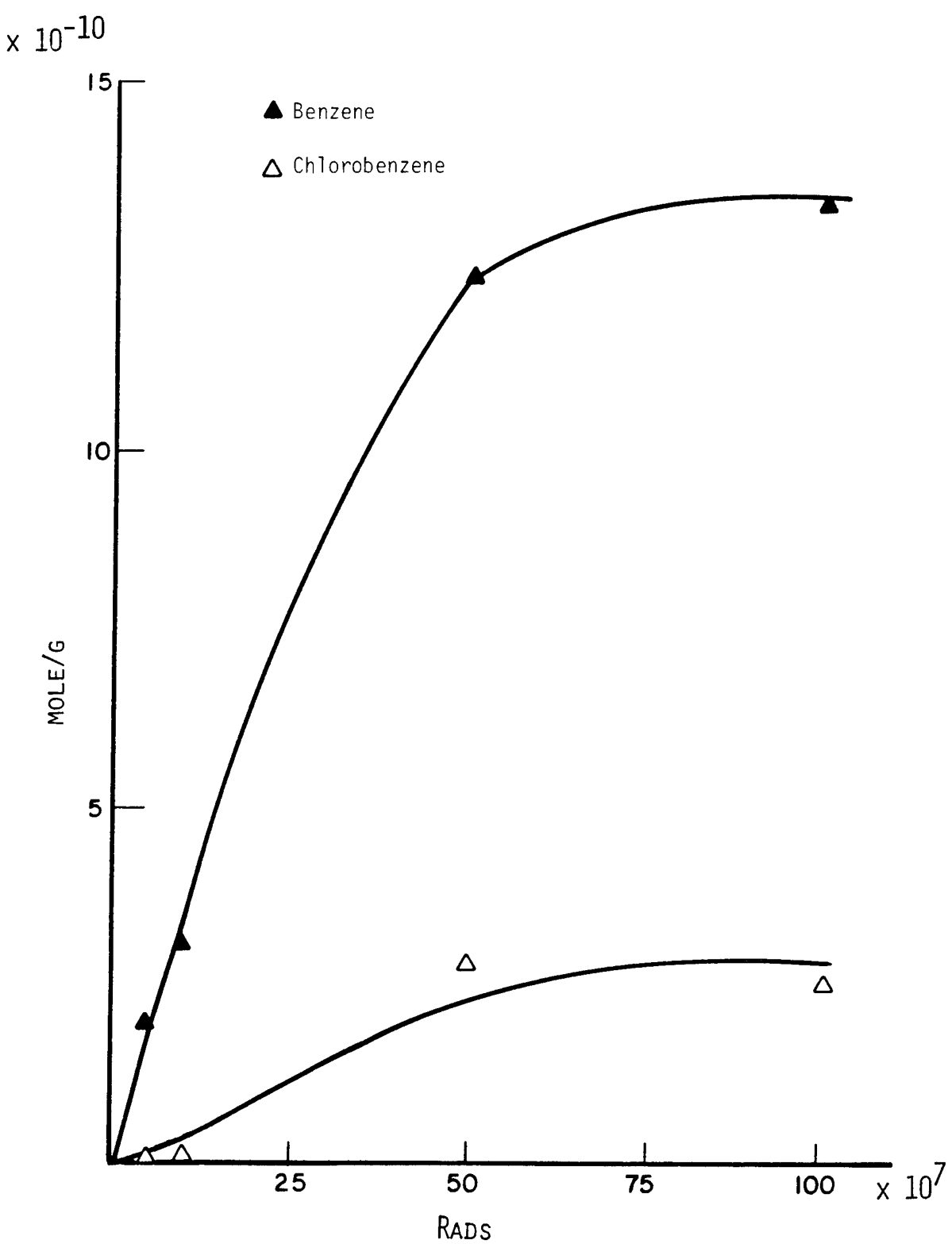


Figure 29. Benzene and Chlorobenzene formation during electron irradiation of P1700/C6000.

Table 28
COMPRESSIVE STRENGTH

<u>Material</u>	<u>Exposure</u>	<u>Strength, MPa (Avg. of 3 Spec.)</u>
934/T300	Control	505
	UV Exposed, 960 ESH	627
	Electron Exposed, 10^9 rads	573
P1700/C6000	Control	365
	UV Exposed, 960 ESH	253
	Electron Exposed, 10^9 rads	418
5208/T300	Control	480
	UV Exposed, 960 ESH	489
	Electron Exposed, 10^9 rads	532

Table 29
FLEXURAL STRENGTH

<u>Material</u>	<u>Exposure</u>	<u>Strength, MPa (Avg. of 3 Spec.)</u>
934/T300	Control	1370
	UV Exposed, 960 ESH	1580
	Electron Exposed, 10^9 rads	1560
P1700/C6000	Control	1100
	UV Exposed, 960 ESH	710
	Electron Exposed, 10^9 rads	850
5208/T300	Control	1870
	UV Exposed, 960 ESH	2000
	Electron Exposed, 10^9 rads	2020

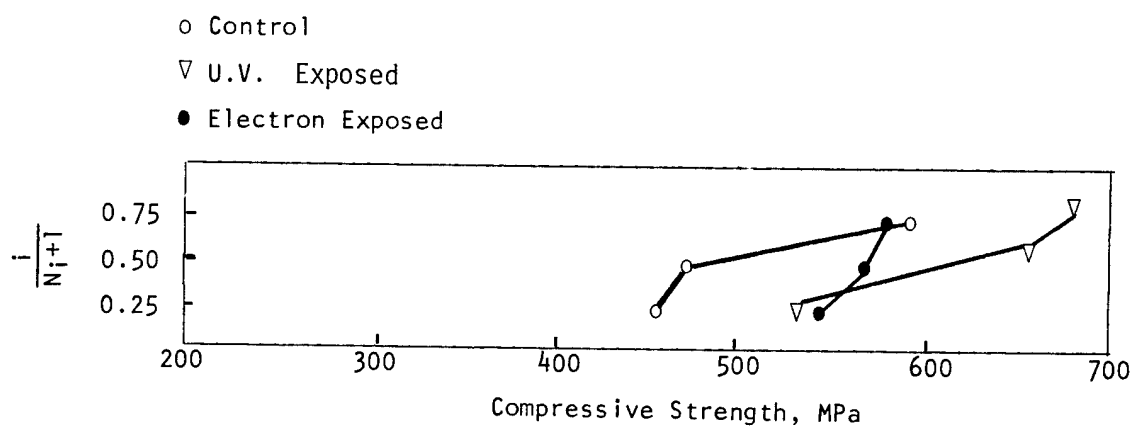


Figure 30. Compressive Strength Distribution for 934/T300

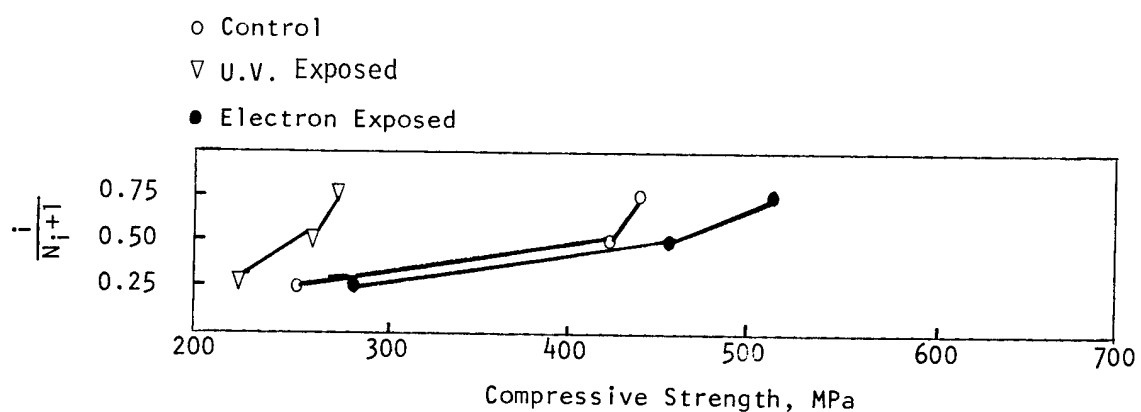


Figure 31. Compressive Strength Distribution for P1700/C6000

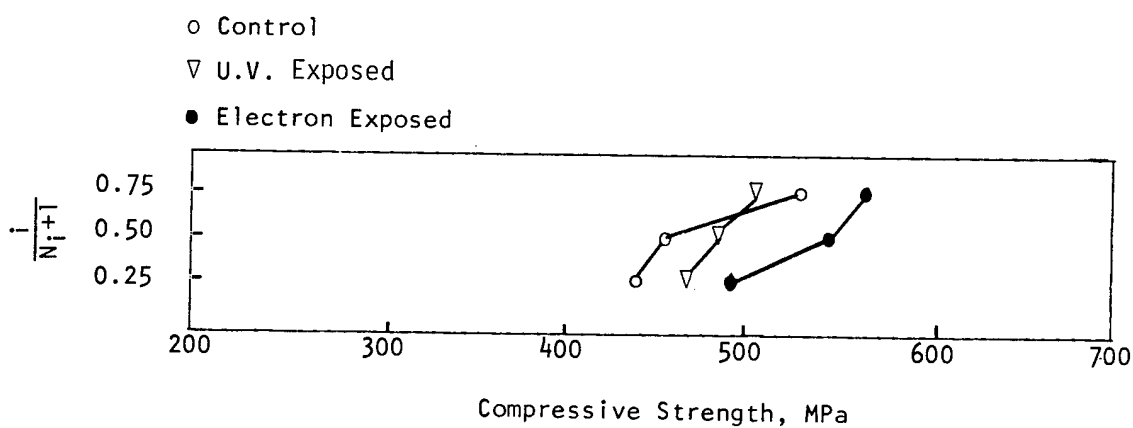


Figure 32. Compressive Strength Distribution for 5208/T300

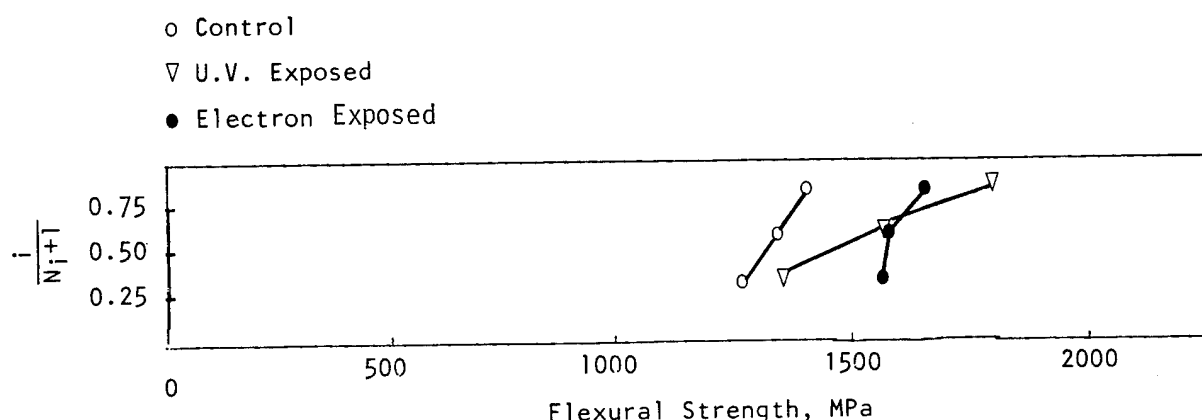


Figure 33. Flexural Strength Distribution for 934/T300

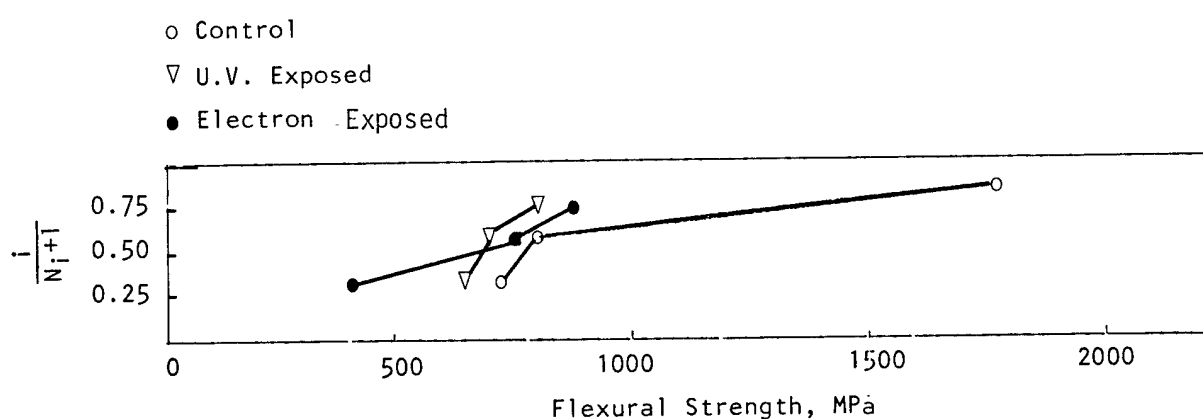


Figure 34. Flexural Strength Distribution for P1700/C6000

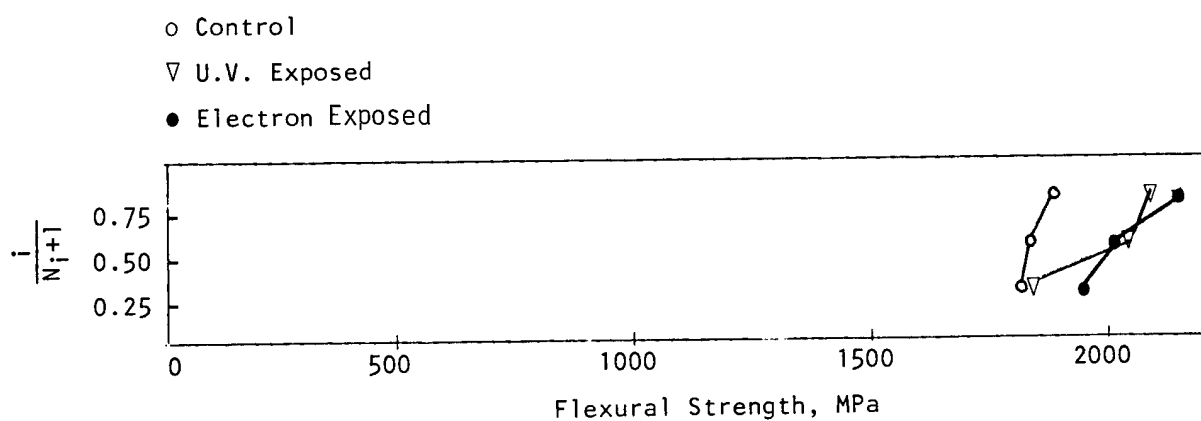


Figure 35. Flexural Strength Distribution for 5208/T300

exposed graphite fibers appear to be somewhat more pronounced in the irradiated sample relative to the control (Figures 36 and 37).

4.2.3. Dynamic Mechanical Analysis of Electron Exposed Samples

The dynamic mechanical behavior of Fiberite 934/T300 and Narmco 5208/T300 has been measured in the sample transverse direction. The elastic modulus and the loss modulus of electron irradiated samples (10^9 rads) and control samples are compared in Figures 38, 39, 40 and 41, for 934/T300 and 5208/T300 respectively. The elastic modulus of the two epoxy systems is virtually unchanged over a wide temperature range after irradiation, but the point of inflection of the modulus curve for 5208/T300 occurs at slightly higher temperature, indicating a higher α transition due to radiation induced cross-linking. The same phenomenon can be observed by comparing the temperatures at which maxima occur in the loss modulus plots. The loss modulus curves show that both 934/T300 and 5208/T300 have high temperature (α) and low temperature (β) transitions. The temperature at which these transitions occur (as measured by the temperature of the transition peak) appears to change as a result of electron irradiation, but the direction of the change is not the same for the two resins. According to the loss modulus plots, irradiation increases the α peak temperature in the case of 5208/T300, but decreases it for 934/T300. The precision of the technique is adequate to detect changes of this magnitude, but because of some variability in the samples used, additional measurements will be required before drawing definite conclusions. The increase in the α transition temperature of Narmco 5208 is probably related to evolution of hydrogen which was particularly high at 10^9 rads, as can be seen from Table 20 and Figure 22. (Polymers which are known to cross-link under the effect of radiation such as polystyrene produce almost exclusively hydrogen as a by-product).

DMA studies of P1700/C6000 and epoxy samples in the fiber direction have not been completed.

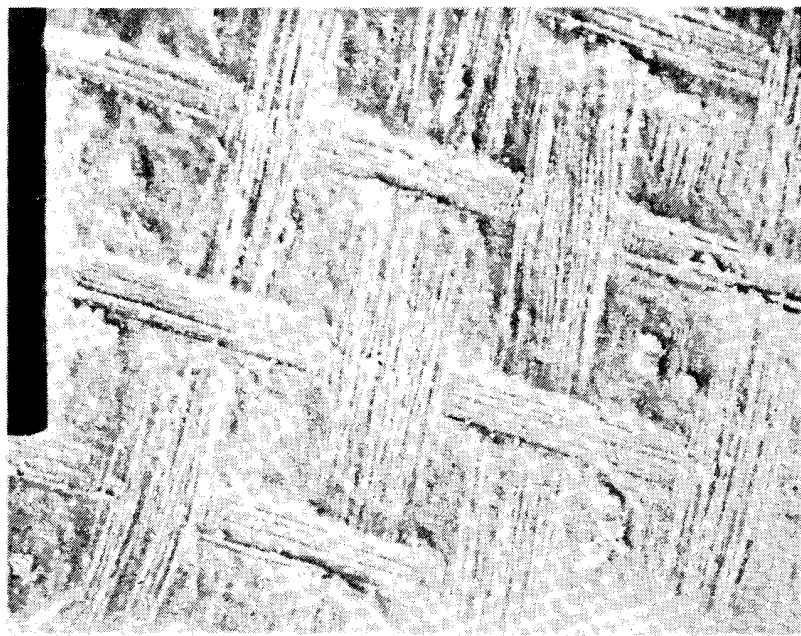
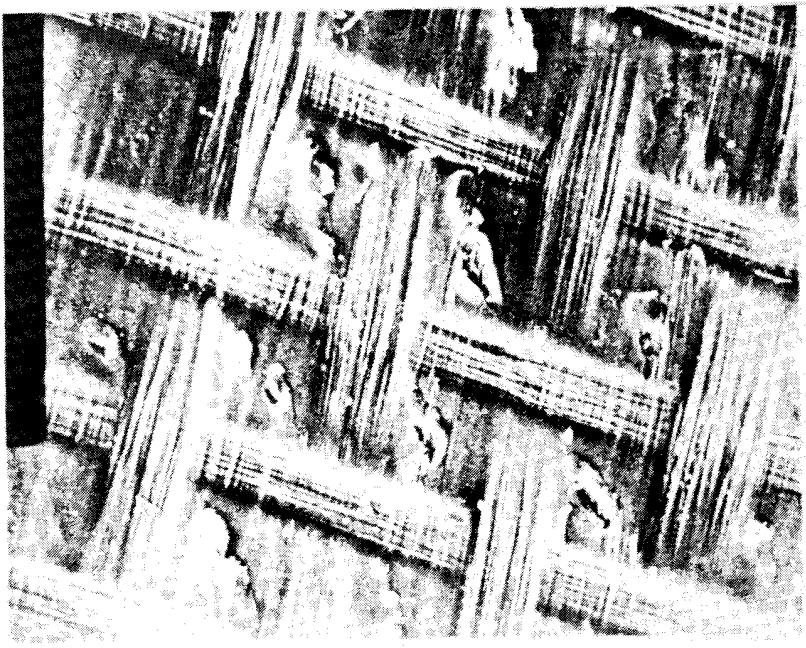


Figure 36. SEM Micrographs (50X) of P1700/C6000 laminate.
Left sample, control. Right sample, UV irradiated (960 ESH)

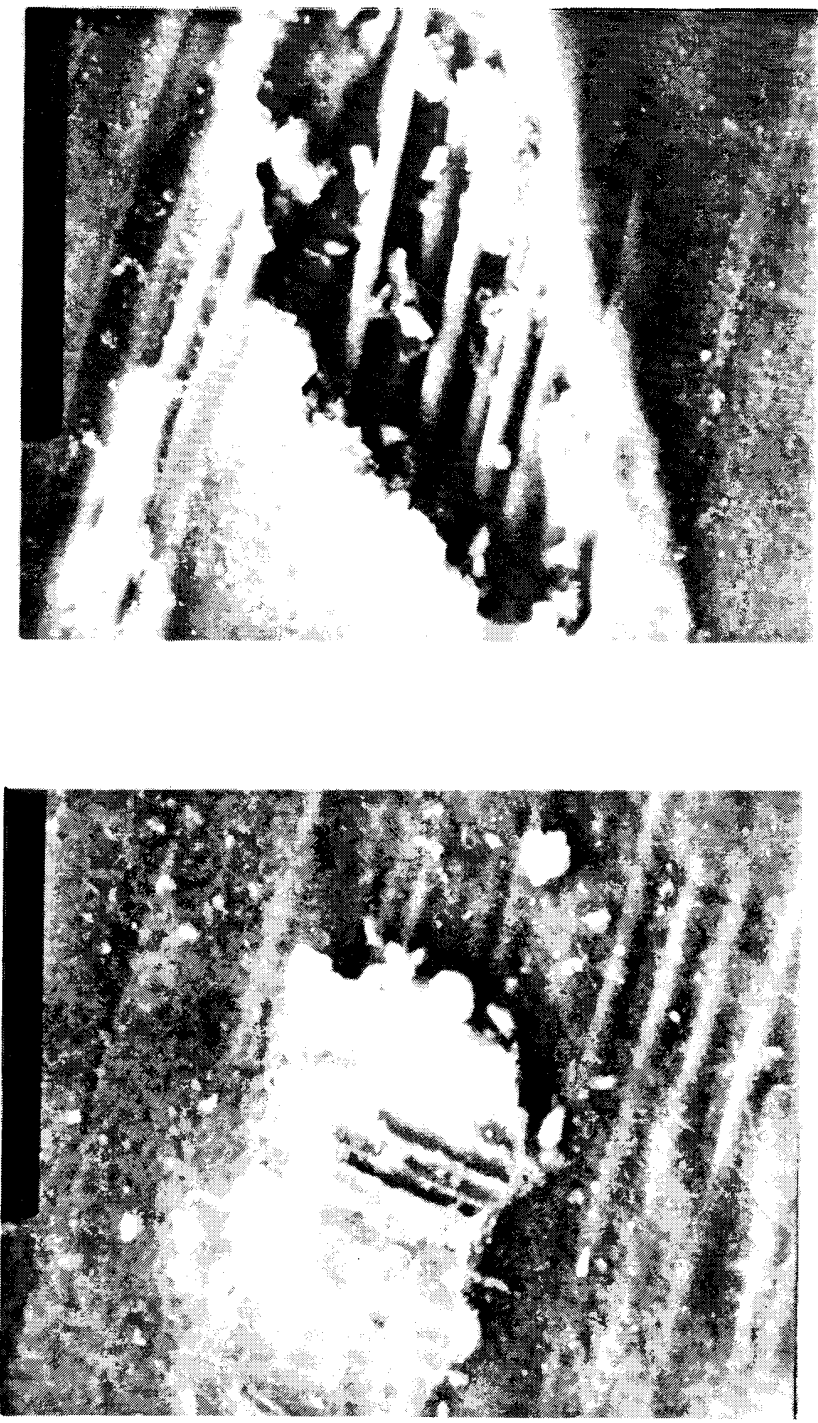


Figure 37. SEM Micrographs (500X) of P1700/C6000 laminate.
Left sample, control. Right sample, UV irradiated (960 ESH)

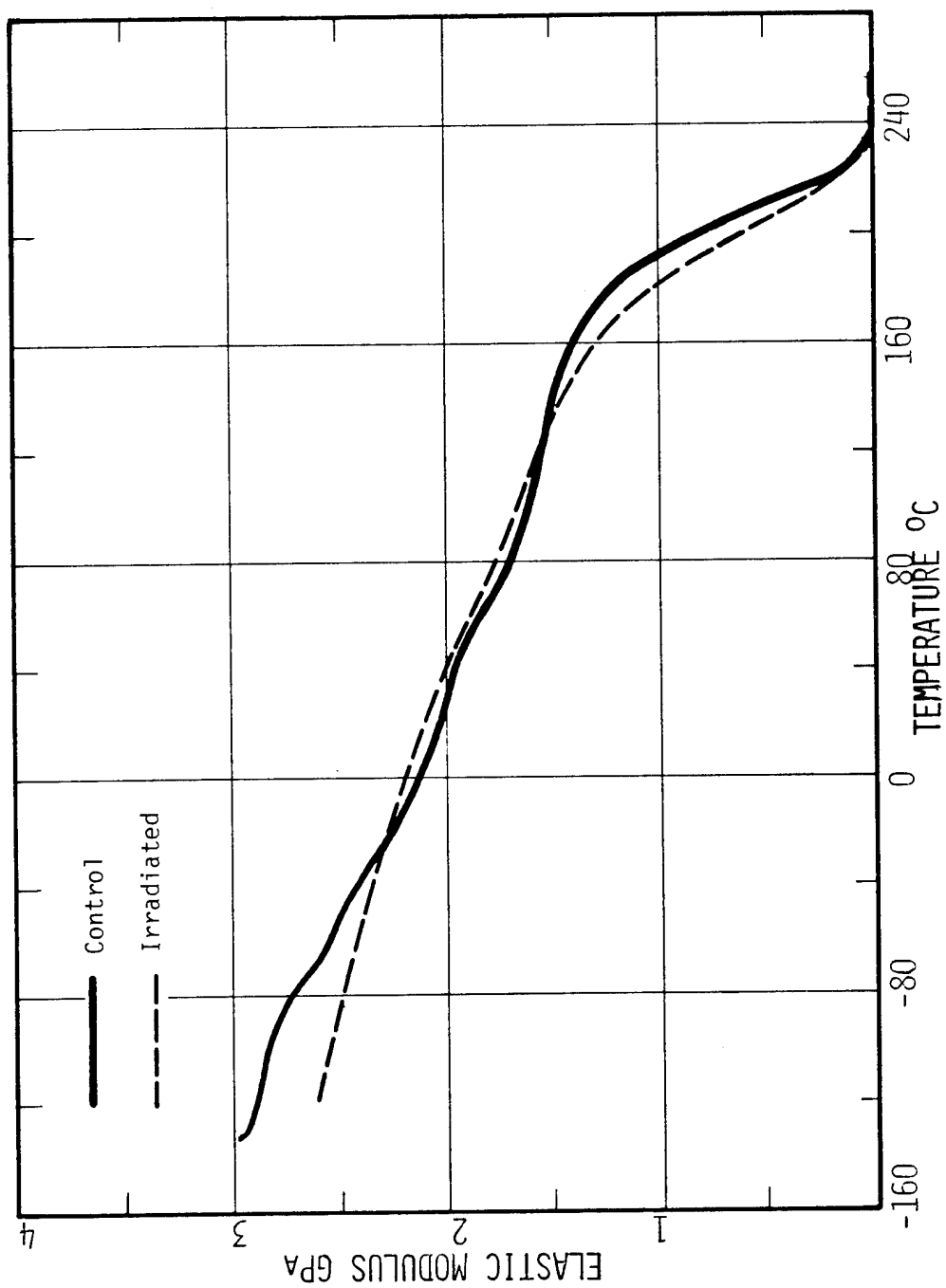


Figure 38. Effect of electron irradiation (10^9 rads) on the elastic modulus of Fiberite 934/T300.

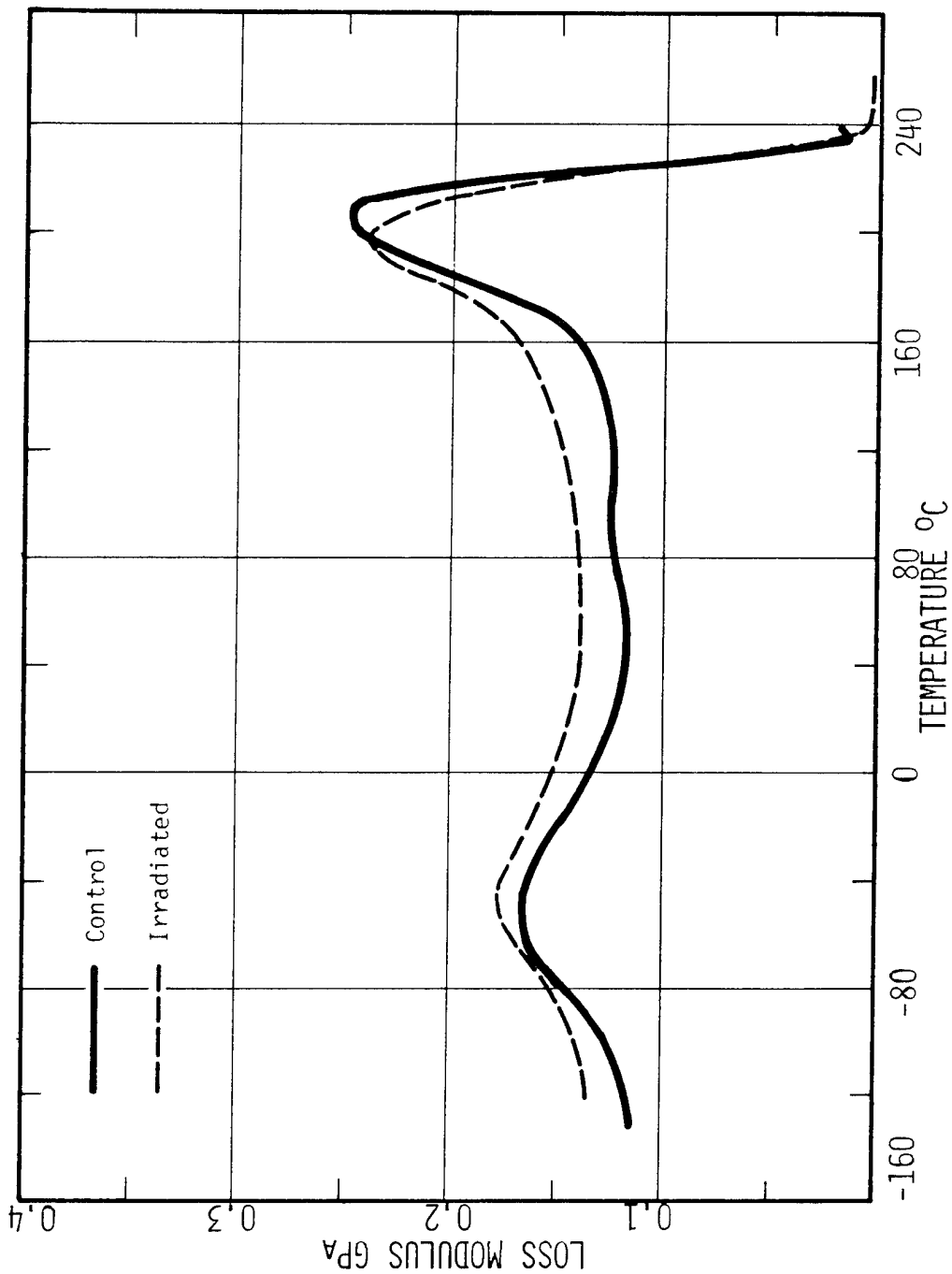


Figure 39. Effect of electron irradiation (10^9 rads) on the loss modulus of Fiberite 934/T300.

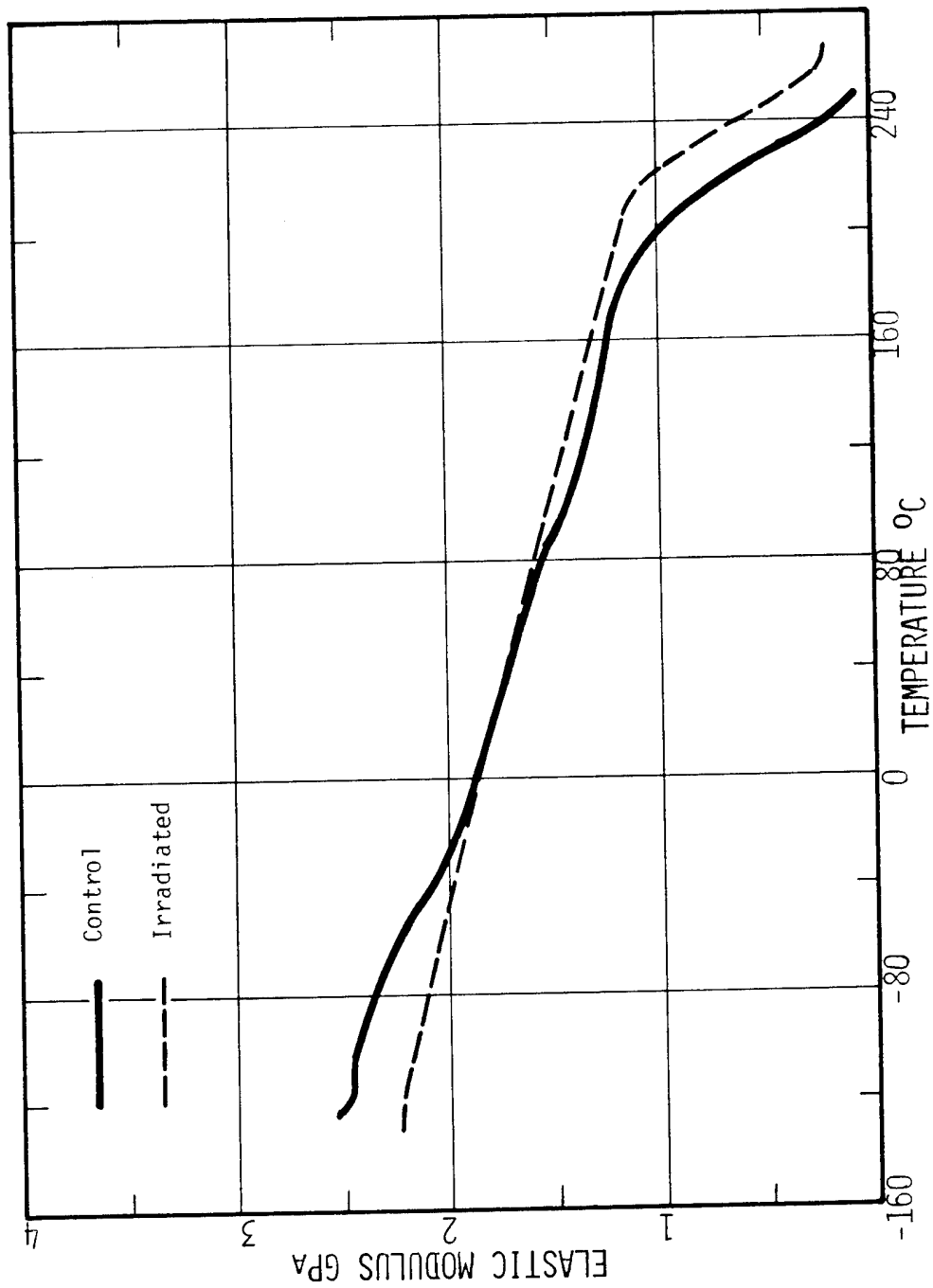


Figure 40. Effect of electron irradiation (10^9 rads) on the elastic modulus of Narmco 5208/T300.

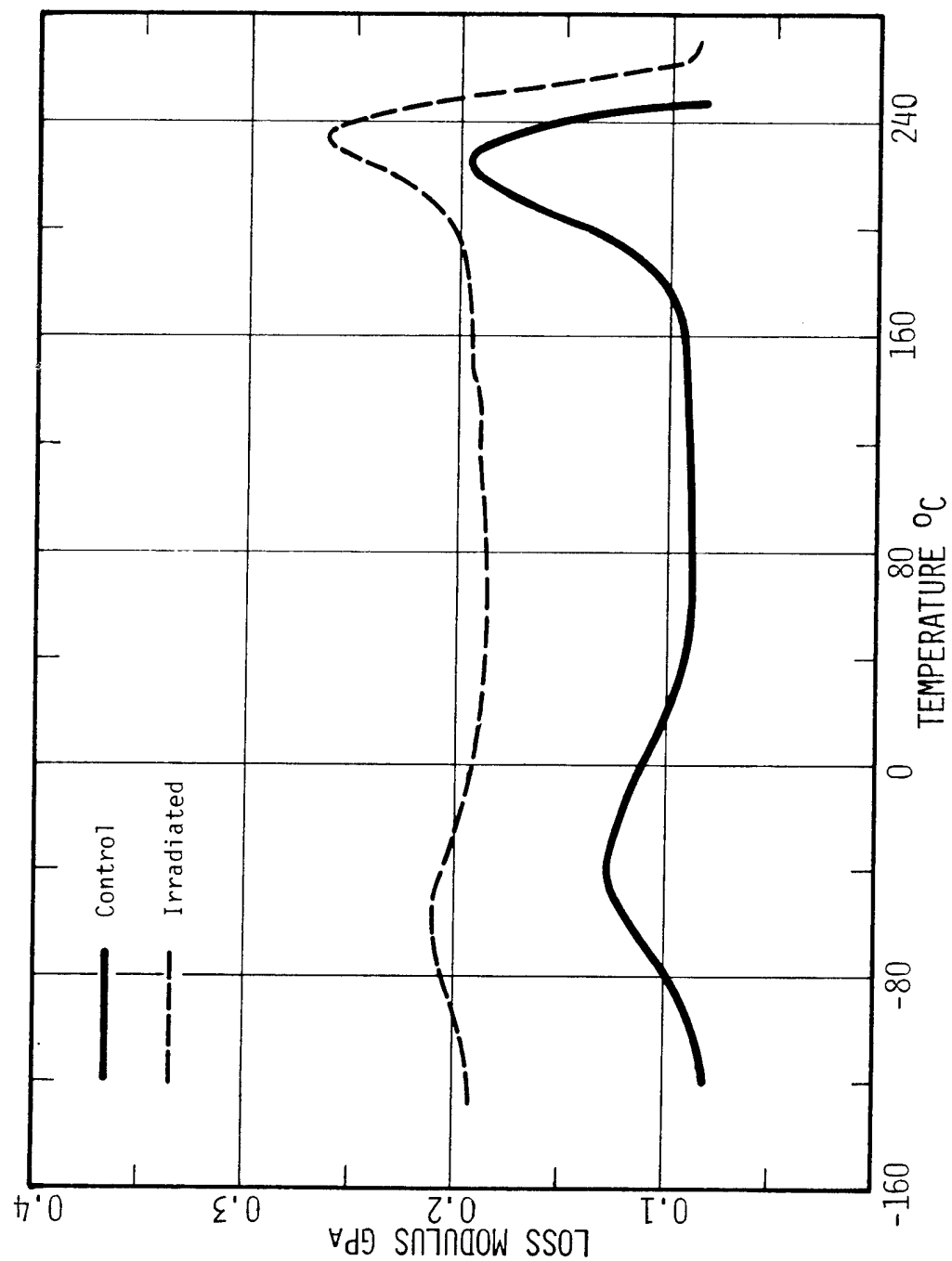


Figure 41. Effect of electron irradiation (10^9 rads) on the modulus of Narmco 5208/T300.

4.3 CONCLUSIONS AND RECOMMENDATIONS

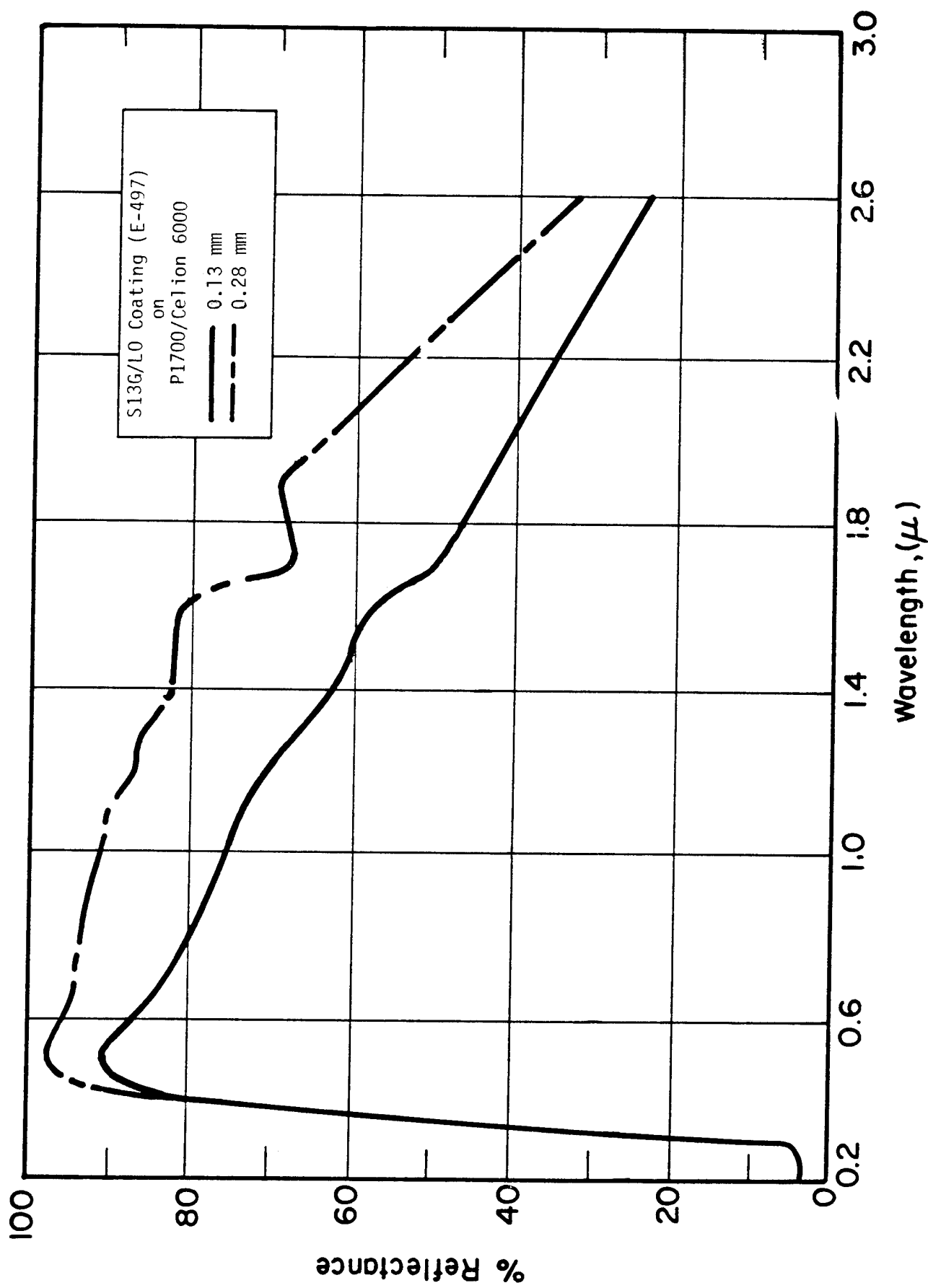
The composite materials evaluated have shown good electron radiation stability as indicated by low G values for gas formation and no evidence of mechanical property changes up to radiation doses of 10^9 rads. The same composites have shown poor stability to ultraviolet radiation in terms of quantum yields for gas formation. In terms of mechanical properties, no measurable changes have been detected up to 960 ESH, with the possible exception of PI700/C6000. Because of the high aromaticity of the matrix resins investigated, ultraviolet radiation is totally absorbed at the surface and a "skin effect" is produced.

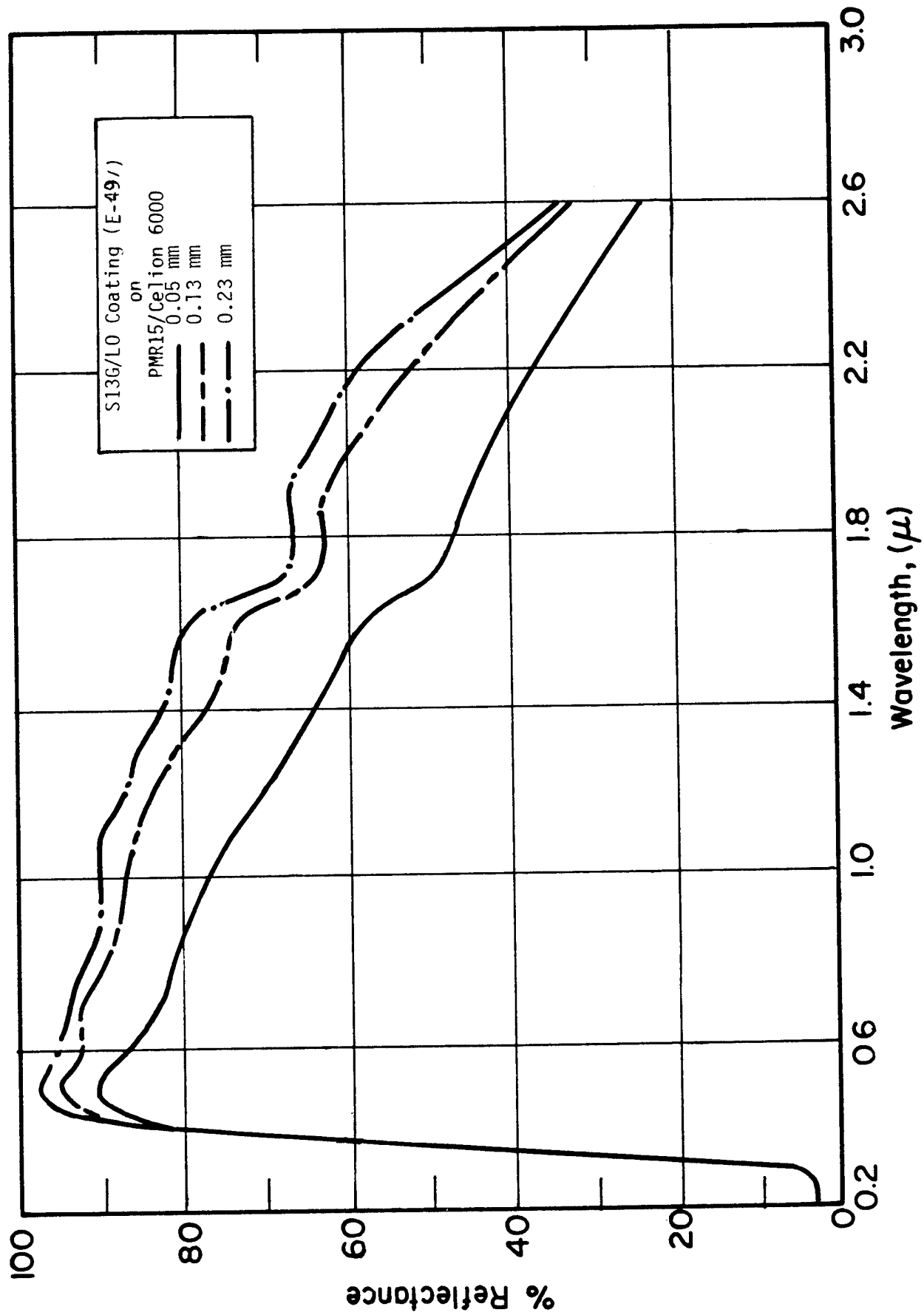
Quantitative analysis of volatile products evolved during radiation exposure has been found to be very useful for determining "molecular" radiation stability. Gas formation in irradiated polymers reflects the occurrence of chain scission and cross-linking reactions, which are ultimately responsible for mechanical failure. Plots of main gas formation versus exposure doses generally follow well-defined curves that could be simply described mathematically and utilized for a kinetic model of the degradation process. The gas analysis technique is very sensitive and reveals changes occurring at the molecular level long before these become apparent in terms of physical property changes. The method is particularly useful for the study of thermosets, which because of their insolubility cannot be analyzed by conventional polymer characterization methods. We have identified several free radical mechanisms of matrix degradation and have compared the radiation resistance of different matrices on the basis of their rates of gas evolution. Correlations between molecular effects of degradation (gas formation) and gross effects (changes in mechanical properties) have not been established because the radiation doses employed were insufficient to produce measurable physical property changes in the laminates tested. An increase in the Tg of 5208/T300 at 10^9 rads appears to be related to hydrogen formation, which is particularly high at this dose.

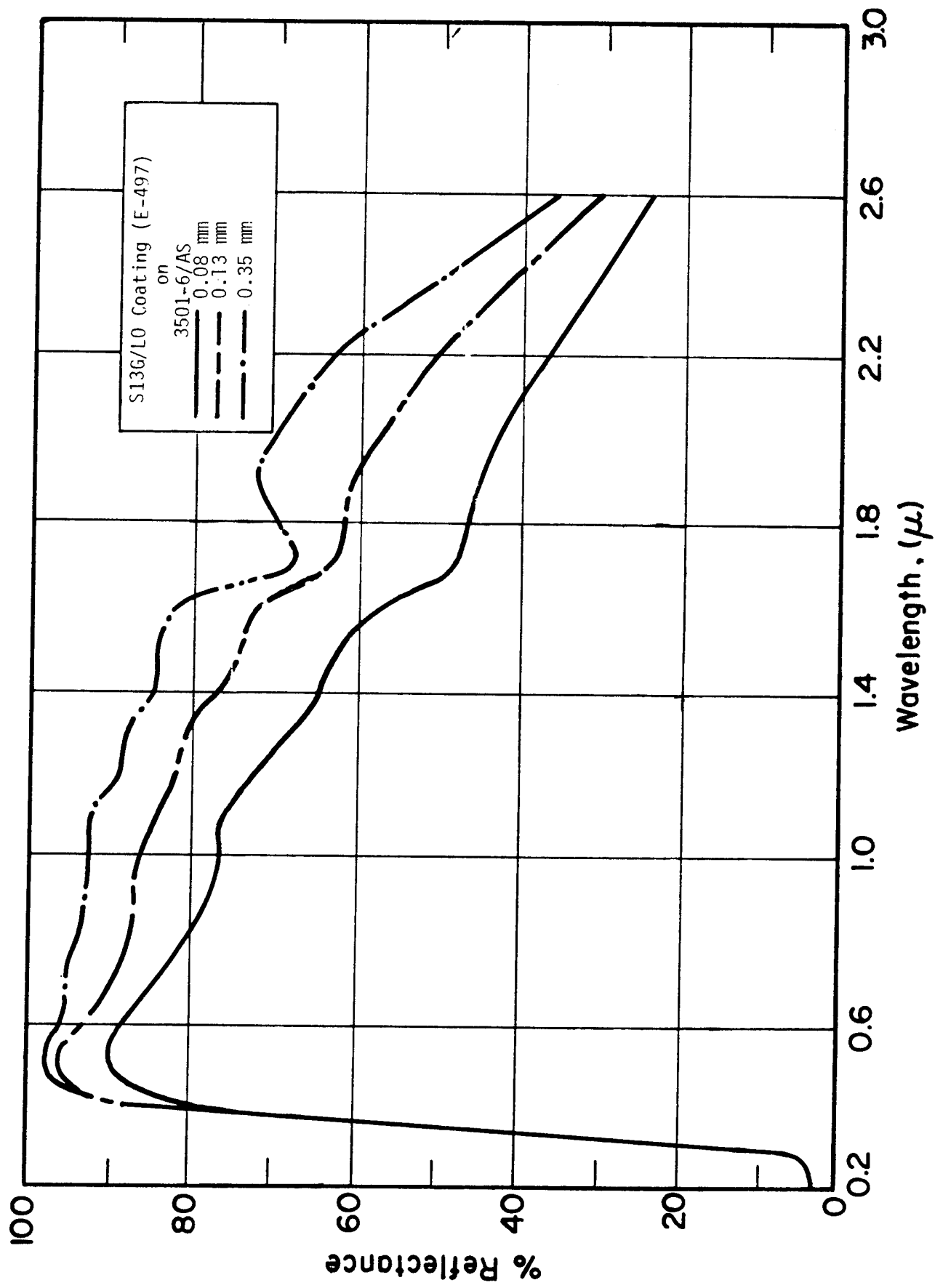
Of particular concern was the identification of diethyl and di-n-butyl phthalate among the by-products obtained. The presence of these compounds was most likely due to insufficient cleaning of prepregger's resin mixing vat. It is doubtful that this trace quantity of plasticizer could have a major effect on the degradation of the epoxy resin system. The fact that it was found emphasizes the need for cleanliness by the prepregger.

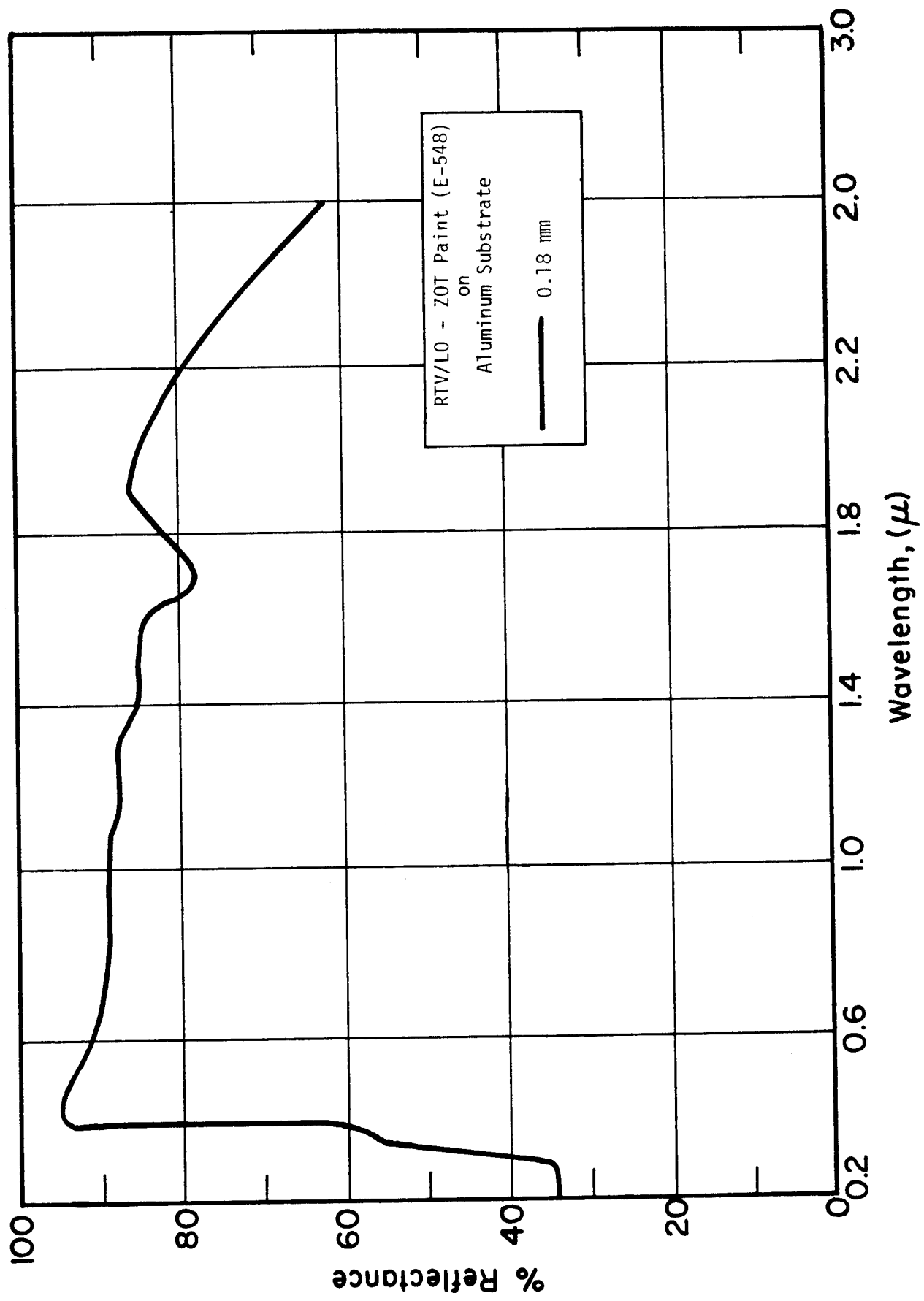
Dose rate effects have not been investigated and should be considered in future work. High-energy radiation exposure tests at dose rates substantially lower than the ones employed in this work would be very expensive and time consuming, if total doses in excess of 10^9 rads are to be attained. Again, gas analysis can be very useful for a study of dose rate effects, since the method is very sensitive and fluences as low as 5×10^7 rads would be sufficient to evaluate gas formation as a function of energy flux.

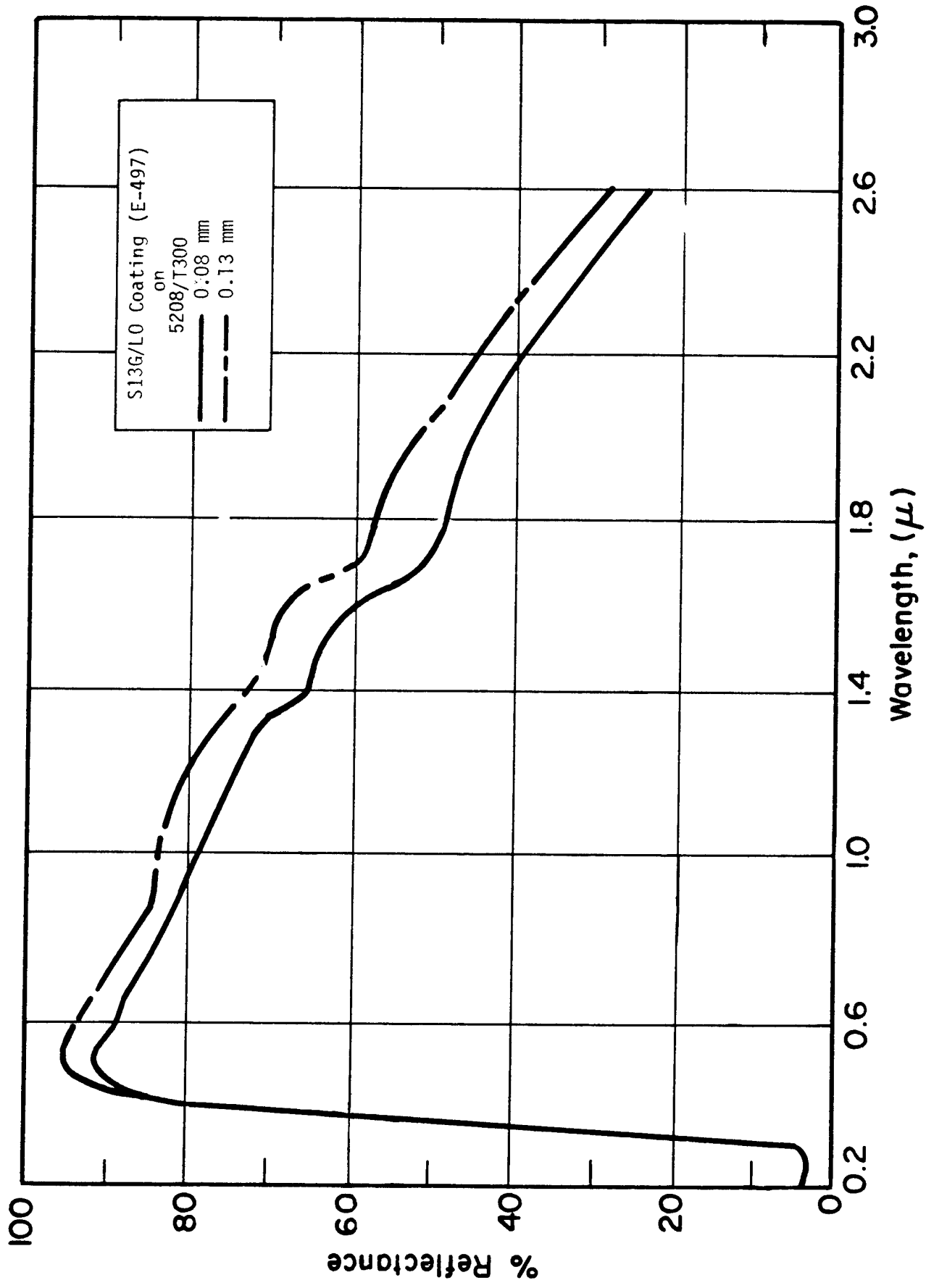
APPENDIX
REFLECTANCE CURVES











1. Report No. NASA CR-3559	2. Government Accession No.	3. Recipient's Catalog No.	
4. Title and Subtitle INVESTIGATION OF DEGRADATION MECHANISMS IN COMPOSITE MATRICES		5. Report Date June 1982	
		6. Performing Organization Code	
7. Author(s) C. Giori and T. Yamauchi		8. Performing Organization Report No. C06428-17	
9. Performing Organization Name and Address IIT Research Institute 10 W. 35th Street Chicago, Illinois 60616		10. Work Unit No.	
		11. Contract or Grant No. NAS1-15469	
12. Sponsoring Agency Name and Address National Aeronautics and Space Administration Washington, DC 20546		13. Type of Report and Period Covered Contractor Report 7/25/78 to 3/25/80	
		14. Sponsoring Agency Code	
15. Supplementary Notes Langley Technical Monitor: Wayne S. Slemp Final Report			
16. Abstract Degradation mechanisms have been investigated for graphite/polysulfone and graphite/epoxy laminates exposed to ultraviolet and high-energy electron radiations in vacuum up to 960 equivalent sun hours and 10^9 rads respectively. Based on GC and combined GC/MS analysis of volatile by-products evolved during irradiation, several free radical mechanisms of composite degradation have been identified. The radiation resistance of different matrices has been compared in terms of G values and quantum yields for gas formation. All the composite materials evaluated have shown high electron radiation stability and relatively low ultraviolet stability as indicated by low G values and high quantum yields for gas formation. Mechanical property measurements of irradiated samples did not reveal significant changes, with the possible exception of UV exposed polysulfone laminates. Hydrogen and methane have been identified as the main by-products of irradiation, along with unexpectedly high levels of CO and CO ₂ .			
17. Key Words (Suggested by Author(s)) Space Environment Ultraviolet Radiation Electron Radiation Graphite Composites		18. Distribution Statement Unclassified - Unlimited Subject Category 27	
19. Security Classif. (of this report) Unclassified	20. Security Classif. (of this page) Unclassified	21. No. of Pages 112	22. Price A06

For sale by the National Technical Information Service, Springfield, Virginia 22161

NASA-Langley, 1982